(12) INTERNATIONAL APPLICATION PUBLISHED UNDER THE PATENT COOPERATION TREATY (PCT)

(19) World Intellectual Property Organization
International Bureau

(43) International Publication Date
19 March 2020 (19.03.2020)

WIPO | PCT

(10) International Publication Number
WO 2020/053589 A1

(51) International Patent Classification:
B01D 53/14 (2006.01) *B01J 20/28* (2006.01)
B01J 20/26 (2006.01)

(21) International Application Number:
PCT/GB2019/052557

(22) International Filing Date:
13 September 2019 (13.09.2019)

(25) Filing Language: English

(26) Publication Language: English

(30) Priority Data:
1814881.7 13 September 2018 (13.09.2018) GB

(71) Applicants: **THE UNIVERSITY OF LIVERPOOL** [GB/GB]; Foundation Building, 765 Brownlow Hill, Liverpool L69 7ZX (GB). **THE QUEEN'S UNIVERSITY OF BELFAST** [GB/GB]; University Road, Belfast BT7 1NN (GB).

(72) Inventors: **COOPER, Andrew**; c/o The University of Liverpool, Foundation Building, 765 Brownlow Hill, Liverpool L69 7ZX (GB). **GREENAWAY, Rebecca**; c/o The University of Liverpool, Foundation Building, 765 Brownlow Hill, Liverpool L69 7ZX (GB). **KAI, Aiting**; c/o The University of Liverpool, Foundation Building, 765 Brownlow Hill, Liverpool L69 7ZX (GB). **EGLESTON, Benjamin**; c/o The University of Liverpool, Foundation Building, 765 Brownlow Hill, Liverpool L69 7ZX (GB). **JAMES, Stuart**; c/o The Queen's University of Belfast, University Road, Belfast BT7 1NN (GB).

(74) Agent: **MURGITROYD & COMPANY**; Scotland House, 165-169 Scotland Street, Glasgow Strathclyde G5 8PL (GB).

(81) Designated States *(unless otherwise indicated, for every kind of national protection available)*: AE, AG, AL, AM, AO, AT, AU, AZ, BA, BB, BG, BH, BN, BR, BW, BY, BZ, CA, CH, CL, CN, CO, CR, CU, CZ, DE, DJ, DK, DM, DO, DZ, EC, EE, EG, ES, FI, GB, GD, GE, GH, GM, GT, HN, HR, HU, ID, IL, IN, IR, IS, JO, JP, KE, KG, KH, KN, KP, KR, KW, KZ, LA, LC, LK, LR, LS, LU, LY, MA, MD, ME, MG, MK, MN, MW, MX, MY, MZ, NA, NG, NI, NO, NZ, OM, PA, PE, PG, PH, PL, PT, QA, RO, RS, RU, RW, SA, SC, SD, SE, SG, SK, SL, SM, ST, SV, SY, TH, TJ, TM, TN, TR, TT, TZ, UA, UG, US, UZ, VC, VN, ZA, ZM, ZW.

(54) Title: ORGANIC CAGE MICROPARTICLE DISPERSIONS FOR GAS ABSORPTION

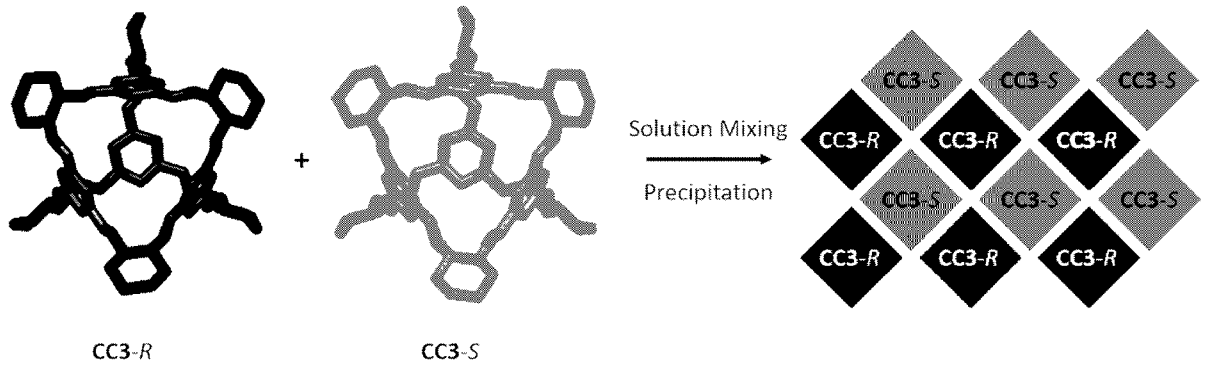

Figure 2

(57) Abstract: This invention relates to adispersion ofporous particles comprisingorganic cage molecules, the porous particles beingdispersed in a liquid phase, wherein the liquid is selected from the group consisting of liquid oligomers, size-excludedliquids, ionic liquids, liquid polymers, silicone oils, halogenated oils, paraffin oils, petroleum oils, triglyceride oils and combinations thereof. The invention also relates to amethod of adsorbing a gas into a liquid, comprising at least the step of bringing the gas into contact with thedispersion. In addition, the invention includes a method for preparing thedispersion comprising at least the step of:mixing (i) porous particles comprisinganorganic cagemolecule,and (ii) a liquid selected from the group consisting of liquid oligomers, size-excludedliquids, ionic liquids, liquid polymers, silicone oils, halogenated oils, paraffin oils, petroleum oils, triglyceride oils and combinations thereof. The invention also relates to an assemblage of the dispersion, the organic cage molecule comprising a cavity and a gas contained within the cavity.

[Continued on next page]

WO 2020/053589 A1

(84) **Designated States** *(unless otherwise indicated, for every kind of regional protection available)*: ARIPO (BW, GH, GM, KE, LR, LS, MW, MZ, NA, RW, SD, SL, ST, SZ, TZ, UG, ZM, ZW), Eurasian (AM, AZ, BY, KG, KZ, RU, TJ, TM), European (AL, AT, BE, BG, CH, CY, CZ, DE, DK, EE, ES, FI, FR, GB, GR, HR, HU, IE, IS, IT, LT, LU, LV, MC, MK, MT, NL, NO, PL, PT, RO, RS, SE, SI, SK, SM, TR), OAPI (BF, BJ, CF, CG, CI, CM, GA, GN, GQ, GW, KM, ML, MR, NE, SN, TD, TG).

Published:

— *with international search report (Art. 21(3))*

ORGANIC CAGE MICROPARTICLE DISPERSIONS FOR GAS ABSORPTION

[001] This invention relates to dispersions of porous particles comprising organic cage molecules, the porous particles being dispersed in a liquid phase, as well as to methods of preparing such dispersions. The invention also relates to a method of adsorbing a gas into a liquid, comprising at least the step of bringing the gas into contact with the dispersions. In addition, the invention relates to an assemblage of such a dispersion, the organic cage molecule comprising a cavity and a gas contained within the cavity.

[002] Background

[003] Porous solids such as zeolites are useful in molecular separation due to their permanent porosity. Porous solid adsorbents have significant advantages, for instance in terms of lower energy penalties in adsorption-desorption cycles when compared with their liquid counterparts, but they are difficult to incorporate into conventional flow processes.

[004] Liquid phases for the dissolution of gases are known. Solutions of various amines in water, or other solvents, are known to dissolve CO_2 and are applied industrially in natural gas “sweetening”. However, these methodologies comprise the use of toxic materials; are corrosive towards steel, which limits their uses industrially; and require large amounts of energy to regenerate. They are also non-specific and therefore cannot be used for specific or targeted gas separation.

[005] Porous liquids (liquids with permanent porosity) for use in molecular separation have subsequently been developed. These porous liquids have been categorised into three different types (*Chem. Eur. J.*, **2007**, *13*, 3020) as follows:

- Type 1 – neat liquid hosts comprising molecules having an internal cavity, and that the molecules cannot collapse or interpenetrate,
- Type 2 – host molecules having an internal cavity, the molecules being dissolved in a solvent that cannot occupy the host’s cavities, and

- Type 3 – particles of a host molecular framework dispersed in a liquid that cannot occupy the host's cavities.

Thus, each type of porous liquid comprises a "host" having a cavity into which, for example, gas molecules could be absorbed.

[006] Porous liquids having improved properties, particularly high gas uptake, are sought.

[007] **Statement of invention**

[008] According to one aspect of the invention, there is provided a dispersion of porous particles comprising organic cage molecules, the particles being dispersed in a liquid phase, wherein the liquid is selected from the group consisting of liquid oligomers, size-excluded liquids, ionic liquids, liquid polymers, silicone oils, halogenated oils, paraffin oils, petroleum oils, triglyceride oils and combinations thereof.

[009] Generally, a dispersion is a system in which particles are dispersed in a continuous phase of a different composition. The term "dispersion" is used in relation to the invention to refer to a system in which particles of a porous solid are dispersed in a liquid phase or medium. The dispersion may optionally comprise additives, such as surfactants, in order to increase the stability of the dispersion. Such additives are known to those skilled in the art.

[0010] The term "organic cage molecule" is used in relation to the invention to refer to cage molecules which do not include a metal atom.

[0011] In particular, the porous particles may be microparticles and/or nanoparticles. More particularly, the porous particles may be microparticles. Microparticles are generally defined as particles having a mean diameter in the range 0.1-100 μm (ie 100-100,000 nm). More particularly, the porous particles may have a mean diameter in the range 0.1-2 μm (ie 100-2000 nm). Nanoparticles are generally defined as particles having a mean diameter in the range 1-100 nm.

[0012] More particularly, the porous particles may be microporous (ie that they have a mean pore diameter of less than 2 nm).

[0013] In particular, the porous particles comprising the organic cage molecules may comprise co-crystals of two chiral forms, or enantiomers, of the same organic cage molecule. In alternative embodiments, the porous particles comprising the organic cage molecules may comprise at least 90 wt%, more particularly at least 95 wt%, of a single chiral form, or enantiomer, of the organic cage molecule. In other embodiments, the porous particles comprising the organic cage molecules may comprise co-crystals of more than one type of organic cage molecules, for example, two or three different types.

[0014] In particular, the porous particles comprising the organic cage molecules may comprise co-crystals of:

(i) the same organic cage molecule, but in different homochiral forms – for example **CC3**-*S*/**CC3**-*R* as included, another example is **FT-RCC3**-*R*/**FT-RCC3**-*S* (*CrystEngComm*, 2017, **19**, 4933),

(ii) two different organic cage molecules (i.e. binary systems) – these can be selected to have complimentary chirality but differ based on their functionalisation, derivative, or topology – examples include **CC1**/**CC3**-*R* and **CC1**/**CC4**-*R* (*Angew. Chem. Int. Ed.* **2012**, 51, 7154); **FT-RCC3**-*R*/**CC1**, **FT-RCC3**-*R*/**CC2**-*S,* and **FT-RCC3**-*R*/**CC4**-*S* (*CrystEngComm*, 2017, **19**, 4933); **CC3**-*R*/**CC2**-*S* and **CC13**/**CC3**-*R* (*Nanoscale*, 2017, **9**, 6783); **CC3**-*S*/**CC15**-*R* (*ACS Cent. Sci.* 2017, 3, 734); **TCC2**-*R*/**CC3**-*S* and **TCC1**-*R*/**CC3**-*S* (*Nat. Chem.*, 2017, 9, 17); **CC3**-*R*/**CC19**-*S* (*Angew. Chem. Int. Ed.*, **2018**, 57, 11228); and

(iii) three different organic cage molecules (i.e. ternary systems) – examples include **CC1**/**CC3**-*R*/**CC4**-*R* (*Angew. Chem. Int. Ed.* **2012**, 51, 7154) and **CC3**-*S*/**CC4**-*S*/**CC13** (*Nanoscale*, 2017, **9**, 6783).

[0015] In this way, the properties of the cage can be controlled, for example allowing porosity to be tuned for certain guest molecules. More particularly, the two chiral forms of the same organic cage molecule may be **CC3**-*R* and **CC3**-*S*, which can be formed using (*R*,*R*)-1,2-diaminocyclohexane and (*S*,*S*)-1,2-diaminocyclohexane respectively.

[0016] In particular, the porous particles comprising a single chiral form, or enantiomer, of the organic cage molecule may comprise **CC3**-*S*, **CC15**-*R*, **CC19**-*R* or **TCC2**-*R*.

[0017] More particularly, the liquid may be an ionic liquid. In particular, the ionic liquid may be 1-butyl- or 1-ethyl- 3-methylimidazolium bis(trifluoromethylsulfonyl) imide, 1-butylpyridinium bis(trifluoromethanesulfonyl)imide, trihexyltetradecylphosphonium bis(trifluoromethanesulfonyl)imide or benzyl(ethyl)dimethylammonium bis(trifluoromethanesulfonyl)imide.

[0018] In particular, the liquid may be a halogenated oil, which may be a chlorinated, brominated or fluorinated oil. Suitable halogenated oils include, for example a perfluoropolyether oil such as Fomblin Y (RTM) oil, a fluorinated silicone such as Fluorosil J15 (RTM), a fluorinated polydimethylsiloxane such as Fluorosil D2 (RTM), a fluorinated alkyl polydimethylsiloxane copolymer such as Fluorosil H418 (RTM), a fluorocarbon ether such as Krytox oil, chlorinated silicone oil and halocarbon oil 27 (RTM).

[0019] More particularly, the liquid may be a triglyceride oil. Suitable triglyceride oils include, for example olive oil, castor oil, sesame oil, sunflower oil, safflower oil, rapeseed oil, walnut oil, peanut oil, almond oil, clove oil, soybean oil, corn oil, cottonseed oil, anise oil and linseed oil.

[0020] In particular, the liquid may be a liquid polymer.

[0021] More particularly, the liquid may be selected from the group consisting of silicone oils, halogenated oils, triglyceride oils, paraffin oils, ionic liquids and size-excluded liquids.

[0022] In particular, the liquid may be a silicone oil (e.g. polydimethylsiloxane). Suitable silicone oils include, for example, pure silicone oil (more particularly silicone oil 5 cSt, silicone oil 20 cSt, and/or silicone oil 50 cSt) and silicone oil AR 20. Silicone oils are cheap, readily available and biocompatible making them

advantageous for use in the dispersions of the present invention. In addition, silicone oil has high thermal stability which facilitates material regeneration.

[0023] In particular, the liquid may be an ionic liquid. Ionic liquids are generally defined as salts in a liquid state. More particularly, the ionic liquid may be 1-butyl-3-methylimidazolium bis(trifluoromethylsulfonyl)imide (ie BMIM.NTf_2), 1-butylpyridinium bis(trifluoromethanesulfonyl)imide (ie BPy.NTf_2), trihexyltetradecylphosphonium bis(trifluoromethanesulfonyl)imide (ie P_{66614}.NTf_2) and benzyl(ethyl)dimethylammonium bis(trifluoromethanesulfonyl)imide (ie BEMA.NTf_2).

[0024] More particularly, the liquid may be a size-excluded liquid. A size-excluded liquid may be defined in the context of the invention as a liquid which is excluded from the pores (ie the cavities) within the organic cage molecule. This can be because the size-excluded liquid has a molecular size which is too large to enter the pores of the porous particles. Alternatively, entry into the pores of the porous particles may be thermodynamically or kinetically unfavourable. In particular, the size-excluded liquid may be 1-^{t}butyl-3,5-dimethylbenzene, 15-crown-5, hexachloropropene, methyl salicylate, 2,4-dichlorotoluene or 4-(trifluoromethoxy)benzyl alcohol. More particularly, the size-excluded liquid may be 1-^{t}butyl-3,5-dimethylbenzene or 15-crown-5.

[0025] In particular, the dispersion may comprise 0.1-50 wt% of the porous particles, more particularly 0.5-30 wt%. Even more particularly, the dispersion may comprise 1-20 wt% of the porous particles. More particularly, the dispersion may comprise 10-15 wt% of the porous particles. In some embodiments, the dispersion may comprise 11-14 wt% of the porous particles, more particularly 12-13 wt% of the porous particles.

[0026] In the dispersion according to the present invention, the pores of the porous particles are accessible to a gas. Optionally, the gas is CO_2, CH_4, N_2, C_2H_4, C_2H_6, Xe, SF_6, C_3H_8 or H_2, or a mixture thereof.

[0027] Particular embodiments of the dispersion are as follows:

(i) the porous particles comprising the organic cage molecules comprise co-crystals of **CC3**-*R* and **CC3**-*S* and the liquid is silicone oil, more particularly silicone oil 5 cSt or silicone oil AR 20;

(ii) the porous particles comprising the organic cage molecules comprise co-crystals of **CC3**-*R* and **CC3**-*S* and the liquid is an ionic liquid, more particularly $P_{66614}.NTf_2$ or $BPy.NTf_2$, even more particularly $BPy.NTf_2$;

(iii) the porous particles comprising the organic cage molecules comprise **CC3**-*S*, **CC15**-*R*, **CC19**-*R* or **TCC2**-*R* and the liquid is silicone oil, more particularly silicone oil 5 cSt.

[0028] According to a further aspect of the present invention, there is provided a method of adsorbing a gas into a liquid, comprising at least the step of bringing the gas into contact with a dispersion of porous particles comprising an organic cage molecule, the porous particles being dispersed in a liquid phase, wherein the liquid is selected from the group consisting of liquid oligomers, size-excluded liquids, ionic liquids, liquid polymers, silicone oils, halogenated oils, paraffin oils, petroleum oils, triglyceride oils and combinations thereof. More particularly, the dispersion may be as defined above.

[0029] In particular, the gas may be CO_2, CH_4, N_2, C_2H_4, C_2H_6, Xe, SF_6, C_3H_8 or H_2, or a mixture thereof. In particular, the gas may be CH_4 or CO_2.

[0030] According to a further aspect of the present invention, there is provided a method for preparing a dispersion comprising at least the step of: mixing (i) porous particles comprising an organic cage molecule, and (ii) a liquid selected from the group consisting of liquid oligomers, size-excluded liquids, ionic liquids, liquid polymers, silicone oils, halogenated oils, paraffin oils, petroleum oils, triglyceride oils and combinations thereof. The porous particles may be as defined above. More particularly, the dispersion formed by the method may be as defined above.

[0031] Optionally, the mixing includes agitating, stirring, sonication or grinding or a combination thereof. More particularly, the method comprises sonicating the mixture.

[0032] According to a further aspect of the present invention, there is provided an assemblage of a dispersion of porous particles comprising an organic cage molecule, the porous particles being dispersed in a liquid phase, wherein the liquid is selected from the group consisting of liquid oligomers, size-excluded liquids, ionic liquids, liquid polymers, silicone oils, halogenated oils, paraffin oils, petroleum oils, triglyceride oils and combinations thereof, wherein the organic cage molecule comprises a cavity and a gas contained within the cavity. More particularly, the gas may be CO_2, CH_4, N_2, C_2H_4, C_2H_6, Xe, SF_6, C_3H_8 or H_2, or a mixture thereof. In particular, the gas may be CO_2 or CH_4.

[0033] **Brief description of the drawings**

[0034] This invention will be further described by reference to the following Figures which are not intended to limit the scope of the invention claimed, in which:

Figure 1 shows a reaction scheme for the synthesis of porous organic cages **CC3**-*R* and **CC3**-*S*, the dashed bond being a cyclohexane ring,

Figure 2 illustrates the formation of microporous organic particles by chiral recognition between **CC3**-*R* and **CC3**-*S* upon mixing in solution, with a schematic of the packing in the **CC3**-*R/S* particles

Figure 3 shows a series of PXRD traces of the individual cages **CC3**-*R* and **CC3**-*S*, as well as for the **CC3**-*R/S* microparticles formed by Examples 1-6 and 7,

Figure 4 shows SEM images of the **CC3**-*R/S* microparticles formed by Examples 1-6 and 7,

Figure 5a-5d show DLS histograms comparing the particle sizes and distributions of **CC3**-*R/S* microparticles formed by Examples 1-6 and 7,

Figure 5e shows a series of PXRD traces of the **CC3**-*R/S* microparticles formed by Examples 7, 8, 9, 10 and 11 of the scale-up procedure,

Figure 5f shows DLS histograms comparing the reproducibility of the **CC3**-*R/S* microparticle sizes and distributions formed by Examples 7, 8 and 9 of the scale-up procedure,

Figure 5g shows DLS histograms comparing the reproducibility of the **CC3**-*R/S* microparticle sizes and distributions formed by Examples 10 and 11 of the scale-up procedure,

Figure 6 shows the structures of liquid dispersants which were investigated for the formation of cage microparticle dispersions,

Figure 7 shows the structure of the control molecule, homochiral cage **CC3**-*R*, homochiral **CC15**-*R*, homochiral **CC19**-*R*, homochiral **TCC2**-*R* and a schematic of the packing of the **CC3**-*R/S* particles,

Figure 8 shows the experimental setup for the measurement of volumetric uptake of gases by porous liquids on a Quantachrome Nova 4200e, with stirrer plates in place to ensure agitation of the liquid samples during degas and adsorption,

Figure 9 shows FTIR traces for the **CC3**-*R/S* microparticles of Example 7, a 12.5 wt% dispersion of **CC3**-*R/S* microparticles in silicone oil (5 cSt), and of silicone oil (5 cSt),

Figure 10 shows PXRD traces for the **CC3**-*R/S* microparticles of Example 7 in air (lower trace) and a 12.5 wt% dispersion of **CC3**-*R/S* microparticles in silicone oil (5 cSt) (upper trace),

Figure 11 shows DLS histograms comparing the particle sizes and distributions of **CC3**-*R/S* microparticles dispersed in DCM (left most peak), a 12.5 wt% dispersion of **CC3**-*R/S* microparticles in silicone oil (5 cSt) after 1 day (middle peak), and a 12.5 wt% dispersion of **CC3**-*R/S* microparticles in silicone oil (5 cSt) after 24 days (right most peak),

Figure 12a shows TGA analysis of the **CC3**-*R/S* solid microparticles, silicone oil (5 cSt), and the 12.5 wt% dispersion of **CC3**-*R/S* microparticles in silicone oil (5 cSt) under air,

Figure 12b shows TGA analysis of the **CC3**-*R/S* solid microparticles, $BPy.NTf_2$, and the 5 wt%, 12.5 wt% and 20 wt% dispersions of **CC3**-*R/S* microparticles in $BPy.NTf_2$ under nitrogen,

Figure 13 shows CO_2 uptake (298-303 K) in an ionic liquid ($BMIM.NTf_2$, left) and a size-excluded solvent (15-crown-5, right),

Figure 14 shows CO_2 (left) and CH_4 (right) isotherms on the solid **CC3**-*R/S* microparticles of Examples 7 and 9,

Figure 15a-p shows CO_2 uptake isotherms (298-303 K) for a range of dispersions and dispersants investigated,

Figure 16 shows a comparison of CO_2 uptake isotherms (298-303 K) for the 12.5 wt% **CC3**-*R/S* microparticle dispersions in silicone oil (5 cSt),

Figure 17a shows repeated CO_2 uptake isotherms for the 12.5 wt% **CC3**-*R/S* microparticle dispersions in silicone oil (5 cSt),

Figure 17b shows repeated CO_2 uptake isotherms for the 12.5 wt% **CC3**-*R/S* microparticle dispersions in BPy.NTf_2,

Figure 18a shows repeated CO_2 uptakes at 1 bar for the 12.5 wt% **CC3**-*R/S* microparticle dispersions in silicone oil (5 cSt),

Figure 18b shows repeated CO_2 uptakes at 1 bar for the 12.5 wt% **CC3**-*R/S* microparticle dispersions in BPy.NTf_2,

Figure 19a shows repeated CO_2 uptake isotherms for fresh and aged 12.5 wt% **CC3**-*R/S* microparticle dispersions in silicone oil (5 cSt),

Figure 19b shows repeated CO_2 uptake isotherms for fresh and aged 12.5 wt% **CC3**-*R/S* microparticle dispersions in BPy.NTf_2,

Figure 20a shows a comparison of CH_4 uptake isotherms (298-303 K) for the 12.5 wt% and 20 wt% **CC3**-*R/S* microparticle dispersions in silicone oil (5 cSt), with neat silicone oil (5 cSt),

Figure 20b shows a comparison of CH_4 uptake isotherms (298-303 K) for the 5 wt%, 12.5 wt% and 20 wt% **CC3**-*R/S* microparticle dispersions in BPy.NTf_2, with neat BPy.NTf_2,

Figure 21a shows a Lumisizer image for a longer term stability test on 12.5 wt% **CC3**-*R/S* (9) microparticles in silicone oil (5cSt),

Figure 21b shows a Lumisizer image for a longer term stability test on 12.5 wt% **CC3**-*R* in silicone oil (5cSt),

Figure 21c shows a Lumisizer image for a longer term stability test on 12.5 wt% **CC3**-*R/S* (9) microparticles in silicone oil AR 20,

Figure 21d shows a Lumisizer image for a longer term stability test on 12.5 wt% **CC3**-*R/S* (9) microparticles in olive oil,

Figure 21e shows a Lumisizer image for a longer term stability test on 12.5 wt% **CC3**-*R/S* (9) microparticles in Fomblin Y,

Figure 21f shows a Lumisizer image for a longer term stability test on 12.5 wt% **CC3**-*R/S* (9) microparticles in Halocarbon 27,

Figure 21g shows a Lumisizer image for a longer term stability test on 5 wt% **CC3**-*R/S* (10) microparticles in BPy.NTf_2.

Figure 21h shows a Lumisizer image for a longer term stability test on 12.5 wt% **CC3**-*R/S* (10) microparticles in BPy.NTf_2.

[0035] **Examples**

[0036] Porous Organic Cage Microparticle Screen

[0037] **CC3**-*R* and **CC3**-*S* were synthesised according to the procedure shown in *JACS*, **2012**, *134*, 588. The reaction scheme is shown in Figure 1. **CC15**-*R* was synthesised according to the procedure shown in *ACS Cent. Sci.*, **2017**, 3, 7, 734. **CC19**-*R* was synthesised according to the procedure shown in *Angew. Chem. Int. Ed.*, **2018**, 57, 35, 11228. **TCC2**-*R* was synthesised according to the procedure shown in *Nat. Chem.*, **2017**, 9, 17.

[0038] A solution (1.5 mg/mL) of organic cage **CC3**-*S* (150 mg) in dichloromethane (100 mL) was added to a solution (1.5 mg/mL) of **CC3**-*R* (150 mg) in dichloromethane (100 mL) using various addition rates, stirring types and temperatures (see Examples 1-7 in Table 1 below). Example 7 was carried out on a larger scale, i.e. **CC3**-*S* (1.35 g) in dichloromethane (900 mL) was added to **CC3**-*R* (1.35 g) in dichloromethane (900 mL).

[0039] The resulting colourless precipitate (**CC3**-*R/S* microparticles) for each example was collected by vacuum filtration through a 0.2 μm nylon membrane filter paper and dried under vacuum overnight (maximum mass recovery = 300 mg).

Ex. No.	Addition Rate	Stirring Type	Temp	Mass Recovery
1	Rapid	Prolonged, magnetic stirrer bar	20 °C (RT)	252 mg, 84%
2	Rapid	Magnetic stirrer bar	20 °C (RT)	292 mg, 97%
3	0.66 mL/min	Magnetic stirrer bar	20 °C (RT)	217 mg, 72%
4	0.66 mL/min	Magnetic stirrer bar	0 °C	208 mg, 69%
5	0.66 mL/min	Magnetic stirrer bar	-78 °C	154 mg, 51%
6	0.66 mL/min	Overhead	20 °C (RT)	133 mg, 44%
7	Rapid	Overhead	20 °C (RT)	1.42 g, 52%

NB – Example 7 was carried out on a larger scale (**CC3**-*R* (1.35g) in dichloromethane (900 mL) + **CC3**-*S* (1.35g) in dichloromethane (900 mL)) to allow dispersion studies to be carried out.

Table 1

[0040] The resulting collected microparticles from Examples 1-7 were analysed by powder X-ray diffraction (PXRD) (see Figure 3) to confirm formation of the **CC3**-*R*/*S* co-crystal. The PXRD patterns of the **CC3**-*R*/*S* microparticles suggest phase-pure material, and closely resemble that observed for homochiral **CC3**-*R* and **CC3**-*S*. This suggests a similar crystal packing, but the peak angles are displaced slightly due to changes in the unit cell volume. This has been previously reported where the unit cell size of **CC3**-*R*/*S* is smaller than **CC3**-*R* and **CC3**-*S* due to the ability of homochiral cages to pack more closely together than their chiral counterparts (*JACS*, **2012**, *134*, 588).

[0041] The samples were also analysed by scanning electron microscopy (SEM) (see Figure 4) and dynamic light scattering (DLS) (see Figure 5) to determine particle morphology, size and distribution. SEM was conducted on a Hitachi (RTM) S4800 scanning electron microscope, and powdered samples of the particles were deposited on to adhesive graphite tabs mounted on 15 mm aluminium stages. DLS was carried out on a Zetasizer (RTM) Nano Particle Sizer by re-dispersing the powdered samples into dichloromethane in a quartz cuvette. Laboratory powder X-ray diffraction data (PXRD) were collected in transmission mode on samples held on thin Mylar (RTM) film in aluminium well plates on a Panalytical (RTM) X'Pert PRO MPD equipped with a high throughput screening (HTS) XYZ stage, X-ray focusing mirror and PIXcel detector, using Ni-filtered Cu Kα radiation. Data were measured over the range 4-40° in ~0.013° steps over 60 minutes.

[0042] The SEM images show that spherical particles are obtained when magnetic stirring with a stirrer bar and hotplate are used (Examples 1-5), or on rapid mixing of the two solutions even when overhead stirring is employed (Example 7), whilst octahedral particles are formed on slow addition with overhead stirring (Example 6). It is worth noting that the particle sizes are similar on rapid mixing at room temperature whether the stirring be magnetic or overhead (Example 2 *vs* Example 7), and that whilst the morphology of the particles can be changed, the PXRDs confirm the same co-crystallised species are present.

[0043] The DLS histograms in Figure 5 are used to compare the **CC3**-*R*/*S* microparticle sizes and distributions formed by a range of methods. Figure 5(a) is a

comparison of the effect of rapid solution mixing with either prolonged magnetic stirring (Example 1), magnetic stirring and immediate filtration (Example 2), or overhead stirring and immediate filtration (Example 7) at the same temperature. Figure 5(b) is a comparison of the effect of rapid solution mixing (Example 2) and slow addition (Example 3) with the same stirring method at the same temperature. Figure 5(c) is a comparison of the effect of different temperatures for solution mixing – ambient or room temperature (RT) (Example 3), 0 °C (Example 4) and -78 °C (Example 5) with the same addition rate and stirring method. Figure 5(d) is a comparison of the effect of magnetic stirring (Example 3) and overhead stirring (Example 6) at the same temperature and addition rate.

[0044] A summary of the results from both the SEM and DLS measurements is shown in Table 2 below:

Ex No.	Morphology	SEM Size Range / nm	DLS Size* / nm
1	Spherical	150-750	503
2	Spherical	200-500	442
3	Spherical	300-1300	946
4	Spherical	200-900	787
5	Spherical	500-1200	1316
6	Octahedral	500-900	943
7	Spherical	250-550	540

*Reported size is the z-average over 3 runs

Table 2

[0045] Due to the ease of scaling the procedure up, Example 7 was used to investigate dispersion formation in oils, ionic liquids and size-excluded solvents.

[0046] Scale-up of Porous Organic Cage Microparticles

[0047] A solution (1.5 mg/mL) of organic cage **CC3**-*S* (1.35 g) in dichloromethane (900 mL) was rapidly added in a single addition to a solution (1.5 mg/mL) of **CC3**-*R*

(1.35 g) in dichloromethane (900 mL) with overhead stirring at room temperature (ie the Example 7 procedure). The resulting colourless precipitate (**CC3**-*R/S* microparticles) was collected by vacuum filtration through a 0.2 μm nylon membrane filter paper and dried under vacuum overnight (52% mass recovery, maximum mass recovery = 2.7 g).

[0048] This preparation was repeated a further four times to ensure reproducibility in particle size/distribution as determined by DLS – for a summary of the five runs see Table 2a below. PXRD and DLS data for Examples 7, 8 and 9 is shown in Figures 5e and 5f, and Examples 10 and 11 are shown in Figures 5e and 5g. In Figure 5f, the particle size can be seen to vary slightly between the three Examples, but all particle sizes are within the range 200-2000 nm.

Ex No.	Addition Rate	Stirring Type	Temperature	Mass Recovery	DLS Size* / nm
7	Rapid	Overhead	20 °C (RT)	1.42 g, 52%	540
8				2.15 g, 80%	601
9				1.80 g, 66%	1206
10				2.32 g, 86%	721
11				2.02 g, 75%	632

*Reported size is the z-average over 3 runs

Table 2a

[0049] Cage Microparticle Dispersions – Formation, Characterisation and Gas Uptake

[0050] Dispersions of the scaled-up microparticles (Examples 7-11) were investigated in silicone oil (PDMS, 5 cSt and 50 cSt), size-excluded ionic liquids (1-butyl-3-methylimidazolium bis(trifluoromethylsulfonyl)imide (BMIM.NTf_2), 1-butylpyridinium bis(trifluoromethanesulfonyl)imide (BPy.NTf_2) and a size-excluded solvent (15-Crown-5) that is known to be size-excluded from the cage cavity. Other oils were also tested, including triglycerides, hydrocarbon oils, halocarbon oils, and polyethyleneglycol (PEG) derivatives (see Figure 6) using the scaled-up microparticles of Examples 7-11.

[0051] The solid microparticles and the potential liquid dispersants were stirred or sonicated and the resulting suspension visually inspected. In silicone oil (5 cSt), the ionic liquid and the size-excluded solvent, a 12.5 wt% flowable dispersion, that visually remains dispersed, was formed. The microparticles in 5 cSt silicone oil and BPy.NTf_2 were also made up to a 20 wt% dispersion.

[0052] A series of other oils were also investigated as dispersants at a 12.5 wt% loading of **CC3**-*R/S* microparticles (Examples 7-9) including: silicone oil AR 20, olive oil and sunflower oil (triglycerides), paraffin oil (hydrocarbon) and Genesorb (RTM)

1753. For both Halocarbon 27 (RTM) and Fomblin Y (RTM), 5 wt% dispersions were made.

[0053] Representative Procedure for formation of 5 wt% microparticle dispersions

[0054] The **CC3**-*R/S* microparticles (150 mg) were desolvated at 90 °C overnight in a vacuum oven, before the direct addition of the liquid dispersant (2.85 g), and the resulting suspension sonicated for 10 minutes to afford a 5 wt% dispersion.

[0055] Representative Procedure for formation of 12.5 wt% microparticle dispersions

[0056] The **CC3**-*R/S* microparticles (200 mg) were desolvated at 90 °C overnight in a vacuum oven, before the direct addition of the liquid dispersant (1.4 g), and the resulting suspension sonicated for 10 minutes to afford a 12.5 wt% dispersion.

[0057] Representative Procedure for formation of 20 wt% microparticle dispersions

[0058] The **CC3**-*R/S* microparticles (100 mg) were desolvated at 90 °C overnight in a vacuum oven, before the direct addition of the liquid dispersant (0.4 g), and the resulting suspension sonicated for 10 minutes to afford a 20 wt% dispersion.

[0059] Alongside this, to confirm that the gas uptake was due to the cavities in the cages, a control liquid using a molecule that contains all the functionality of the porous organic cages used (**CC3**-*R* and **CC3**-*S*), but no cavity, was investigated as a 12.5 wt% dispersion in silicone oil (5 cSt). To determine if the homochiral cage **CC3**-*R* has the same uptake capacity as the formed **CC3**-*R/S* microparticles, the solid was ground in a mortar and pestle and the powder investigated as a 12.5 wt% dispersion in silicone oil (5 cSt) (see Figure 7 for the structure of the control molecule (left), resulting homochiral cage (middle), and a schematic of the packing of the formed microparticles). Alternative microparticles of a different size (Example 5), and different morphology (Example 6), were also investigated as 12.5 wt% dispersions in silicone oil (5 cSt). These were formed using the same representative particle synthesis and dispersion formation procedures described above.

[0060] Representative Procedure for formation of 10 wt% dispersions using alternative organic cage species

[0061] The alternative organic cages (**CC15**-*R*, **CC19**-*R* and **TCC2**-*R*) were ground in a mortar and pestle. The resulting solid (100 mg) was then desolvated at 90 °C overnight in a vacuum oven, before the direct addition of the liquid dispersant (0.9 g silicone oil, 5 cSt), and the resulting suspension sonicated for 10 minutes to afford a 10 wt% dispersion.

[0062] These materials were prepared in order to test whether alternative cage molecules could modify gas uptake in the resulting dispersions.

[0063] CO_2 uptake of microparticle dispersions

[0064] The uptake of CO_2 was measured for the liquid dispersants and dispersions using a Quantachrome (RTM) Nova 4200e to confirm the formation of Type 3 porous liquids. The equipment is shown in Figure 8.

[0065] To ensure reliable gas uptake measurements, the sorption method on the Quantachrome (RTM) Nova 4200e was optimised to benchmark the system against liquids with known Henry's constants for CO_2 in the literature. The sample size, effect of stirring, stirrer bar type, number of pressure points, pressure tolerance and equilibration time were investigated and optimised, and the CO_2 uptake measured on an ionic liquid (BMIM.NTf_2, literature - Accounts of Chemical Research, **2007**, 40, *11*, 1208-1216) and a size-excluded solvent (15-crown-5, literature - J. Phys. Chem. B, **2017**, *121*, 8367), and compared to those calculated from the literature (see Table 2b below).

[0066] The standardised setup and method was as follows. Adsorption isotherms were measured using an in-house modification of a Quantachrome (RTM) Nova 4200e for liquid samples at ambient temperature (298-303 K). A 9 mm sample cell with large bulb (P/N:74064), filler rod (P/N: 74105-LP), and small glass coated magnetic stirrer bars were used for all measurements. The sample size used was approximately 0.5 mL injected directly into the bulb using a long syringe needle. Liquid samples were degassed under vacuum at ambient temperature for a minimum

of 18 hours, whilst stirring (500 rpm) – no filler rod, He backfill selected to prevent refill with gas being measured. Adsorption of CO_2 was carried out using the following settings: backfill = He, He Pump Down = 60 min, pressure points P/P_0 = 0.05 to 1.0, in 0.05 increments; pressure tolerance = 0.05 mmHg; equilibration time = 1800 seconds; equilibration timeout = 5400 seconds, and was stirred (500 rpm) throughout the measurement, with a filler rod in place. The software automatically measures the free-space and takes this into account when calculating the uptakes. Separate samples of each dispersion were measured a minimum of 2 times to calculate an average uptake and standard deviation.

Sample	Literature H_{CO2} (bar)	Calculated Literature CO_2 Uptake (μmol/g_L)	Average Experimental Uptake (μmol/g_L)
BMIM.NTf_2	33.0±0.3 (298 K, 1 bar)	71-73	75.1 ± 6.8
15-crown-5	45.8 (308 K, 1 bar)	85-113	78.5 ± 3.1

Table 2b

[0067] The CO_2 uptake measurements of both an ionic liquid and size-excluded solvent were comparable to those calculated from the reported Henry's constants in the literature, and the uptakes reproducible between samples (see Figure 13). Therefore, this method was used to measure the uptakes with the dispersants and microparticle dispersions. The results are set out in Table 3 below.

[0068] To enable comparison to a calculated uptake for the amount of porous solid included in the dispersions, CO_2 and CH_4 isotherms at 298 K were measured on the solid **CC3**-*R/S* microparticles (Examples 7 and 9) using a Micromeritics (RTM) ASAP 2020 volumetric adsorption analyser (see Figure 14). The uptakes from the two measurements at 1 bar were used to calculate an expected uptake for the solid present in the dispersions. Powder samples were degassed offline at 90 °C for 15 h under dynamic vacuum (10^{-5} bar) before analysis, followed by degassing on the analysis port under vacuum, also at 90 °C. Whilst the uptakes are in the same region, slight variation is seen between batches so the average uptake at 1 bar was calculated and used to compare to the uptakes in the dispersions – CO_2 = 1895

μmol/g_S (7) and 1690 μmol/g_S (9), therefore average = 1792 ± 72 μmol/g_S; CH_4 = 1119 μmol/g_S (7) and 1009 μmol/g_S (9), therefore average = 1064 ± 77 μmol/g_S.

Disp. No.	Solid	Dispersant	Loading (wt%)	Average CO_2 Uptake, 298-303 K, 1 bar (μmol/g_L unless otherwise stated)	Average increase in uptake over base solvent (μmol/g_L)
1*	**CC3**-*R/S*	-	-	1792 ± 72 μmol/g_S	-
2	-	Silicone oil (5 cSt)	-	84.8 ± 2.4	-
3	**CC3**-*R/S* (8)	Silicone oil (5 cSt)	12.5	199.5 ± 1.9	114
4	**CC3**-*R/S* (9)	Silicone oil (5 cSt)	12.5	198.0 ± 3.8	113
5	**CC3**-*R/S* (8)	Silicone oil (5 cSt)	20	279.7	195
6	**CC3**-*R/S* (5)	Silicone oil (5 cSt)	12.5	198.6 ± 10.4	113
7	**CC3**-*R/S* (6)	Silicone oil (5 cSt)	12.5	199.8 ± 6.4	115
8	Control	Silicone oil (5 cSt)	12.5	83.7 ± 8.7	0
9	**CC3**-*R*	Silicone oil (5 cSt)	12.5	185.2 ± 13.0	100
10	-	Silicone oil AR 20	-	61.0 ± 1.1	-
11	**CC3**-*R/S* (9)	Silicone oil AR 20	12.5	181.8 ± 3.8	120
12	-	Olive Oil	-	61.1 ± 1.8	-
13	**CC3**-*R/S* (9)	Olive Oil	12.5	77.2 ± 4.5	16

14	-	Sunflower Oil	-	74.0 ± 6.3	-
15	**CC3**-*R/S* (9)	Sunflower Oil	12.5	133.2 ± 1.4	59
16	-	Paraffin Oil	-	41.9 ± 0.1	-
17	**CC3**-*R/S* (9)	Paraffin Oil	12.5	65.0 ± 5.3	23
18	-	Halocarbon 27 (RTM)	-	37.0 ± 3.1	-
19	**CC3**-*R/S* (9)	Halocarbon 27 (RTM)	5	74.8 ± 8.1	37
20	-	Fomblin Y (RTM)	-	28.5 ± 1.5	-
21	**CC3**-*R/S* (9)	Fomblin Y (RTM)	5	67.0 ± 0.9	38
22	-	Genesorb (RTM) 1753	-	104.0 ± 4.4	-
23	**CC3**-*R/S* (9)	Genesorb (RTM) 1753	12.5	85.0 ± 16.0	0
24	-	BMIM.NTf_2	-	75.1 ± 6.8	-
25	**CC3**-*R/S* (9)	BMIM.NTf_2	12.5	80.0 ± 1.2	5
26	-	15-crown-5	-	78.5 ± 3.1	-
27	**CC3**-*R/S* (9)	15-crown-5	12.5	94.0 ± 7.7	15
28	-	BPy.NTf_2	-	78.3 ± 4.5	-
29	**CC3**-*R/S* (10)	BPy.NTf_2	5	111.4 ± 6.4	36
30	**CC3**-*R/S* (10)	BPy.NTf_2	12.5	170.1 ± 7.7	92
31	**CC3**-*R/S* (11)	BPy.NTf_2	12.5	172.1 ± 3.6	94
32	**CC3**-*R/S* (11)	BPy.NTf_2	20	209.8 ± 6.7	131

33	-	$P_{66614}.NTf_2$	-	77.6	-
34	**CC3**-*S*	$P_{66614}.NTf_2$	12.2	155.7	78
35	-	$BEMA.NTf_2$	-	86.5	-
36	**CC3**-*S*	$BEMA.NTf_2$	5.8	144.9	58
37	**CC19**-*R*	Silicone oil (5 cSt)	10	216	131
38	**CC3**-*R*	Silicone oil (5 cSt)	10	173	88
39	**CC15**-*R*	Silicone oil (5 cSt)	10	153	68
40	**TCC2**-*R*	Silicone oil (5 cSt)	10	157	72

*Average uptake measurements for **CC3**-*R/S* solid microparticles carried out on a Micromeritics (RTM) ASAP 2020 (CO_2, 298 K, 1 bar)

Table 3

[0069] For the CO_2 uptake measurements, the isotherms and uptakes of duplicate samples for each example dispersion were comparable and reproducible, and all showed an increase in uptake over the neat dispersant with the exception of Genesorb 1753 (see Figure 15).

[0070] On comparison of the CO_2 uptake in dispersions consisting of different **CC3**-*R/S* microparticles (varying the sizes and morphologies), and using homochiral **CC3**-*R* not formed into microparticles, in silicone oil (5 cSt), the uptake was comparable. This suggests that particle size and morphology does not have a direct effect on the porosity of the dispersion (see Figure 15c). Furthermore, the control molecule dispersed in silicone oil (5 cSt) at 12.5 wt% showed no increase in CO_2 uptake over neat silicone oil (5 cSt), confirming that the observed uptake is reliant on the presence of the cage cavities (see Figure 15a). There was, however, variation in the uptake depending on which liquid dispersant was used – see Table 4 below for more information. Compared to the CO_2 uptake in a previously reported 'scrambled' cage porous liquid of ~55 μmol/g_{PL} (*Chem. Sci.*, **2017**, *8*, 2640), the dispersions of

microparticles in silicone oil (5 cSt) showed an approximate 4-6 fold increase in gas uptake.

[0071] In Table 4 below, the average CO_2 volumetric uptake measurement (1 bar, 298-303 K) on the different **CC3**-*R/S* microparticle dispersions was compared to the calculated theoretical maximum uptake for the dispersion based on the ratio of solid and liquid present in that dispersion. For example, for a 12.5 wt% dispersion, the calculated uptake (μmol/g) would be 0.125 times the uptake in the solid (μmol/g_S), plus 0.875 times the uptake in the neat liquid (μmol/g_L).

Disp. No.	Solid	Dispersant	Loading (wt%)	Average dispersant Uptake (μmol/g_L)	Average dispersion Uptake (μmol/g_L)	Calculated uptake for dispersion (μmol/g)*	Percentage Porosity Obtained (%) (Measured vs Calculated)
1	**CC3**-*R/S* (9)	Silicone oil (5 cSt)	12.5	85	198	298	66
2	**CC3**-*R/S* (8)	Silicone oil (5 cSt)	20	85	280	426	66
3	**CC3**-*R/S* (9)	Silicone oil AR 20	12.5	61	182	277	66
4	**CC3**-*R/S* (9)	Olive oil	12.5	61	77	277	28
5	**CC3**-*R/S* (9)	Sunflower oil	12.5	74	133	289	46
6	**CC3**-*R/S* (9)	Paraffin oil	12.5	42	65	261	25
7	**CC3**-*R/S* (9)	Halocarbon 27 (RTM)	5	37	75	125	60
8	**CC3**-*R/S* (9)	Fomblin Y (RTM)	5	29	67	117	57
9	**CC3**-*R/S* (9)	Genesorb (RTM)1753	12.5	104	85	315	27
10	**CC3**-*R/S* (9)	BMIM.NTf_2	12.5	75	80	290	28
11	**CC3**-*R/S* (9)	15-crown-5	12.5	79	94	293	32
12	**CC3**-*R/S* (10)	BPy.NTf_2	5	78	111	164	68
13	**CC3**-*R/S* (11)	BPy.NTf_2	12.5	78	172	292	59
14	**CC3**-*R/S* (11)	BPy.NTf_2	20	78	210	421	50

*Calculated using the average CO_2 uptake in the solid **CC3**-*R/S* microparticles - 1792 μmol/g_S

Table 4

WO 2020/053589 PCT/GB2019/052557
22

[0072] Overall, two thirds (66%) of the calculated theoretical porosity from the solid microparticles and liquid dispersant is maintained in the dispersions in silicone oils (Silicone oil 5 cSt and Silicone AR20) and some ionic liquids ($BPy.NTf_2$), even at different weight loadings. On changing to halocarbon oils (Halocarbon 27 (RTM) and Fomblin Y (RTM)) the percentage porosity is slightly reduced compared to the theoretical calculated uptake for the dispersion, with ~57-60% of the calculated uptake being achieved. This reduction in porosity is also observed with triglyceride and hydrocarbon oils, although to differing extents depending on the oil used – paraffin oil and olive oil had 25-28% of the calculated uptake being achieved, and sunflower oil achieved 46% of the calculated uptake. The use of an alternative ionic liquid ($BMIM.NTf_2$), or a size-excluded solvent (15-crown-5), also showed a reduction in porosity compared to the calculated uptake, but still exhibited ~25-32% of the calculated theoretical porosity. The porosity of the microparticles is lost when dispersed in Genesorb (RTM) 1753, with a lower uptake than the neat liquid itself, likely due to interpenetration of the polyethylene glycol dimethyl ethers into the cage cavities.

[0073] The use of fewer pressure points and the effect on the measured CO_2 uptake was investigated using the 12.5 wt% **CC3**-*R/S* microparticle dispersion in silicone oil (5 cSt). As shown in Figure 16, the uptakes measured using 4 pressure points (0.25, 0.5, 0.75, and 1.0 bar, the squares in Figure 16) are comparable to those measured using 20 pressure points (0.05 to 1.0, in 0.05 bar increments, the triangles in Figure 16) showing that the gas does not need long equilibration times in order for gas uptake to occur in the porous liquid.

[0074] <u>CH_4 uptake of microparticle dispersions</u>

[0075] An alternative gas (CH_4) was investigated for uptake in the porous dispersions using the 12.5 wt% and 20 wt% **CC3**-*R/S* microparticle dispersions in silicone oil (5 cSt)), and the 5 wt%, 12.5 wt% and 20 wt% **CC3**-*R/S* microparticle dispersions in $BPy.NTf_2$ – see Figure 20a and 20b. Both dispersions showed an increased uptake compared to the dispersant alone. These results are shown in Table 5 below.

Disp. No.	Solid	Dispersant	Loading (wt%)	Average CH_4 Uptake, 298-303 K, 1 bar ($\mu mol/g_L$ unless otherwise stated)	Increase in uptake over base solvent ($\mu mol/g_L$)
1*	**CC3**-*R/S*	-	-	1064 ± 77 $\mu mol/g_S$	-
2	-	Silicone oil (5 cSt)	-	17.1 ± 1.4	-
3	**CC3**-*R/S* (9)	Silicone oil (5 cSt)	12.5	88.6	71
4	**CC3**-*R/S* (8)	Silicone oil (5 cSt)	20	121.7	104
5	-	BPy.NTf_2	-	7.9 ± 0.11	-
6	**CC3**-*R/S* (10)	BPy.NTf_2	5	36 ± 0.32	28
7	**CC3**-*R/S* (10)	BPy.NTf_2	12.5	71.3 ± 3.9	63
8	**CC3**-*R/S* (11)	BPy.NTf_2	20	103.1	95

*Average update measurements for **CC3**-*R/S* solid microparticles carried out on a Micromeritics (RTM) ASAP 2020 (CH_4, 298 K, 1 bar)

Table 5

[0076] In Table 6 below, the average CH_4 volumetric uptake measurement (1 bar, 298-303 K) on the different **CC3**-*R/S* microparticle dispersions was compared to the calculated theoretical maximum uptake for the dispersion based on the ratio of solid and liquid present in that dispersion, as described above.

Disp. No.	Solid	Dispersant	Loading (wt%)	Average dispersant uptake ($\mu mol/g_L$)	Average dispersion uptake ($\mu mol/g_L$)	Calculated uptake for dispersion ($\mu mol/g$)*	Percentage Porosity Obtained (%) (Measured vs Calculated)
1	**CC3**-*R/S* (9)	Silicone oil (5 cSt)	12.5	17	89	148	60
2	**CC3**-*R/S*	Silicone oil (5 cSt)	20	17	122	226	54

	(8)						
3	**CC3**-*R/S* (10)	$BPy.NTf_2$	5	7.9	36	61	59
4	**CC3**-*R/S* (10)	$BPy.NTf_2$	12.5	7.9	71	140	51
5	**CC3**-*R/S* (11)	$BPy.NTf_2$	20	7.9	103	219	47

*Calculated using the average CH_4 uptake in the solid **CC3**-*R/S* microparticles - 1064 $\mu mol/g_S$

Table 6

[0077] Overall, ~47-60% of the calculated theoretical porosity (CH_4) from the solid microparticles and liquid dispersant is maintained in the dispersions in silicone oil (5 cSt) and an ionic liquid ($BPy.NTf_2$). As observed for the CO_2 uptake, on increasing the microparticle dispersion from 12.5 wt% to 20 wt%, the percentage porosity maintained in the dispersion is comparable.

[0078] Recyclability of CO_2 uptake

[0079] The 12.5 wt% **CC3**-*R/S* microparticle (Example 9) dispersion in silicone oil (5 cSt) and the 12.5 wt% **CC3**-*R/S* microparticle in $BPy.NTf_2$ were also investigated for recyclability of CO_2 uptake (see Figures 17a, 18a, 17b and 18b), and the effect of aging on CO_2 uptake (Figures 19a and 19b). For the 12.5 wt% **CC3**-*R/S* microparticle (Example 9) dispersion in silicone oil (5 cSt), two separate samples had sorption measurements repeated over 2 days with a short vacuum degas (He pump down = 60 min) between each measurement. Both samples, and their repeats, showed similar isotherms (Figure 17a) and uptakes at 1 bar (Figure 18a), demonstrating both the ease of removal of gas from the porous liquid, and the recyclability of gas uptake. For the 12.5 wt% **CC3**-*R/S* microparticle (Example 11) dispersion in $BPy.NTf_2$, sorption measurements were only performed on a single

sample but repeated 7 times, with a thorough overnight degas between each measurement. Corresponding isotherms and uptakes at 1 bar are shown in Figure 17b and Figure 18b respectively.

[0080] Figures 19a and 19b then show CO_2 uptake isotherms for aged samples (24 days or 30 days) of 12.5 wt% **CC3**-*R/S* microparticles (Example 9) in silicone oil (5 cSt) and 12.5 wt% **CC3**-*R/S* microparticles (Example 11) in BPy.NTf_2, respectively. These show that the dispersions are still porous after ageing at ambient temperature under normal atmospheric conditions. For the dispersion in silicone oil (5 cSt), the uptake on day 1 = 178 μmol/g_L, compared to uptake on day 24 = 207 μmol/g_L (298-303 K, 1 bar). For the dispersion in BPy.NTf_2, the uptake on day 1 = 170 μmol/g_L, compared to day 30 = 172 μmol/g_L

[0081] Visual stability of dispersions

[0082] Table 7 below shows data on the visual stability of a selection of dispersions after being left to stand at ambient (or room) temperature for one day. A tick indicates that the dispersion was visibly stable, a cross that it wasn't, and a dash if the sample was not tested. Apart from the 12.5 wt% control dispersion in silicone oil (5 cSt), which rapidly settled, the dispersions were visually stable on standing for 1 day. All samples also appeared to be dispersed when stirring was maintained, for example, during the degassing and adsorption studies.

	Silicone Oil 5 cSt	Silicone Oil AR 20	Olive Oil	Sunflower Oil	Paraffin Oil	Halocarbon 27 (RTM)	Fomblin Y (RTM)	Genesorb 1753 (RTM)	BMIM .NTf_2	15-crown-5	BPy.NTf_2
Control	×	-	-	-	-	-	-	-	-	-	×
12.5 wt% CC3-*S*	✓	-	-	-	-	-	-	-	-	-	-
12.5 wt% CC3-*R/S* (9)	✓	✓	✓	✓	✓	-	-	✓	✓	✓	-
20 wt% CC3-*R/S* (8)	✓	-	-	-	-	-	-	-	-	-	-
12.5 wt% CC3-*R/S* (5)	✓	-	-	-	-	-	-	-	-	-	-
12.5 wt% CC3-*R/S* (6)	✓	-	-	-	-	-	-	-	-	-	-
5 wt% CC3-*R/S* (9)	-	-	-	-	-	✓	✓	-	-	-	-
5 wt% CC3-*R/S* (10)	-	-	-	-	-	-	-	-	-	-	✓
12.5 wt% CC3-*R/S*	-	-	-	-	-	-	-	-	-	-	✓

(10)											
20 wt% CC3-*R*/*S* (11)	-	-	-	-	-	-	-	-	-	-	✓
10 wt% **CC19**-*R*	✓	-	-	-	-	-	-	-	-	-	-
10 wt% **CC3**-*R*	✓	-	-	-	-	-	-	-	-	-	-
10 wt% **CC15**-*R*	✓	-	-	-	-	-	-	-	-	-	-
10 wt% **TCC2**-*R*	✓	-	-	-	-	-	-	-	-	-	-

Table 7

[0083] Representative characterisation of 12.5 wt% **CC3**-*R/S* microparticle dispersion in silicone oil (5 cSt, PDMS)

[0084] This dispersion was characterized using FTIR (see Figure 9), PXRD (see Figure 10) and DLS (see Figure 11).

[0085] Figure 9 shows, from top to bottom, stacked FTIR spectra of solid **CC3**-*R/S* microparticles (Example 7), the 12.5 wt% **CC3**-*R/S* microparticle dispersion in silicone oil (5 cSt) and silicone oil (5 cSt).

[0086] In relation to Figure 10, the powder X-ray diffraction data was collected using a Panalytical (RTM) Empyrean diffractometer producing Cu-*Kα* radiation and equipped with an X-ray focusing mirror, PIXcel 3D detector, and capillary spinner. X-ray diffraction data was collected in transmission geometry over the 2θ range, 2-50 (°). Samples were contained in 0.7 mm borosilicate glass capillaries that were spun to improve powder averaging. To improve peak shape, 0.02 mm Soller slits, and 1/2° anti scatter slits were used during data collections.

[0087] In Figure 10, the bottom graph shows powder X-ray diffraction data for solid **CC3**-*R/S* microparticles (Example 7) prepared according to the scale-up procedure. The top graph shows powder X-ray diffraction data for **CC3**-*R/S* microparticles dispersed in silicone oil (PDMS, 5 cSt) at 12.5 wt%.

[0088] Figure 11 is a comparison of particle size and distribution of **CC3**-*R/S* microparticles (Example 9) dispersed in dichloromethane, in silicone oil taken from the 12.5 wt% dispersion at T = 1 day, and in silicone oil taken from the 12.5 wt% dispersion at T = 24 days. Sizes in silicone oil (5 cSt) were based on the measured refractive index – 1.397, with the latter samples prepared by taking a small aliquot from the dispersion and diluting in silicone oil (5 cSt).

[0089] The DLS measurements in Figure 11 show an increase in particle size after the dispersion is left for 24 days, from a z-average of 1206 nm on day 1 (comparable to when the microparticles are dispersed in dichloromethane) to 1573 nm on day 24, which could be due to either aggregation or swelling. However, the aged dispersion still demonstrates the same porosity as a newly formed sample (see Figure 19).

[0090] Thermal stability

[0091] Thermogravimetric analysis (TGA) of the **CC3**-*R/S* solid microparticles, silicone oil (5 cSt) or BPy.NTf_2, and the 12.5 wt% dispersions of **CC3**-*R/S* microparticles in silicone oil (5 cSt) or BPy.NTf_2 were carried out. This data is shown in Figures 12a and 12b. TGA was performed using a Q5000IR analyser (TA instruments) with an automated vertical overhead thermobalance. The samples were heated in platinum pans under nitrogen at a rate of 20 °C/min from ambient (room) temperature to 500 °C or 600 °C, either under air or nitrogen.

[0092] The cage microparticles are stable to a temperature of 310 °C under air, and to 400 °C under nitrogen, before thermal degradation occurs. Whilst the literature boiling point of silicone oil (5 cSt) is reported as >140 °C at 0.002 mmHg (supplier – Sigma Aldrich), under a flow of air the silicone oil is lost from 60 °C, with no sample remaining at 310 °C. In the dispersion once the silicone oil has been lost, approximately 12.5 wt% mass is remaining due to the presence of the cage. The ionic liquid, BPy.NTf_2, was thermally stable until 325 °C under a nitrogen flow. The 5 wt%, 12.5 wt%, 20 wt% dispersions of **CC3**-*R/S* microparticles in BPy.NTf_2 also remained unaffected at 325 °C. There were small differences in the TG curve patterns between pure BPy.NTf_2 and the corresponding dispersions. The curve showed a gradual decrease around the decomposing temperature for BPy.NTf_2, with a steeper drop-off around the decomposition temperature for the 12.5 wt% and 20 wt% dispersions, and increasing mass remained in accordance with the increasing loadings of **CC3**-*R/S* microparticles in the 5 wt%, 12.5 wt%, 20 wt% dispersions.

[0093] Long-term stability

[0094] A series of samples were then studied for long term dispersion stability using a LUMiSizer (RTM) 6512-48 at 25 °C with a wavelength of 865 nm, in disposable sample cells (2 mm, rectangular synthetic cell 110-131 mm), with 700 x 30 (or 1000 x 21) second intervals measured and a total run time of 350 min – see Figures 21a-h. This allows accelerated testing to determine the stability of dispersions (e.g. does sedimentation or creaming occur), and what the sedimentation velocity (V, μm/s) of the particles is at a relative centrifugal force (RCF - calculated using the size of the

centrifuge and rpm), which can be then be converted to a sedimentation velocity at gravity, assuming Newtonian sample behaviour – see Table 8 below. RCF is calculated as follows:

$$RCF = \left(\frac{RPM}{1000}\right)^2 \times r \times 1.118$$

where RCF = relative centrifugal force, RPM = revolutions per minute, and r = centrifugal radius in mm.

Disp. No.	Solid	Dispersant	Loading (wt%)	RPM	Stability	Miniscus (mm)	Bottom of sample (mm)	RCF at midpoint	Average V at RCF (μm/s)	Average V at gravity (μm/s)	Average V at gravity (mm/day)
1	**CC3**-*R/S* (9)	Silicone oil (5 cSt)	12.5	2000	Creaming	107	130	530	1.454	2.744×10^{-3}	0.24
2	**CC3**-*R*	Silicone oil (5 cSt)	12.5	2000	Sedimentation	109	130	534	0.543	1.017×10^{-3}	0.09
3	**CC3**-*R/S* (9)	Silicone Oil AR 20	12.5	2000	Creaming	107	130	530	0.367	6.918×10^{-4}	0.06
4	**CC3**-*R/S* (9)	Olive oil	12.5	2000	Sedimentation	111	130	539	0.304	5.634×10^{-4}	0.05
5	**CC3**-*R/S* (9)	Fomblin Y (RTM)	5	2000	Creaming	108	130	532	3.881	7.293×10^{-3}	0.63
6	**CC3**-*R/S* (9)	Halocarbon 27 (RTM)	5	2000	Creaming	108	130	532	0.441	8.287×10^{-4}	0.07
7	**CC3**-*R/S* (11)	$BPy.NTf_2$	5	2000	Creaming	108	130	532	0.830	1.560×10^{-3}	0.12
8	**CC3**-*R/S* (11)	$BPy.NTf_2$	12.5	2000	Creaming	108	130	532	0.255	4.799×10^{-4}	0.04

Table 8

[0095] By using the same batch of microparticles (9) with different dispersants, and running the stability tests at the same RPM, it is possible to directly compare the stability of the dispersions and the effect of changing the liquid component. Depending on the dispersant used, the stability varied in terms of the sedimentation velocity (V), and whether the dispersion creams (particles go to the top of the sample) or sediments (particles go to the bottom of the sample). If long-term stability is of interest for a particular application, it is possible to design a more stable dispersion of microparticles whilst maintaining a similar level of porosity. For example, for 12.5 wt% **CC3**-*R/S* (Example 9) dispersions in silicone oils a similar uptake is achieved in silicone oil (5 cSt) and Silicone Oil AR 20 (CO_2 = 198.0 ± 3.8, and 181.8 ± 3.8, respectively, see Table 3), but the dispersion is more stable using the latter (V (mm/day) = 0.24 and 0.06 respectively, see Table 8). Further, the oil can be substituted for an ionic liquid (BPy.NTf_2), which has a comparable stability but a lower vapour pressure.

[0096] The Lumisizer (RTM) images obtained for the samples in Table 8 are shown in Figures 21a-h. In Figures 21a, 21c, 21e, 21f, 21g and 21h, propagation from right to left indicates creaming. In Figures 21b and 21d, propagation from left to right indicates sedimentation.

Claims

1. A dispersion of porous particles comprising organic cage molecules, the porous particles being dispersed in a liquid phase, wherein the liquid is selected from the group consisting of liquid oligomers, size-excluded liquids, ionic liquids, liquid polymers, silicone oils, halogenated oils, paraffin oils, petroleum oils, triglyceride oils and combinations thereof.

2. A dispersion as claimed in claim 1, wherein the porous particles have a mean diameter in the range 0.1-100 μm.

3. A dispersion as claimed in either claim 1 or claim 2, wherein the porous particles comprising the organic cage molecules comprise co-crystals of either the same organic cage molecule in two chiral forms, or two or more different organic cage molecules.

4. A dispersion as claimed in claim 3, wherein the porous particles comprising the organic cage molecules comprise co-crystals of **CC3**-*R* and **CC3**-*S*.

5. A dispersion as claimed in either claim 1 or claim 2, wherein the porous particles comprising the organic cage molecules comprise at least 90 wt% of a single chiral form, or enantiomer, of the organic cage molecule.

6. A dispersion as claimed in claim 5, wherein the porous particles comprising the organic cage molecule comprise **CC3**-*S*, **CC15**-*R*, **CC19**-*R* or **TCC2**-*R*.

7. A dispersion as claimed in any one of the preceding claims wherein the liquid is selected from the group consisting of silicone oils, halogenated oils, triglyceride oils, paraffin, oils, ionic liquids and size-excluded liquids.

8. A dispersion as claimed in claim 7, wherein the silicone oil is selected from the group consisting of silicone oil 5 cSt, silicone oil 50 cSt and silicone oil AR 20.

9. A dispersion as claimed in claim 7, wherein the ionic liquid is 1-butyl-3-methylimidazolium bis(trifluoromethylsulfonyl)imide), 1-butylpyridinium

bis(trifluoromethanesulfonyl)imide, trihexyltetradecylphosphonium bis(trifluoromethanesulfonyl)imide or benzyl(ethyl)dimethylammonium bis(trifluoromethanesulfonyl)imide.

10. A dispersion as claimed in claim 7, wherein the size-excluded liquid is 1-^{t}butyl-3,5-dimethylbenzene or 15-crown-5.

11. A dispersion as claimed in any one of the preceding claims comprising 0.1-50 wt% of the porous particles.

12. A dispersion as claimed in claim 11 comprising 1-20 wt% of the porous particles.

13. A method of adsorbing a gas into a liquid, comprising at least the step of bringing the gas into contact with a dispersion as claimed in any one of the preceding claims.

14. A method of adsorbing a gas into a liquid as claimed in claim 13, wherein the gas is selected from the group consisting of CO_2, CH_4, N_2, C_2H_4, C_2H_6, Xe, SF_6, C_3H_8 or H_2.

15. A method for preparing a dispersion as claimed in any one of claims 1-12, comprising at least the step of:

mixing (i) porous particles comprising an organic cage molecule, and (ii) a liquid selected from the group consisting of liquid oligomers, size-excluded liquids, ionic liquids, liquid polymers, silicone oils, halogenated oils, paraffin oils, petroleum oils, triglyceride oils and combinations thereof.

16. An assemblage of a dispersion as claimed in any one of claims 1-12, the organic cage molecule comprising a cavity and a gas contained within the cavity.

17. An assemblage as claimed in claim 16, wherein the gas is selected from the group consisting of CO_2, CH_4, N_2, C_2H_4, C_2H_6, Xe, SF_6, C_3H_8 or H_2.

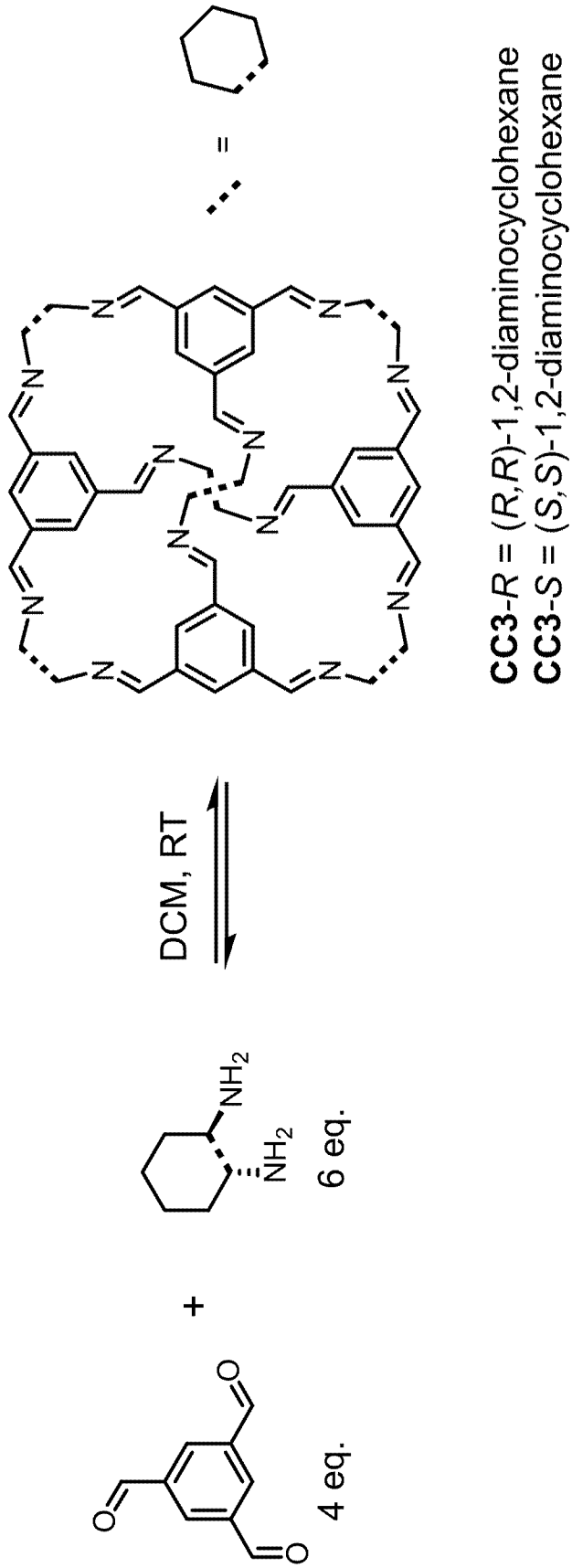

CC3-*R* = (*R*,*R*)-1,2-diaminocyclohexane
CC3-*S* = (*S*,*S*)-1,2-diaminocyclohexane

Figure 1

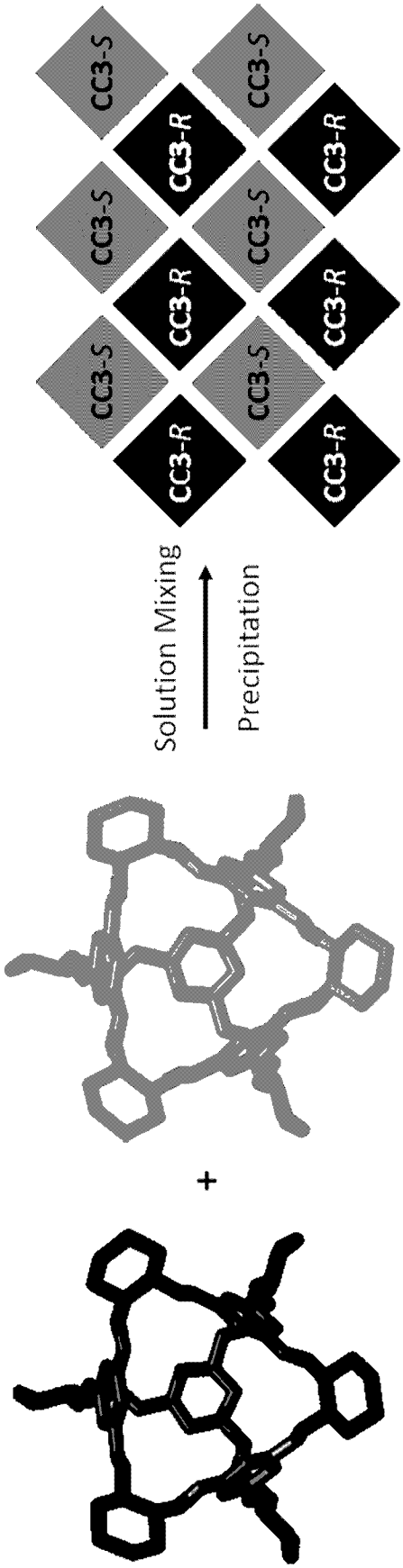
CC3-S
CC3-R
CC3-S
CC3-R
CC3-S
CC3-R
CC3-S
CC3-R
CC3-S
CC3-R
CC3-S
CC3-R
Solution Mixing
Precipitation
CC3-S
+
CC3-R

Figure 2

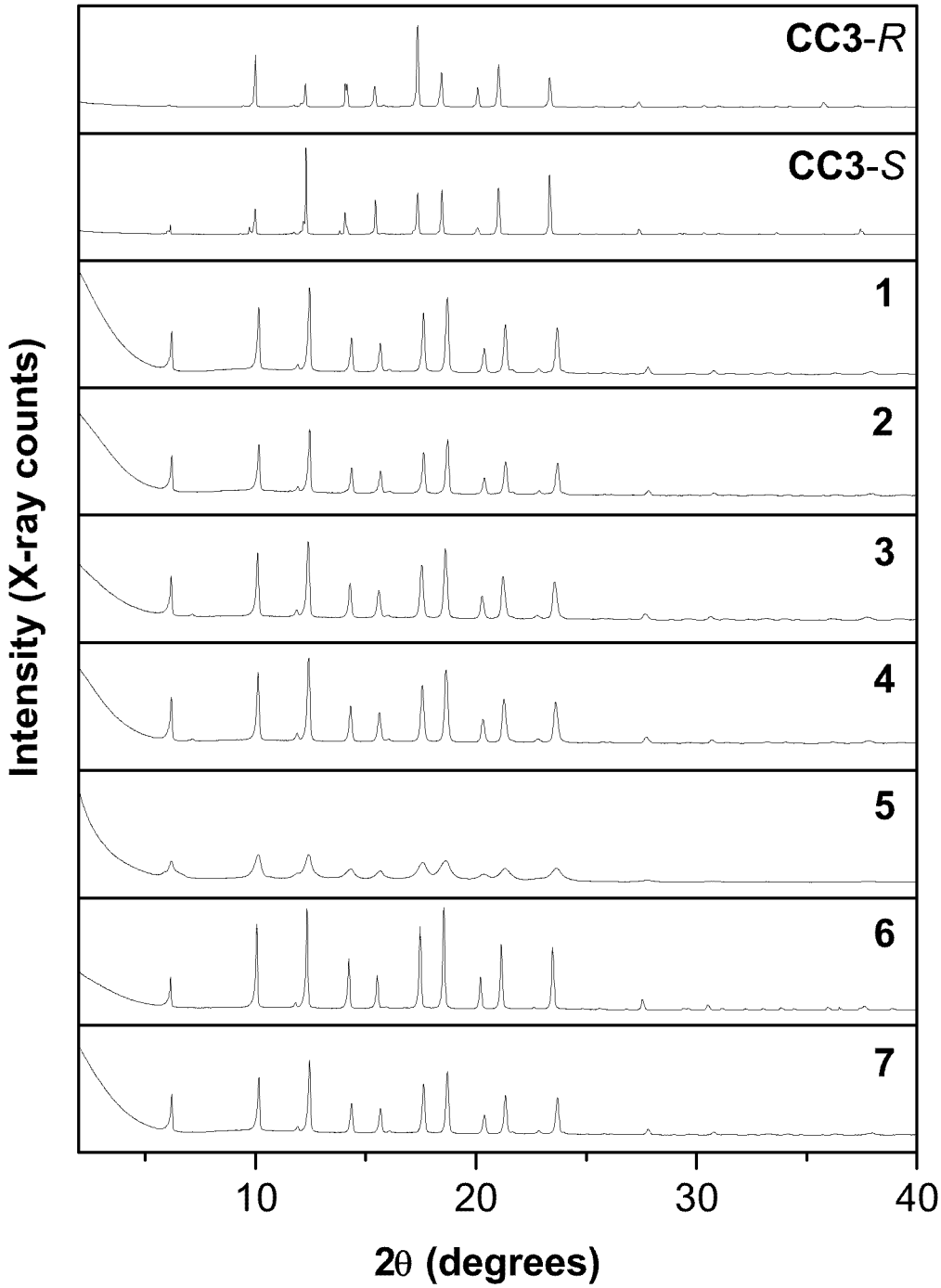
CC3-R
CC3-S
1
2
3
4
5
6
7
Intensity (X-ray counts)
10
20
30
40
2θ (degrees)

Figure 3

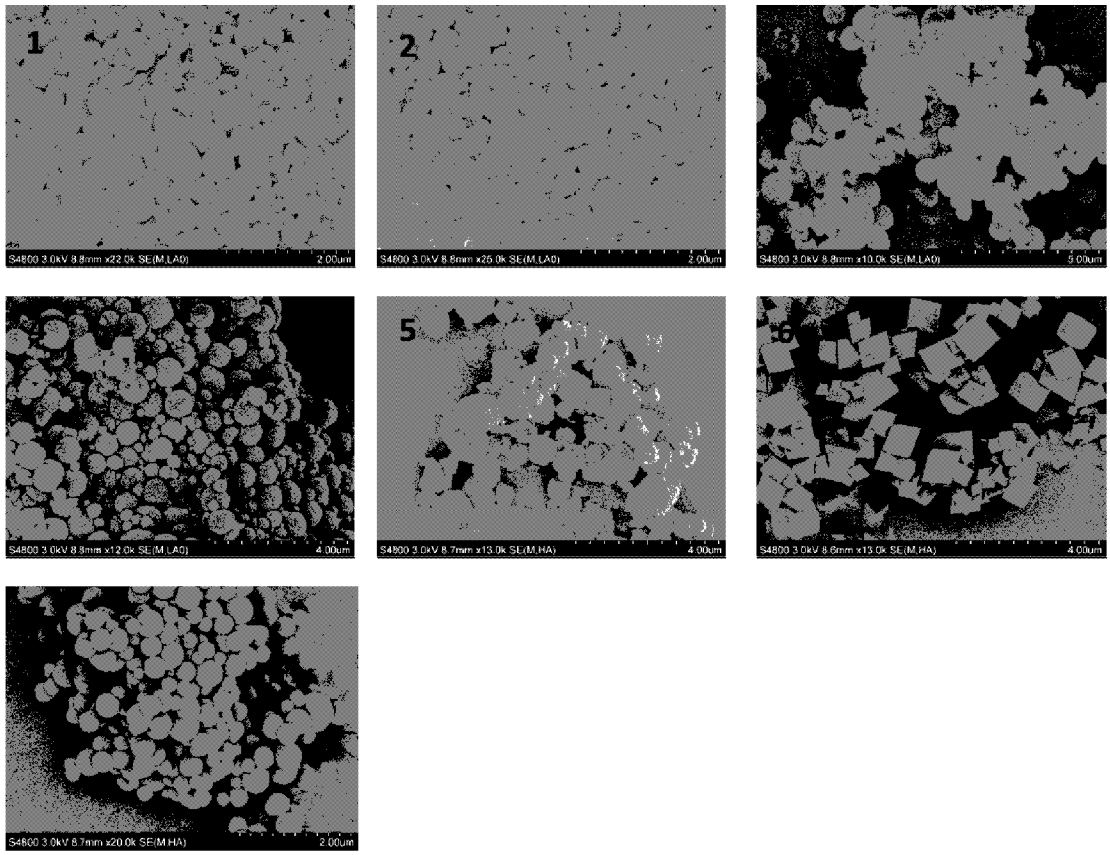

Figure 4

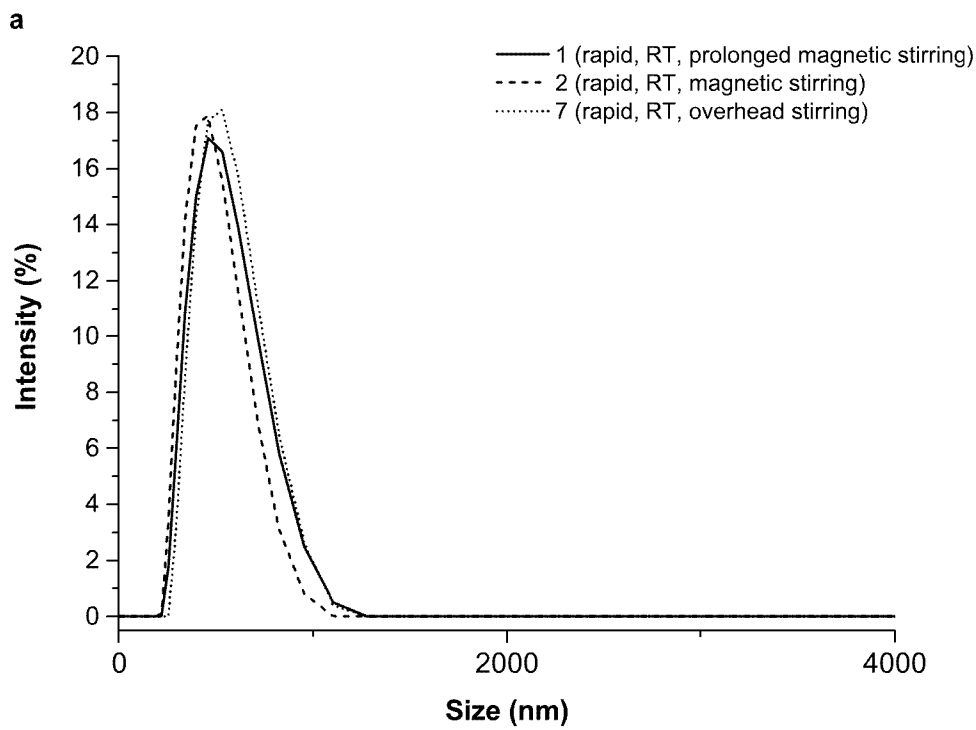

Figure 5a

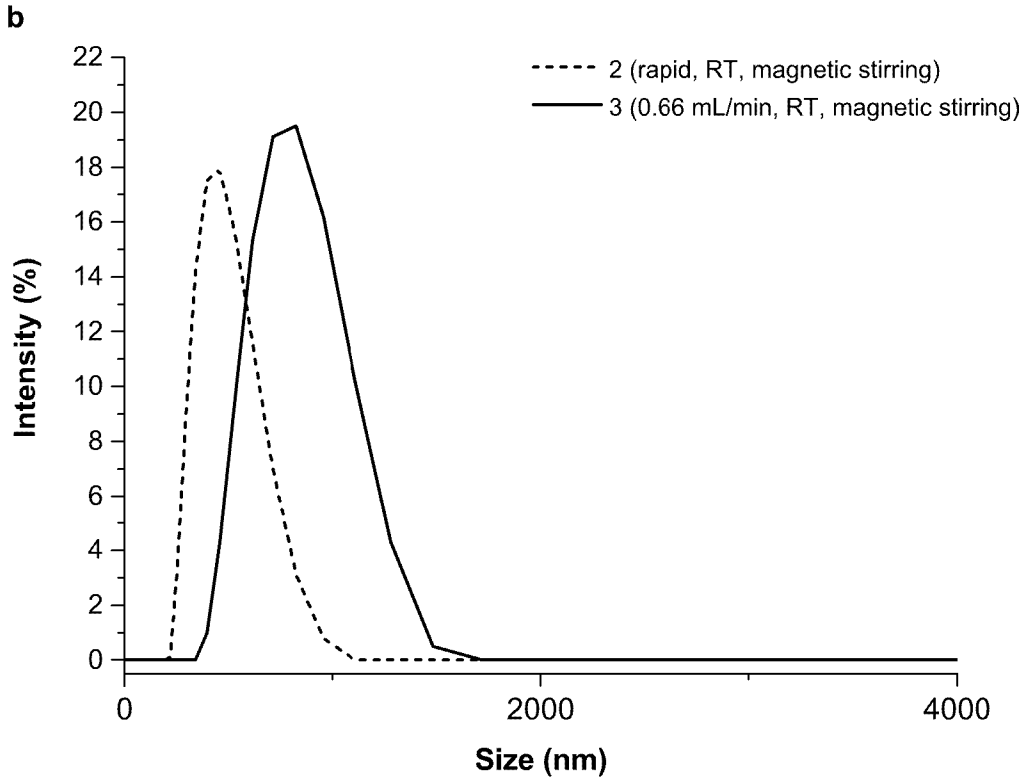

Figure 5b

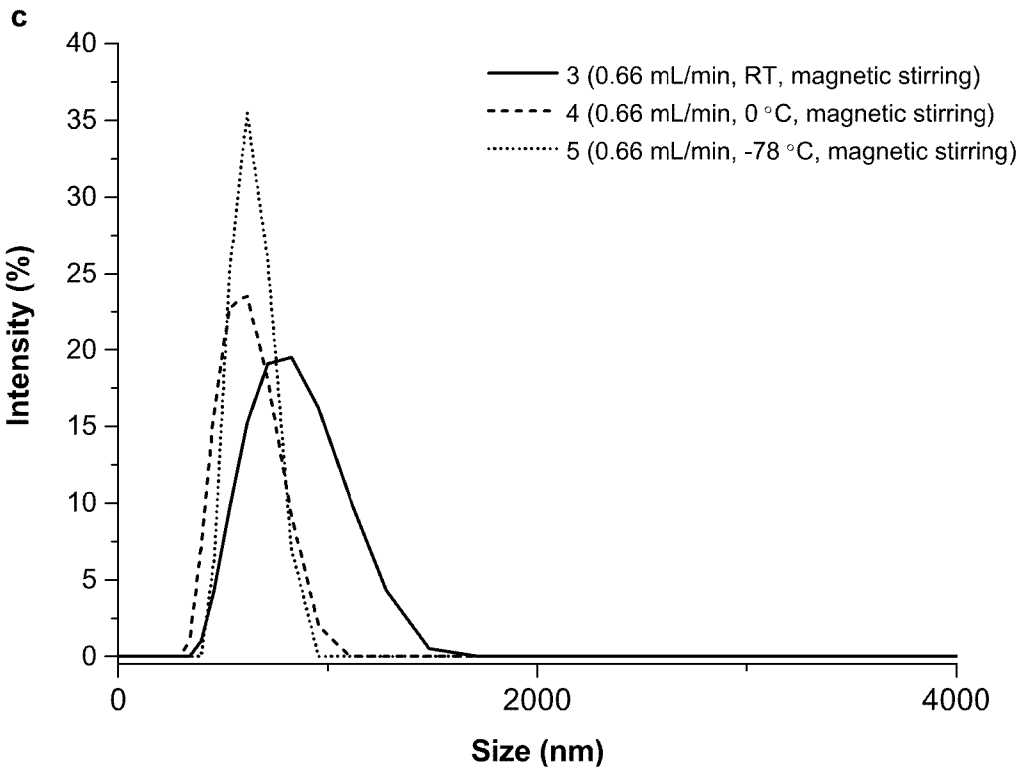

Figure 5c

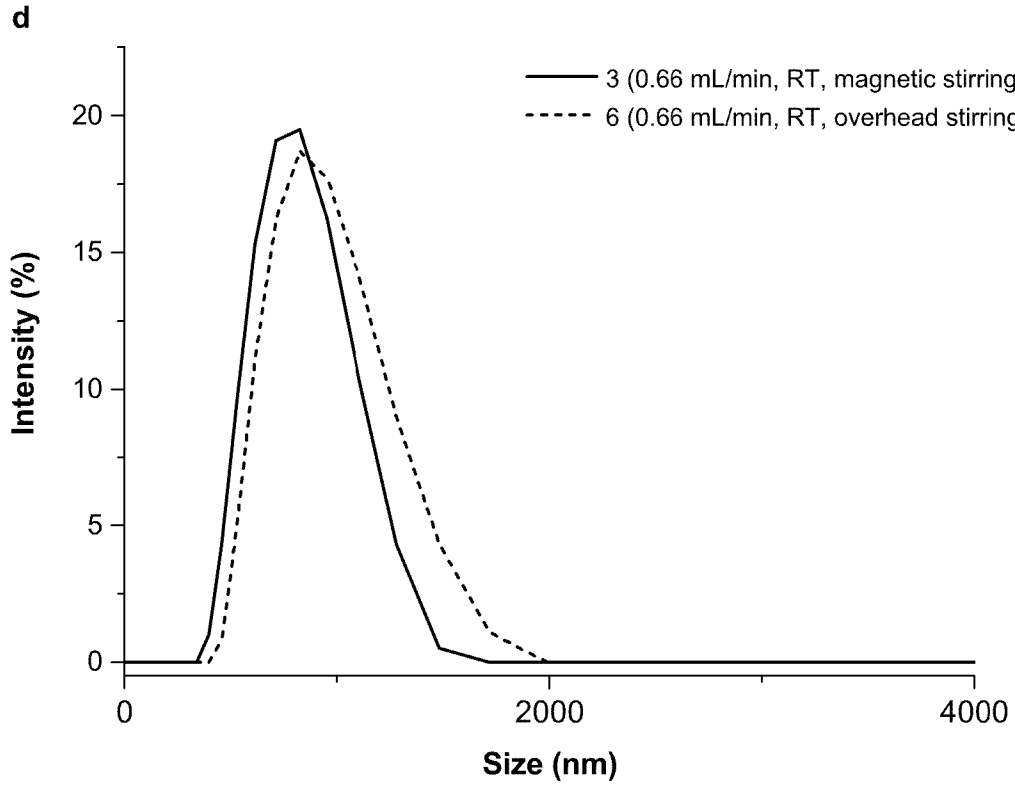
d
3 (0.66 mL/min, RT, magnetic stirring)
6 (0.66 mL/min, RT, overhead stirring)
Intensity (%)
20
15
10
5
0
0
2000
4000
Size (nm)

Figure 5d

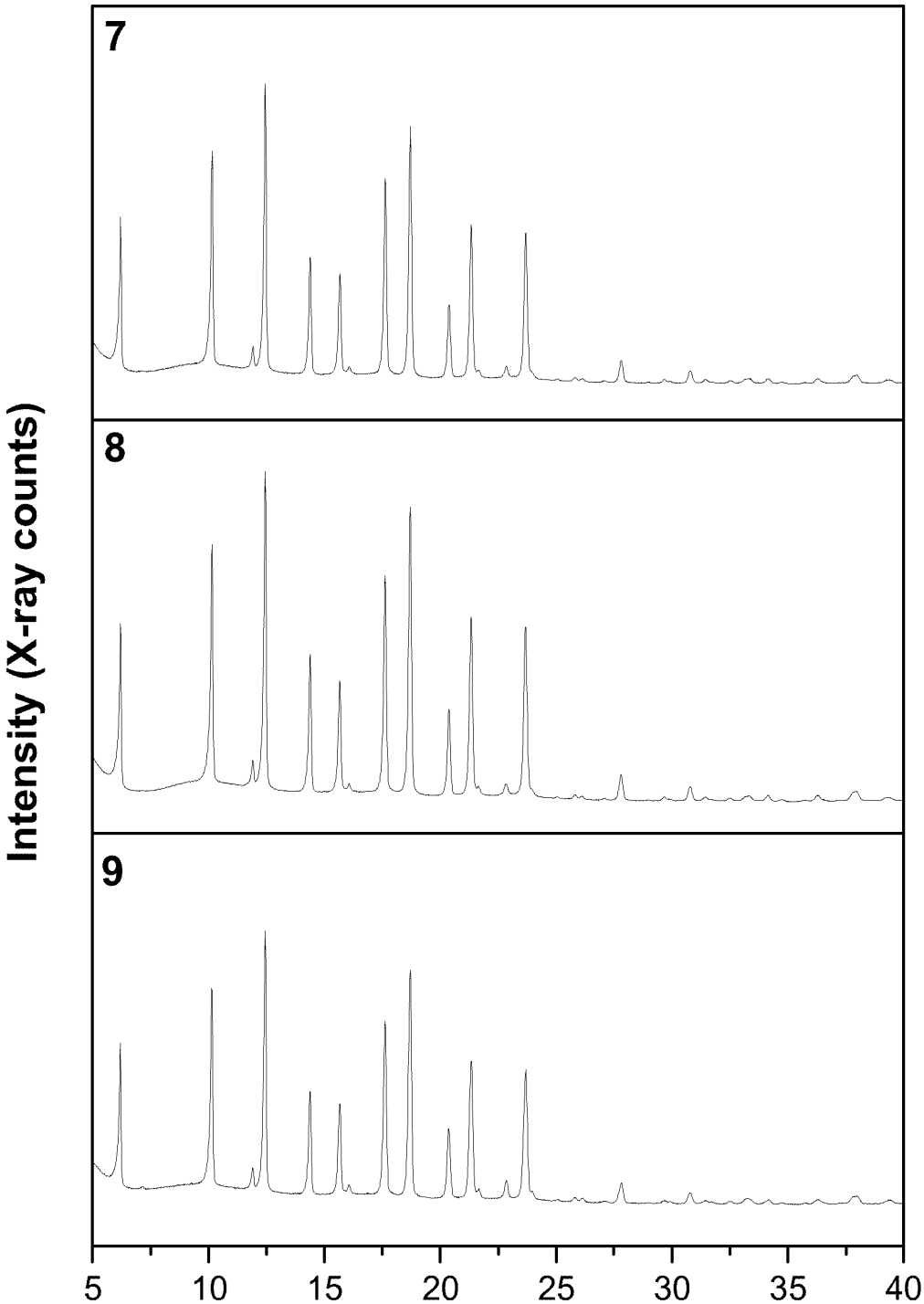

Figure 5e

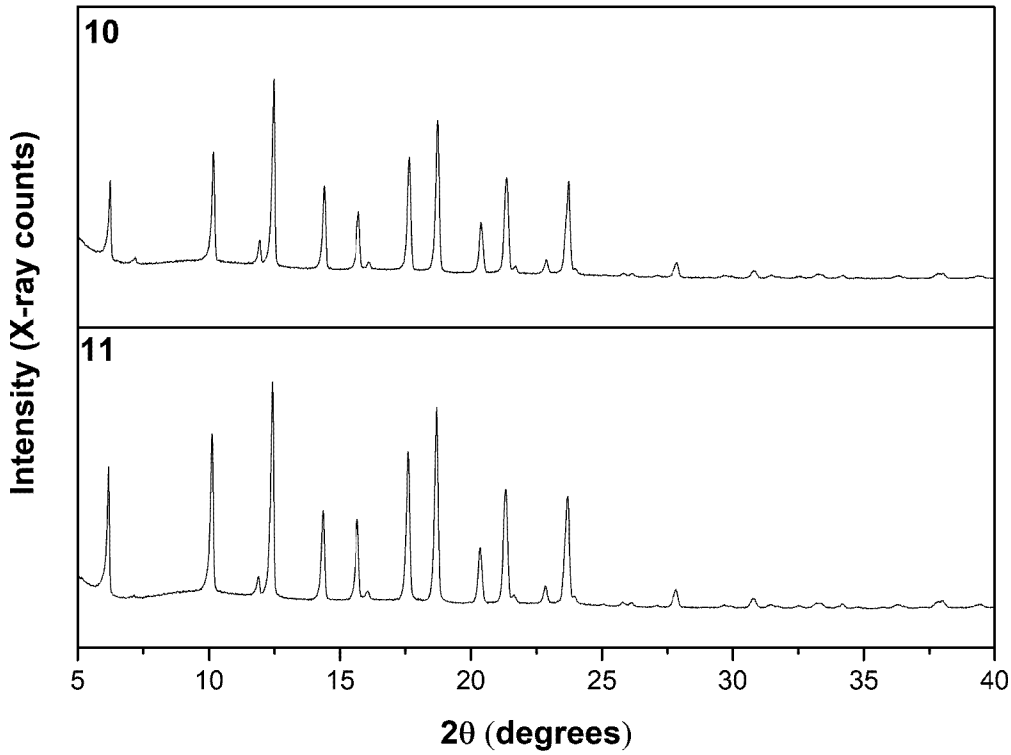

Figure 5e ctd

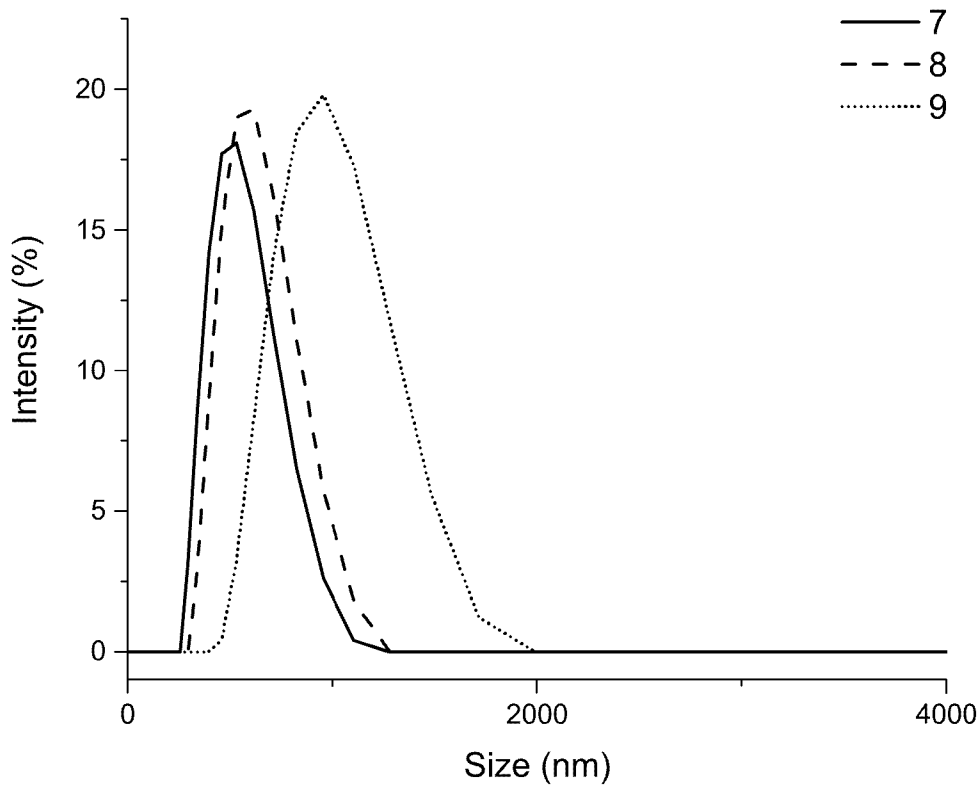

Figure 5f

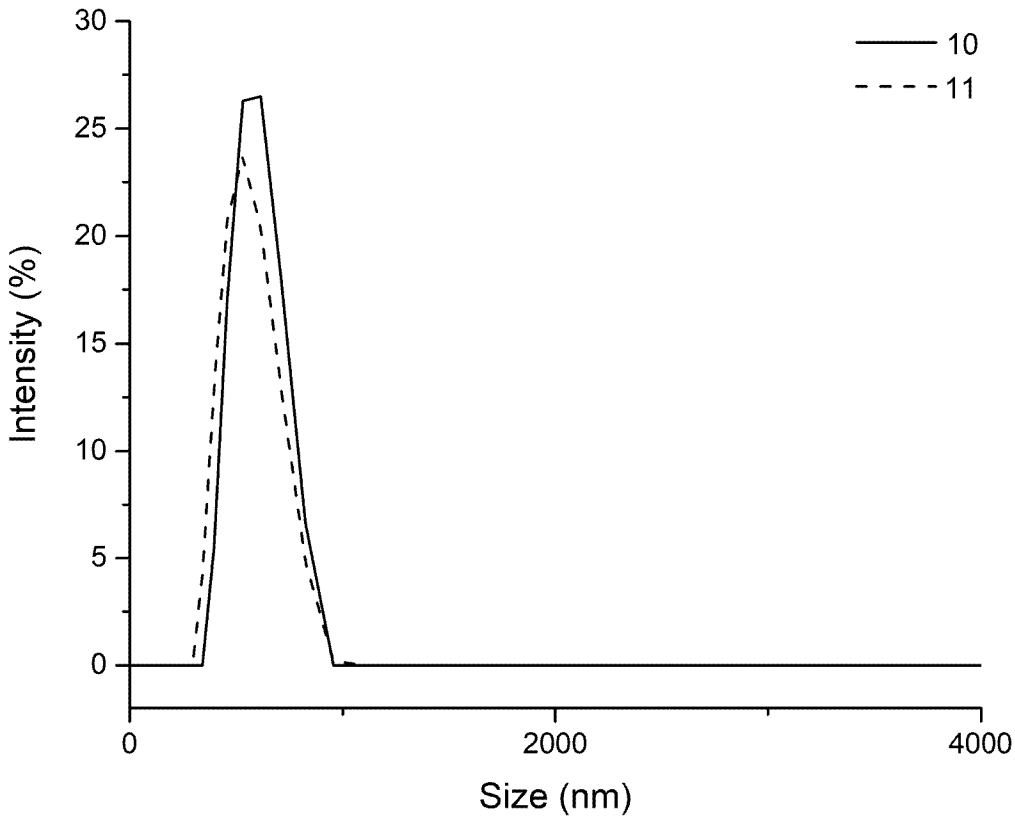

Figure 5g

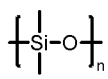

Silicone oil (PDMS)
5 cSt - Sigma Aldrich, 317667
50 cSt - Sigma Aldrich, 378356

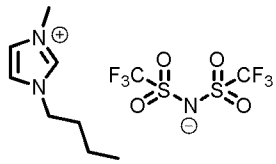

Ionic Liquid (1-butyl-3-methylimidazolium bis(trifluoromethylsulfonyl) imide - BMIM.NTf$_2$
Sigma Aldrich, 711713

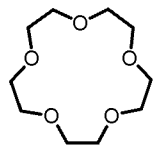

Size-excluded Solvent (15-crown-5)
Sigma Aldrich, 188832

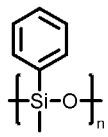

Silicone oil AR 20
~20 cSt - Sigma Aldrich, 10836

Halocarbon 27 (RTM)
Sigma Aldrich, H8773

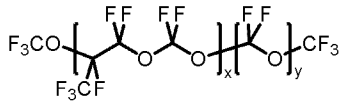

Fomblin Y (RTM)
Sigma Aldrich, 317926

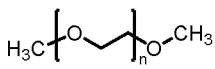

Genesorb 1753 (RTM) (polyethylene glycol dimethyl ethers)

Paraffin Oil
Sigma Aldrich, 18512

Olive oil
Sigma Aldrich, O1514

Sunflower oil
Sigma Aldrich, 88921

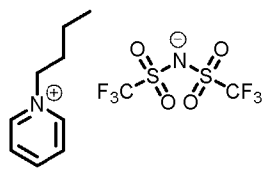

Ionic Liquid 1-butylpyridinium bis(trifluoromethylsulfonyl) imide - BPy.NTf$_2$
TCI, B5571

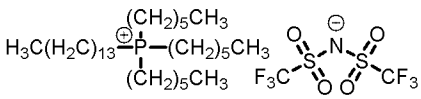

Ionic Liquid trihexyltetradecylphosphonium bis(trifluoromethanesulfonyl)imide - P$_{66614}$.NTf$_2$
Sigma Aldrich, 50971

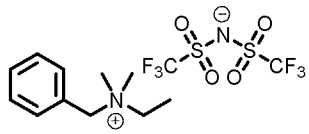

Ionic Liquid benzyl(ethyl)dimethyl ammonium bis(trifluoro-methanesulfonyl)imide - BEMA.NTf$_2$
TCI, B5427

Figure 6

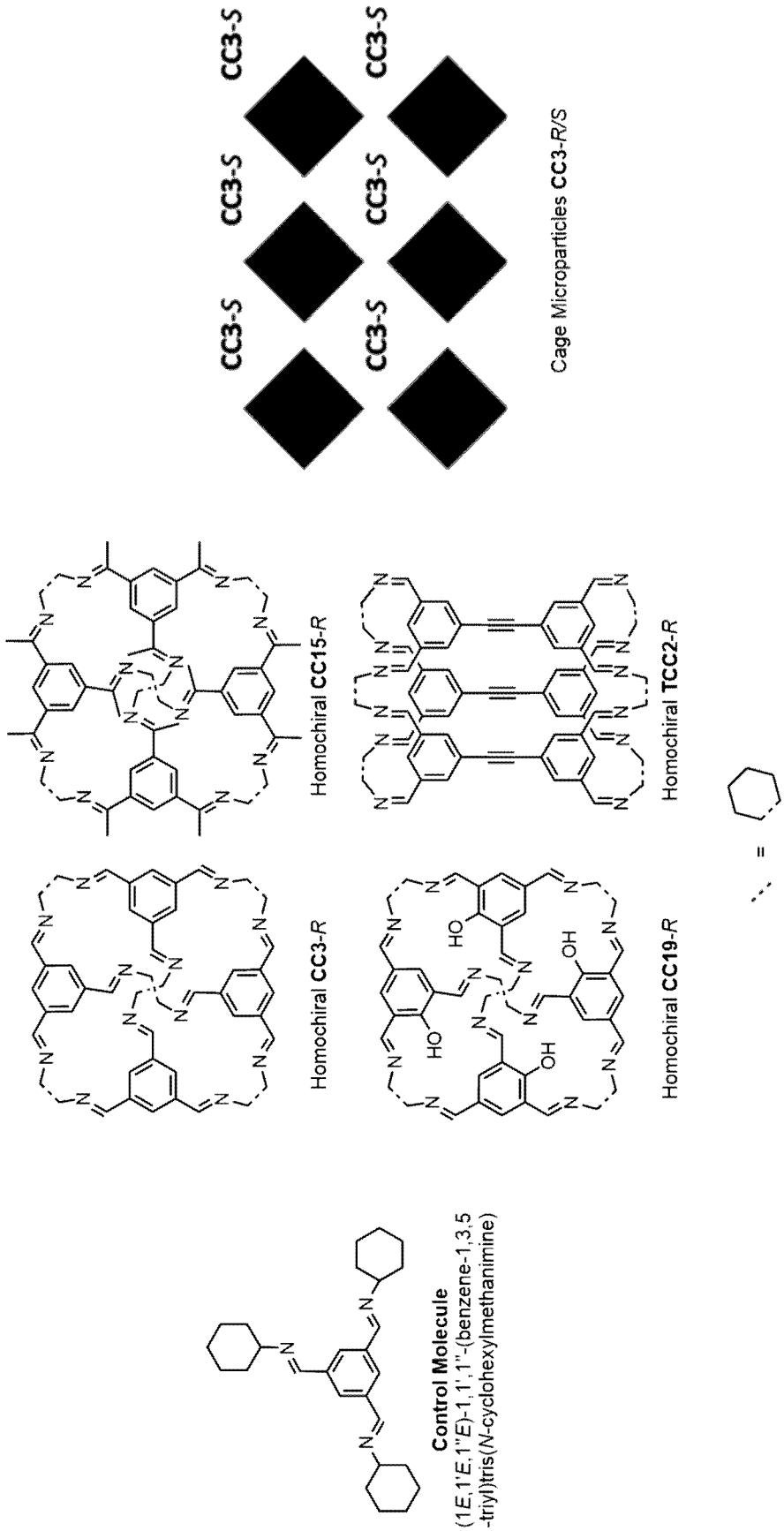
CC3-S
CC3-S
CC3-S
CC3-S
CC3-S
CC3-S
Cage Microparticles CC3-R/S
Homochiral CC15-R
Homochiral TCC2-R
Homochiral CC3-R
Homochiral CC19-R
=
Control Molecule
(1E,1'E,1''E)-1,1',1''-(benzene-1,3,5-triyl)tris(N-cyclohexylmethanimine)

Figure 7

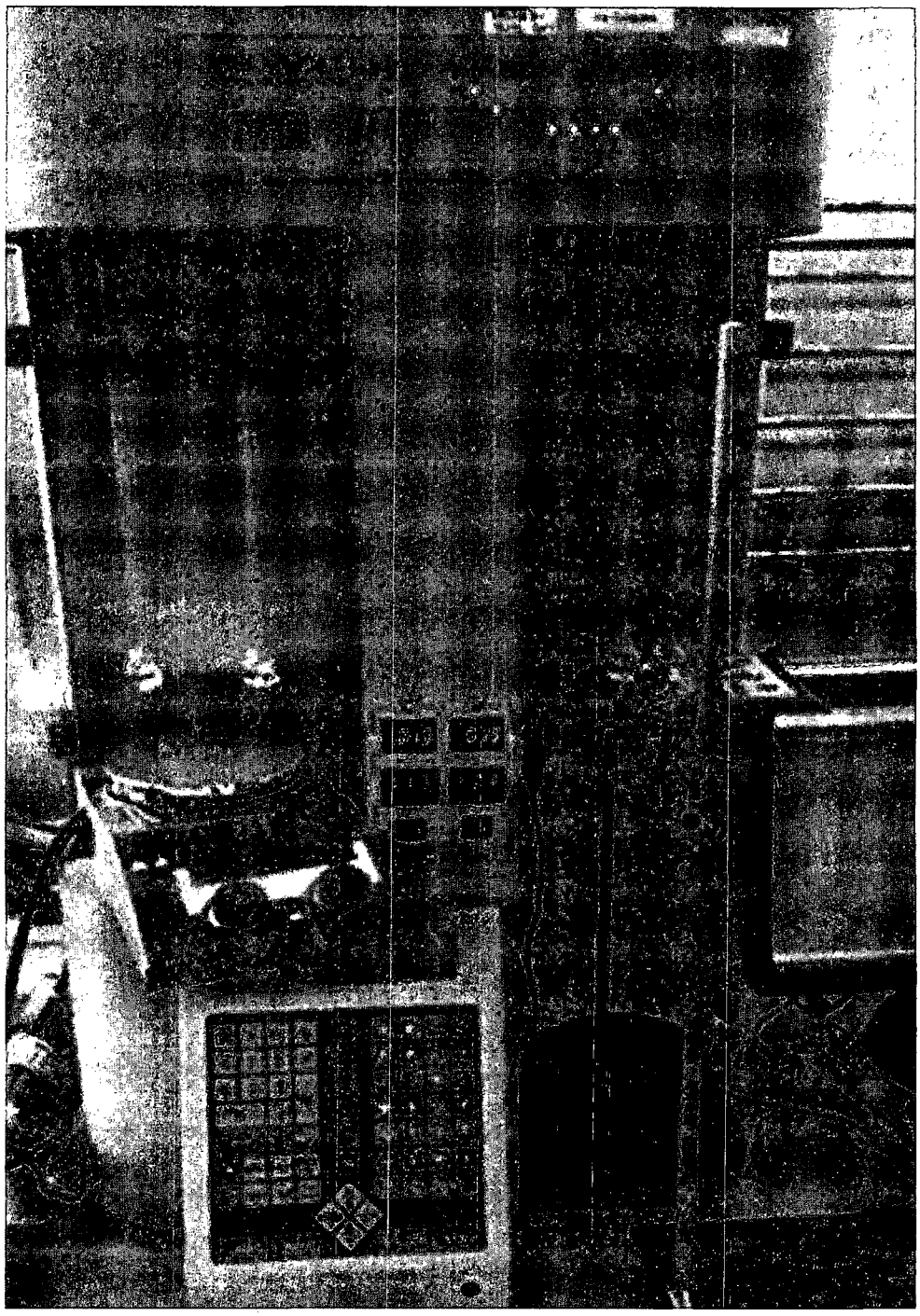

Figure 8

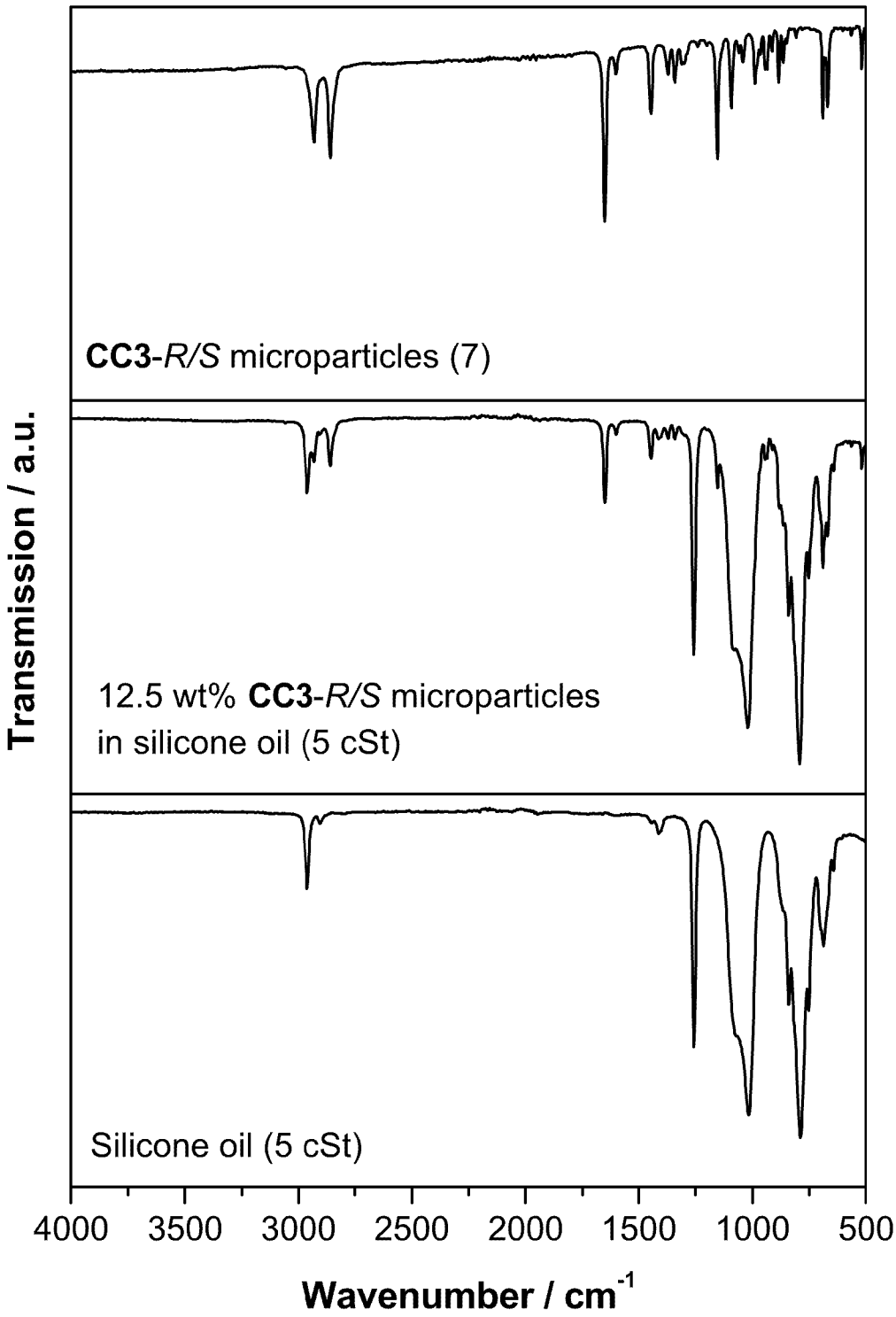
CC3-R/S microparticles (7)
12.5 wt% CC3-R/S microparticles
in silicone oil (5 cSt)
Silicone oil (5 cSt)
Transmission / a.u.
4000
3500
3000
2500
2000
1500
1000
500
Wavenumber / cm-1

Figure 9

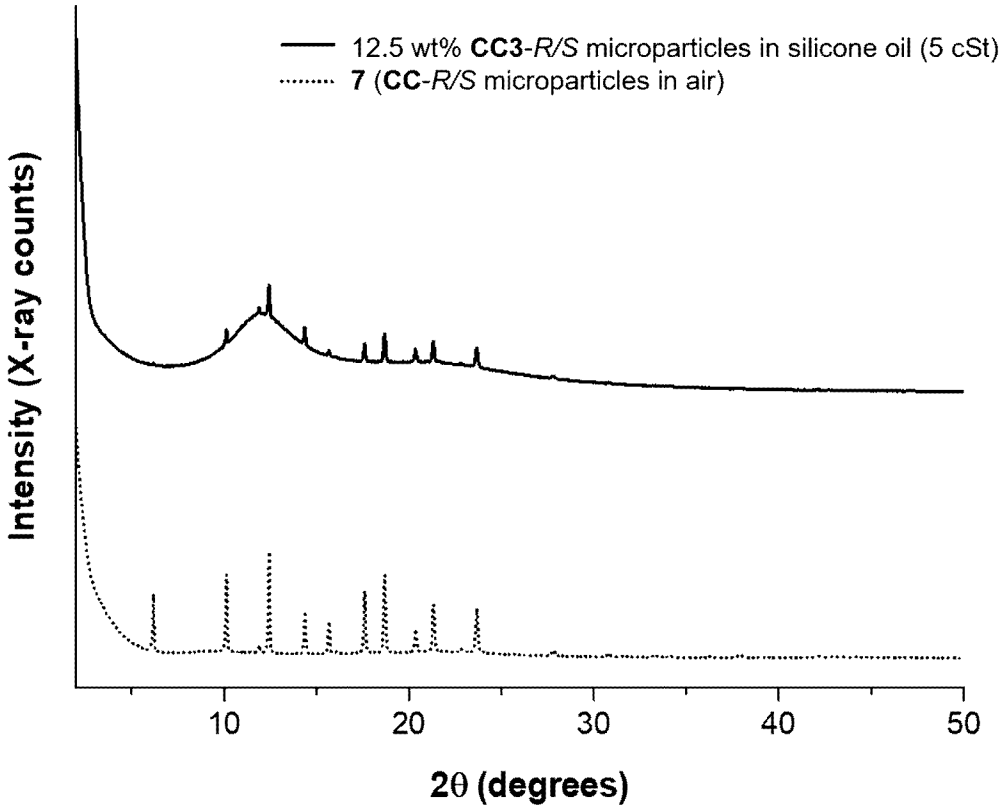

Figure 10

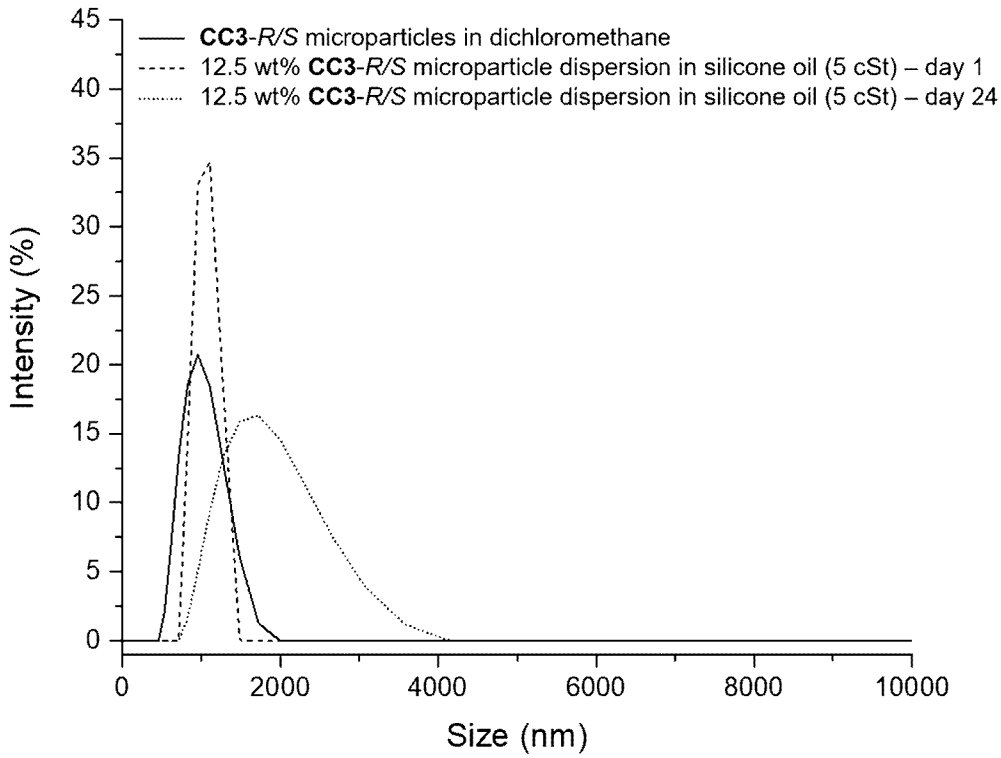

Figure 11

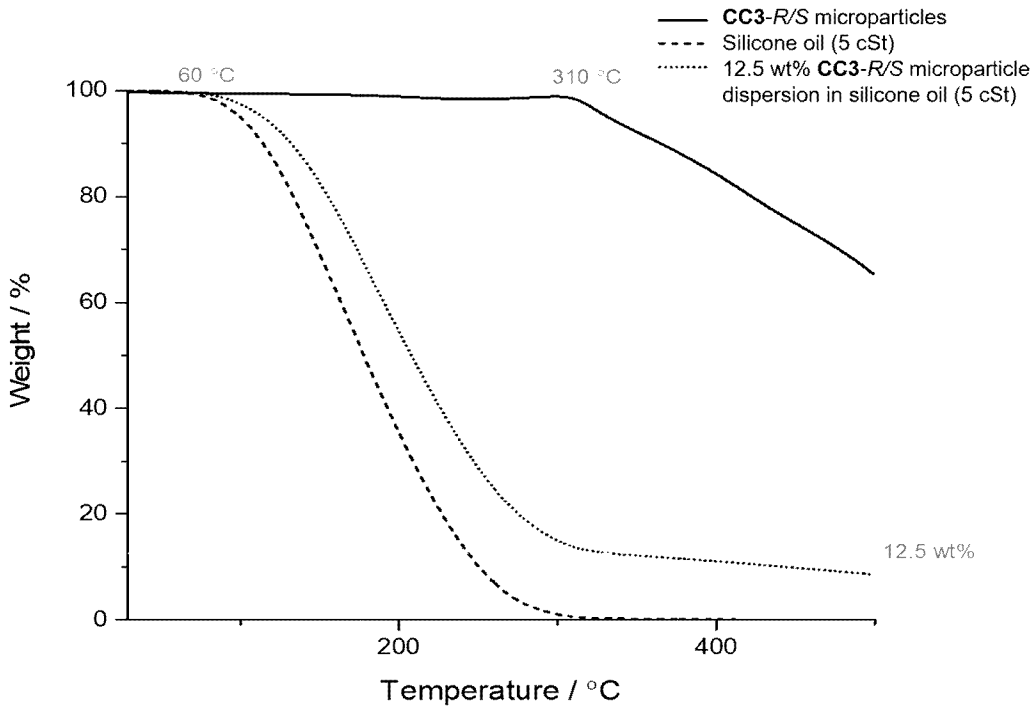

Figure 12a

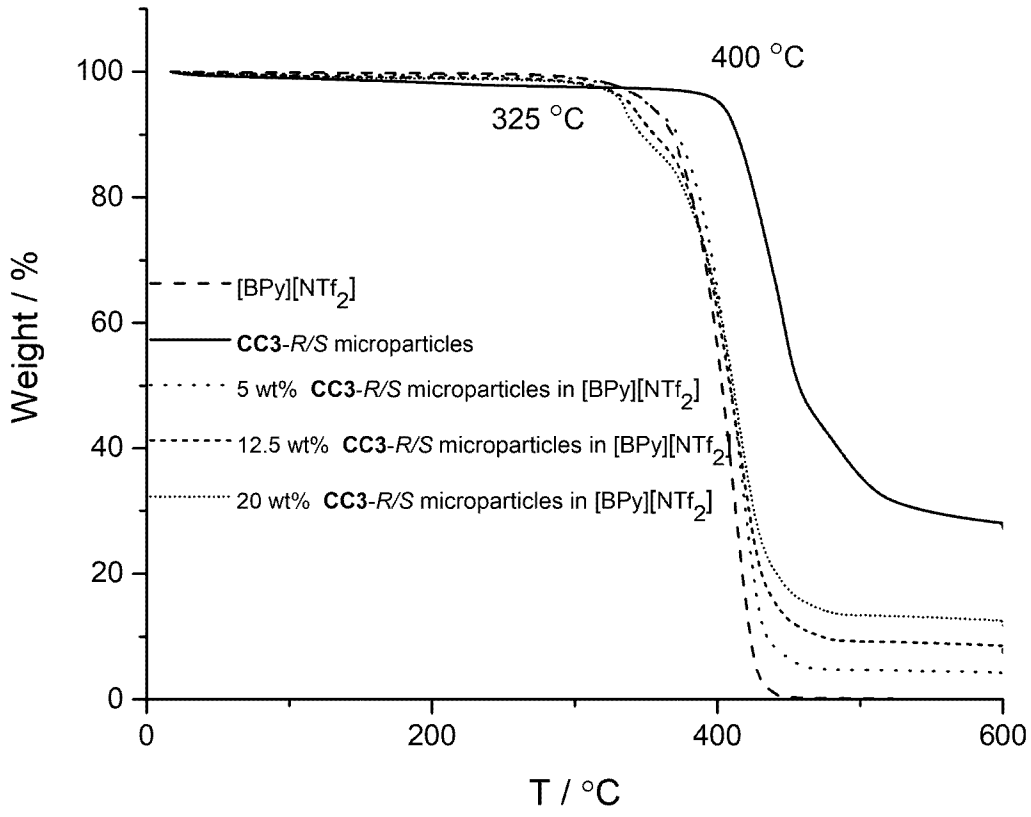

Figure 12b

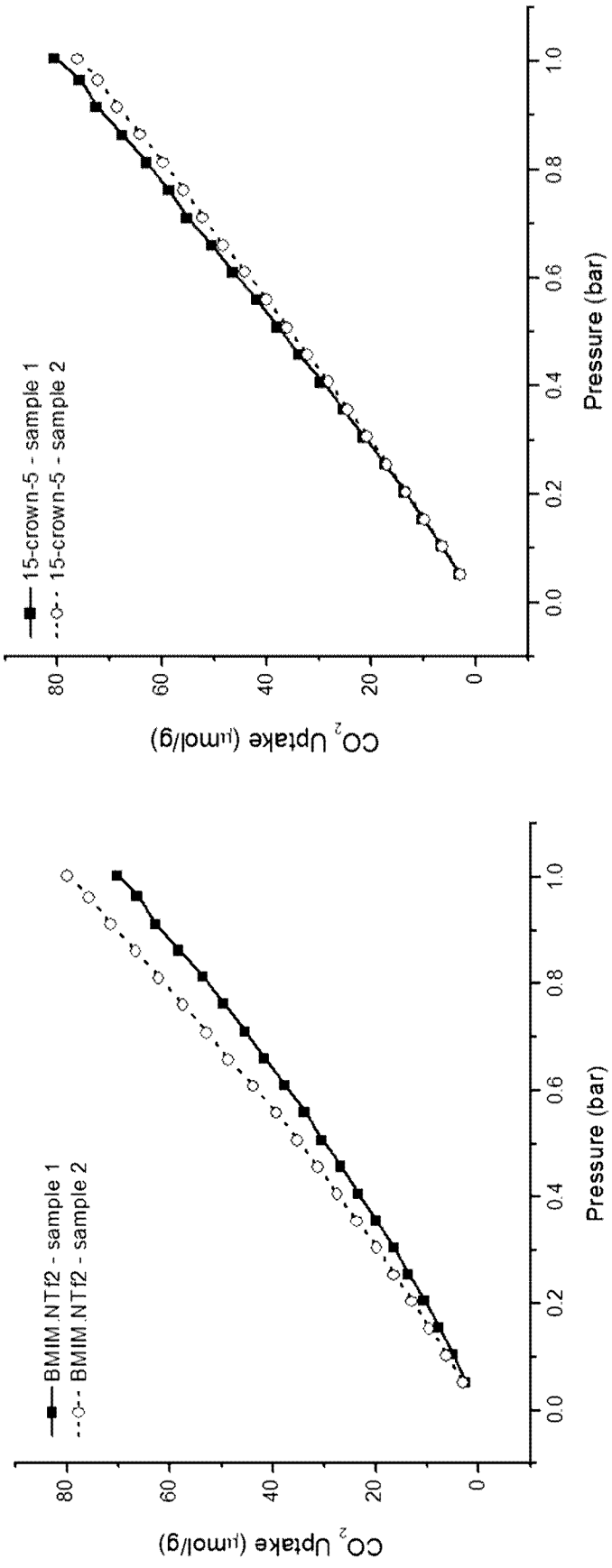
BMIM.NTf2 - sample 1
BMIM.NTf2 - sample 2
CO2 Uptake (μmol/g)
Pressure (bar)
0
20
40
60
80
0.0
0.2
0.4
0.6
0.8
1.0
15-crown-5 - sample 1
15-crown-5 - sample 2
CO2 Uptake (μmol/g)
Pressure (bar)

Figure 13

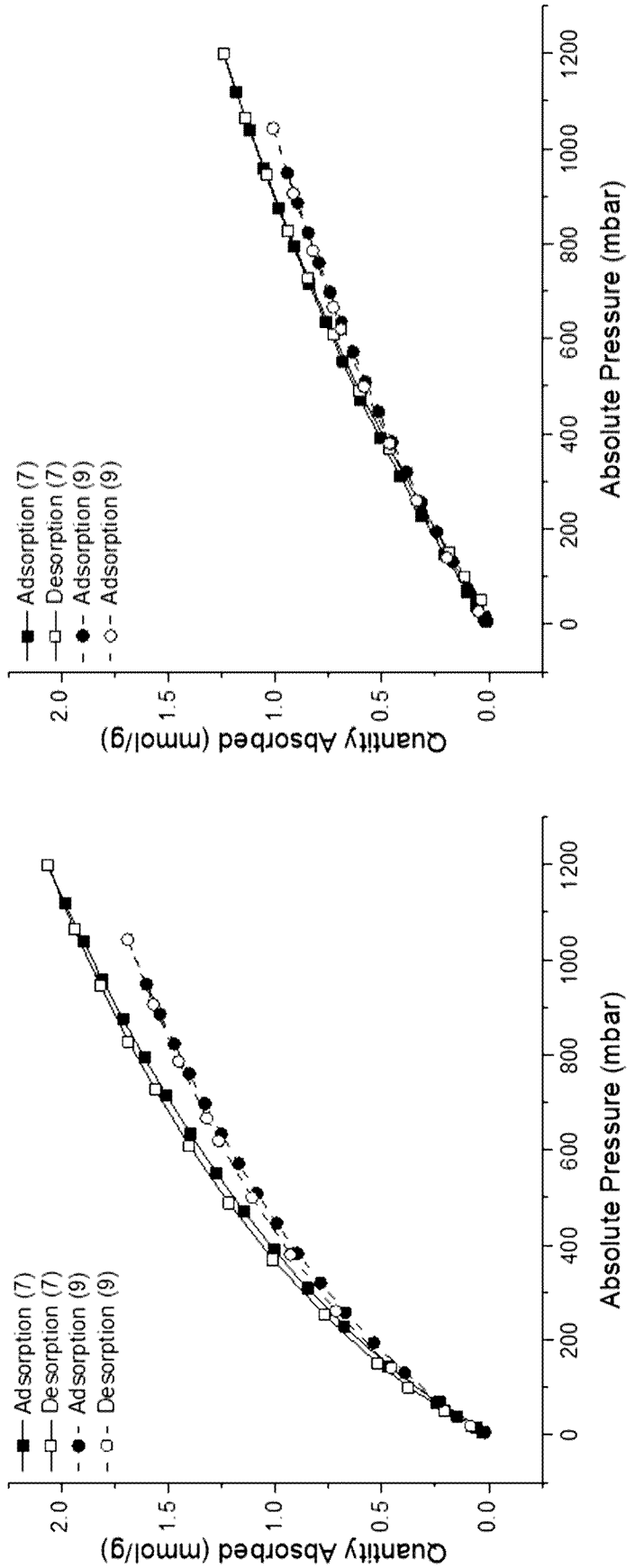
Adsorption (7)
Desorption (7)
Adsorption (9)
Desorption (9)
Quantity Absorbed (mmol/g)
Absolute Pressure (mbar)
0.0
0.5
1.0
1.5
2.0
0
200
400
600
800
1000
1200

Figure 14

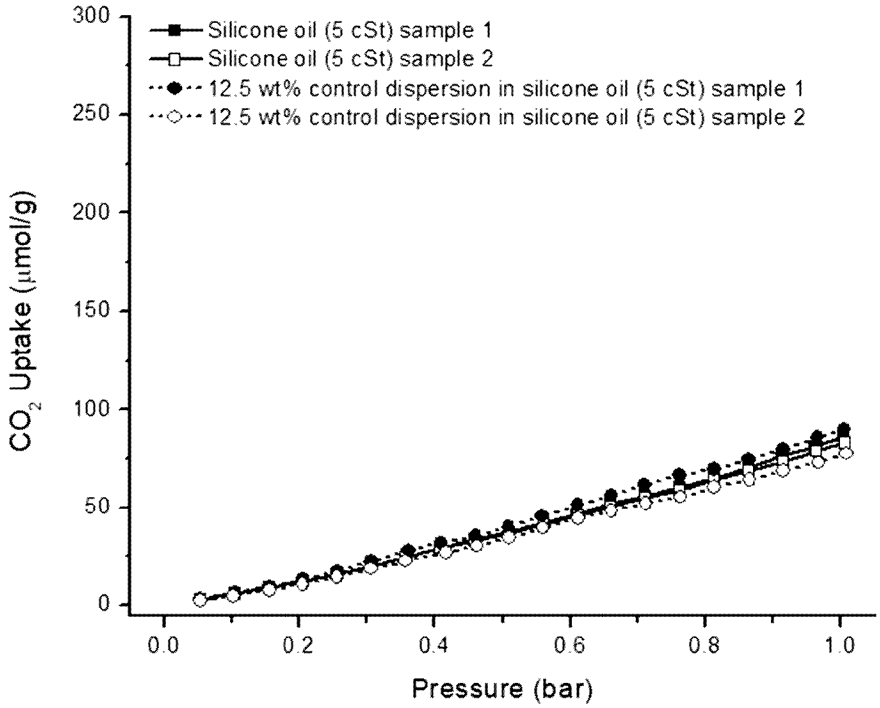

Figure 15a

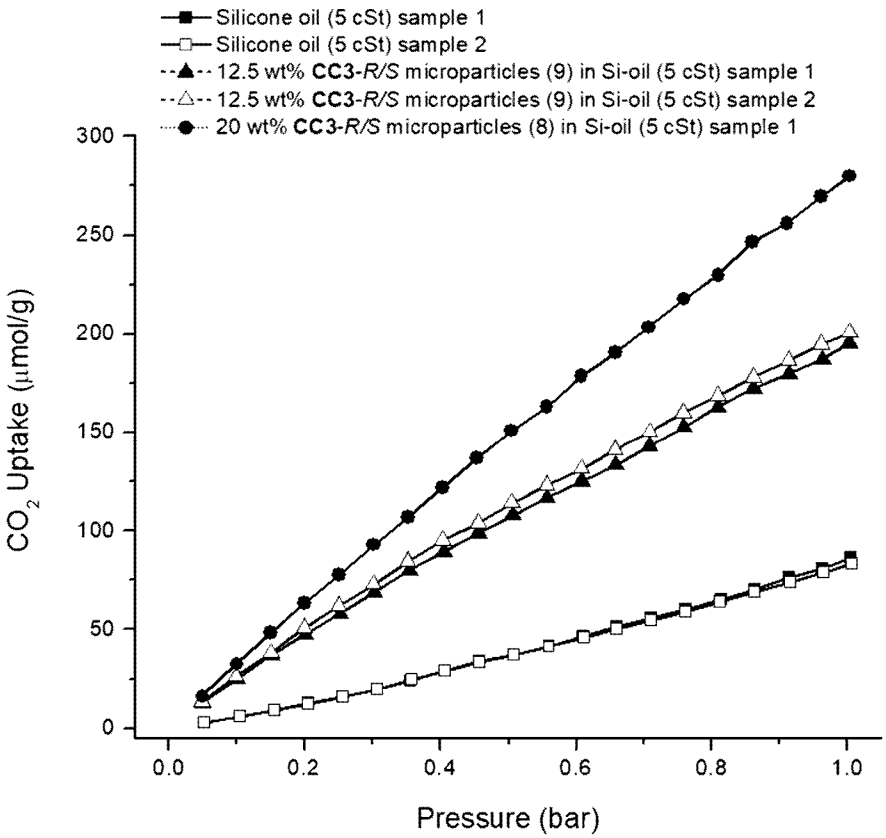

Figure 15b

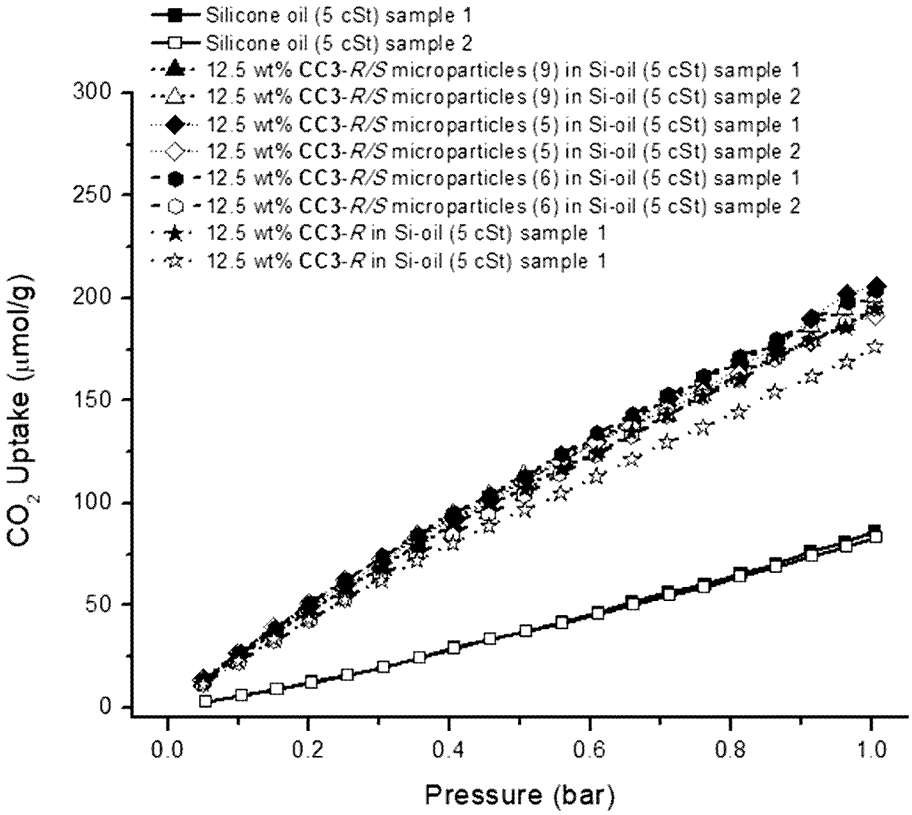

Figure 15c

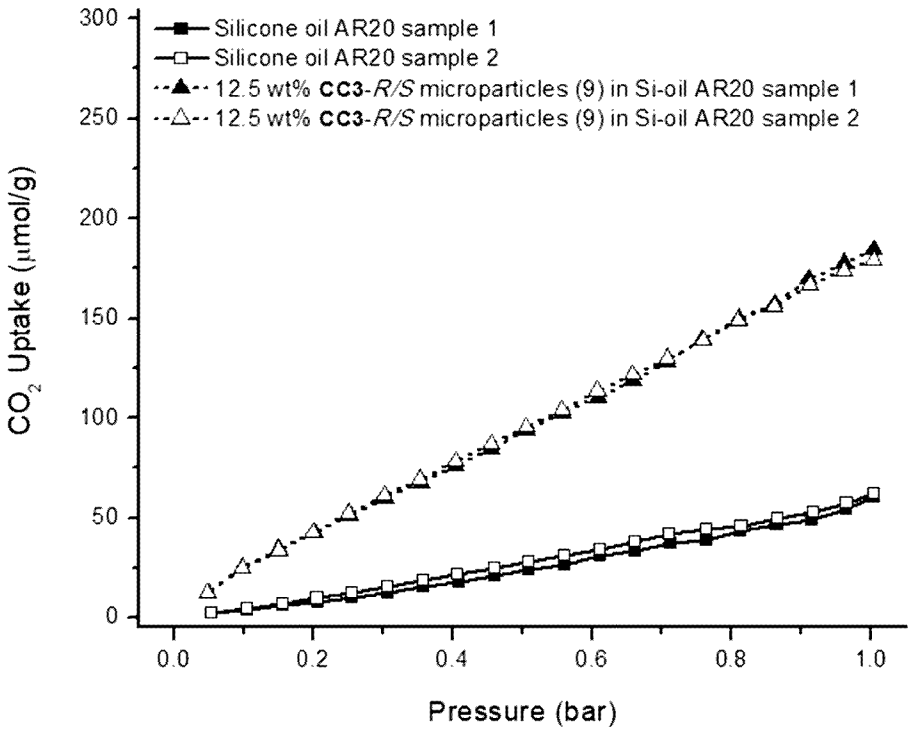

Figure 15d

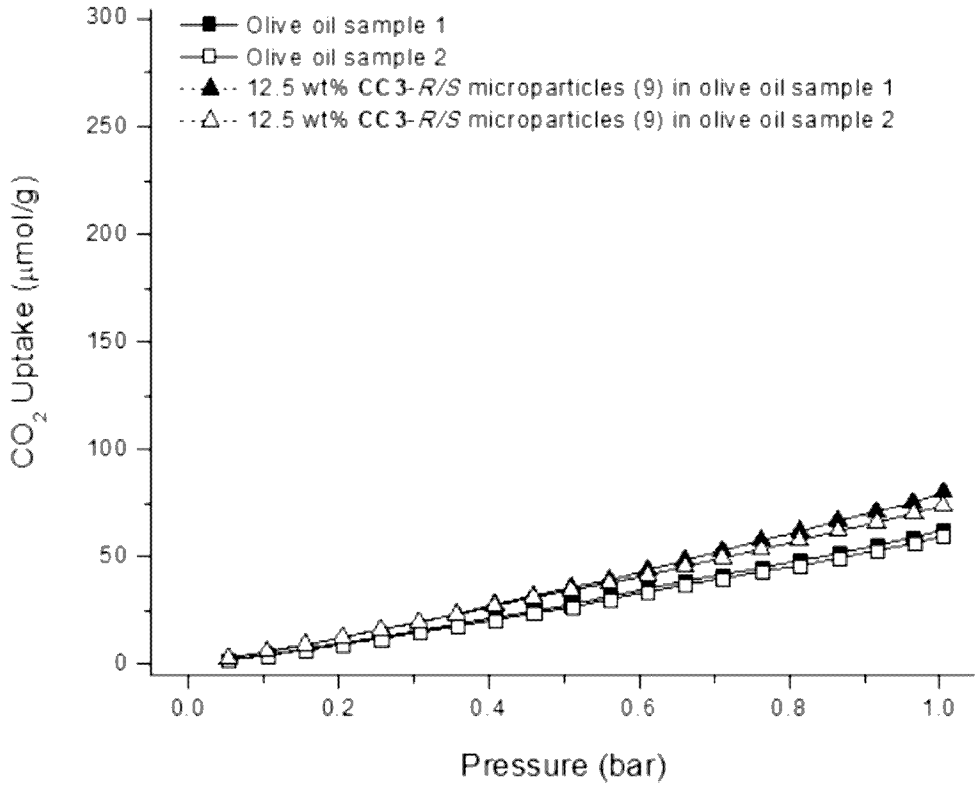

Figure 15e

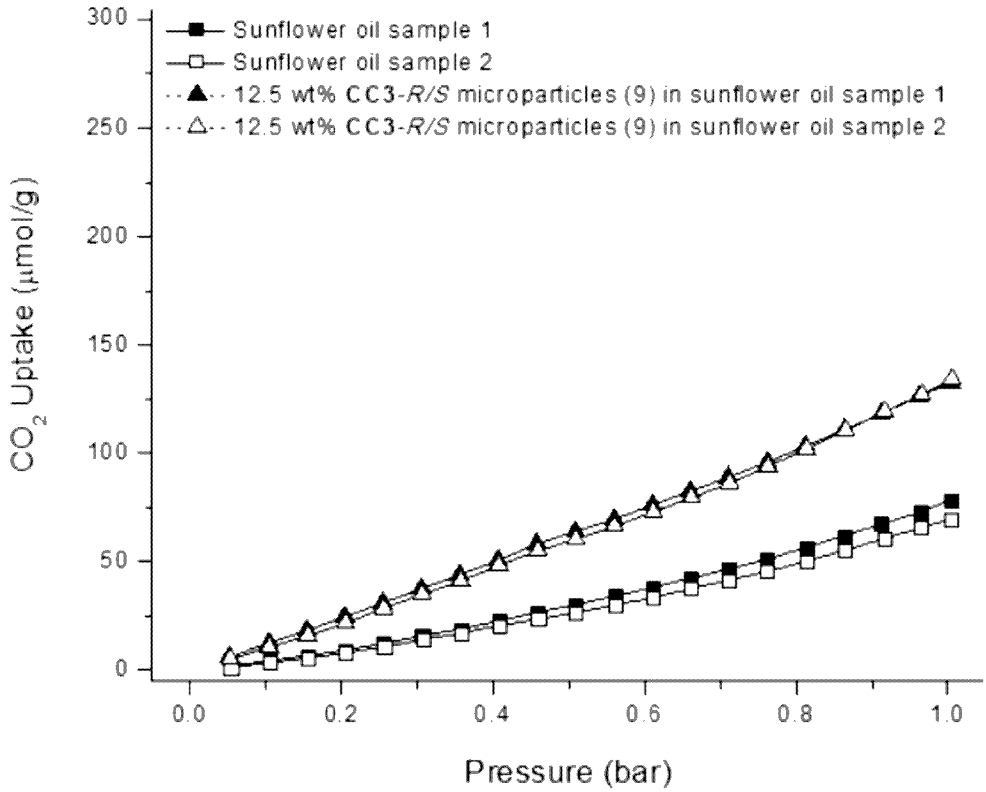

Figure 15f

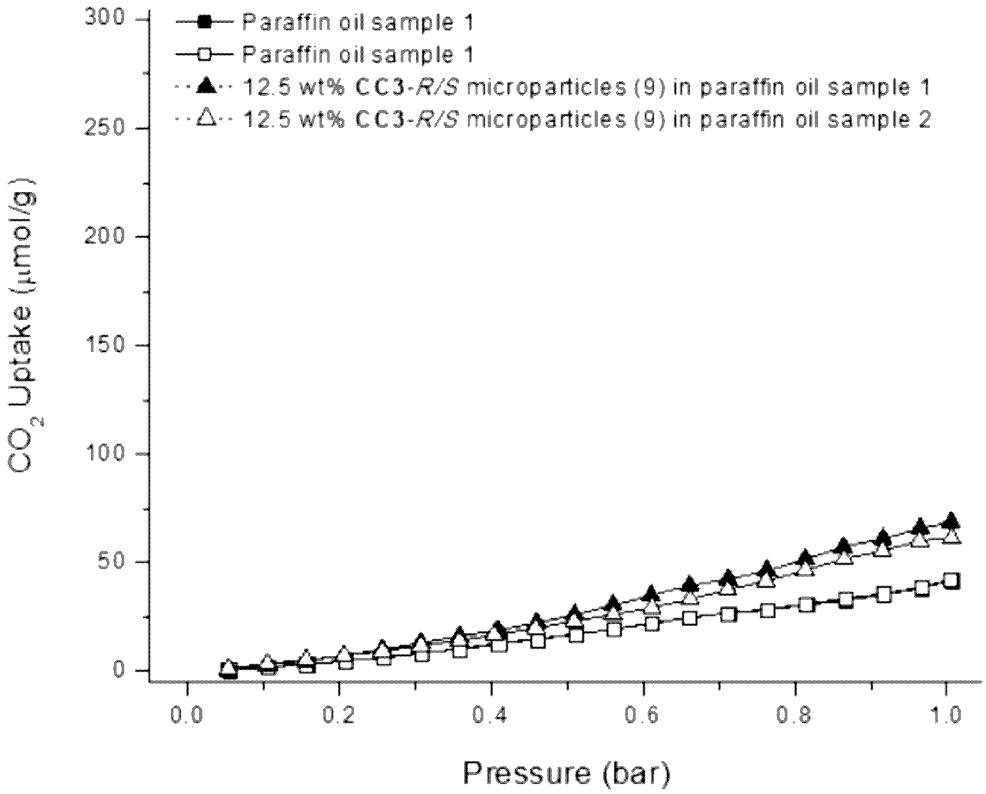

Figure 15g

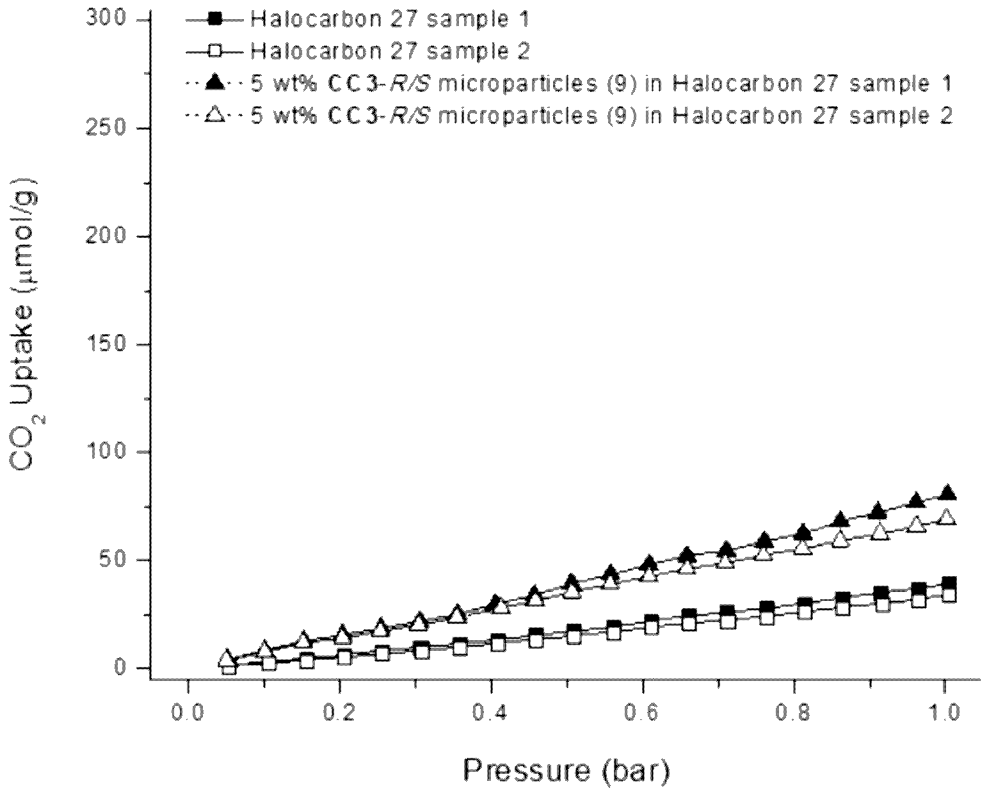

Figure 15h

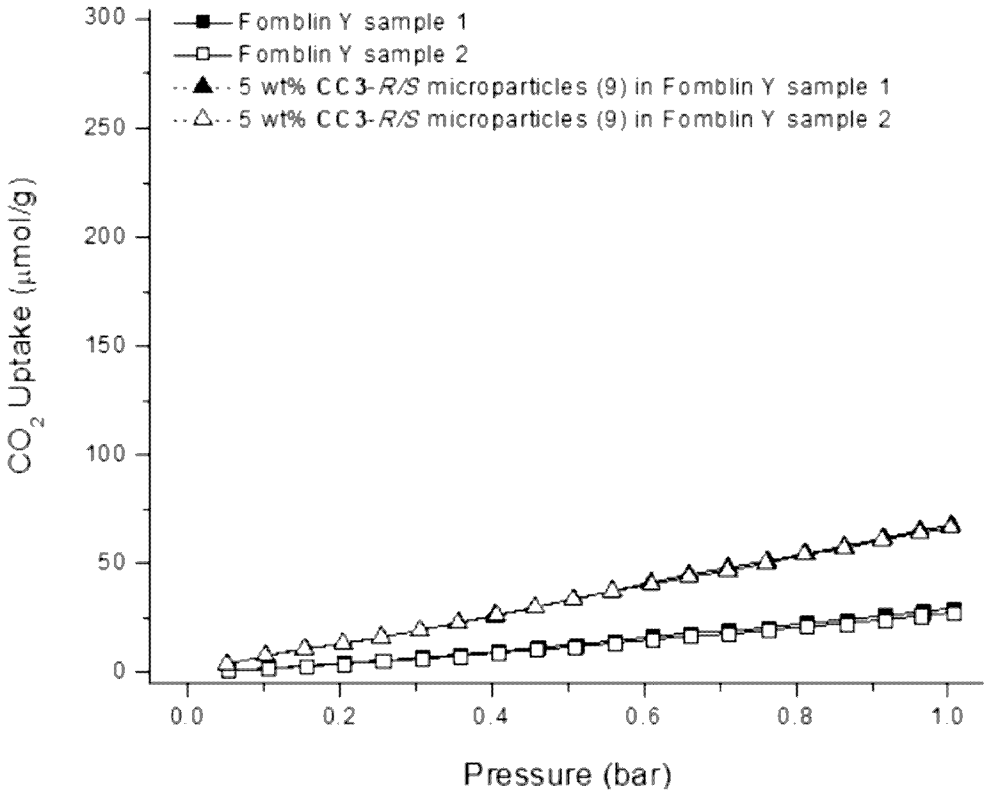

Figure 15i

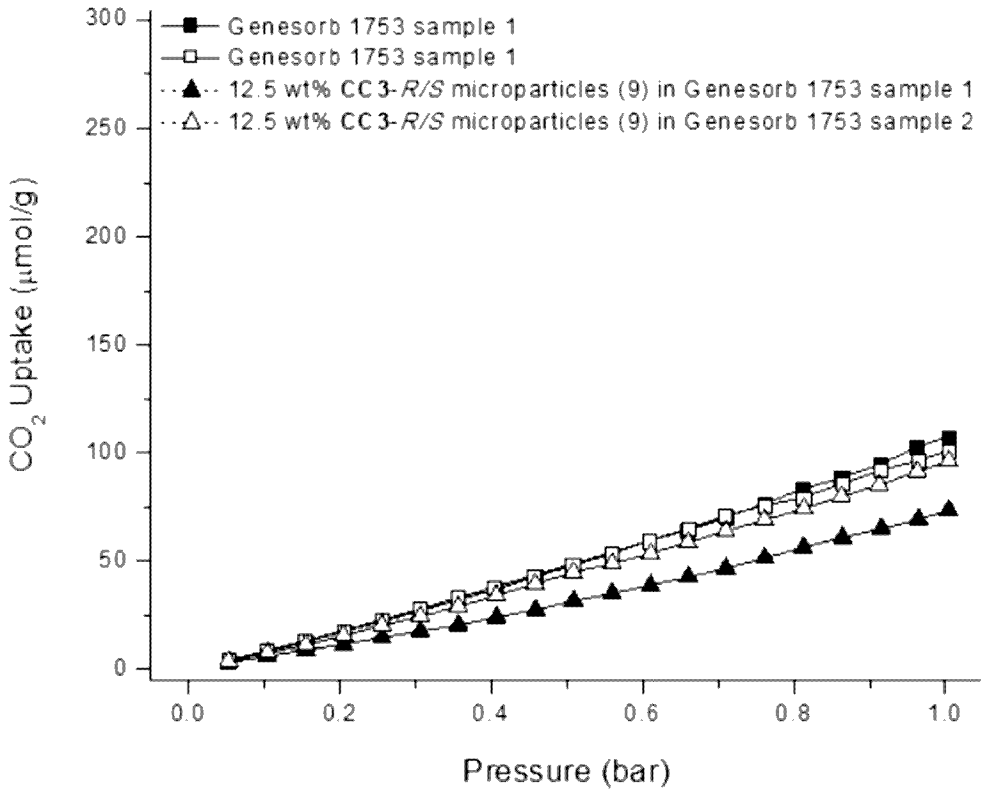

Figure 15j

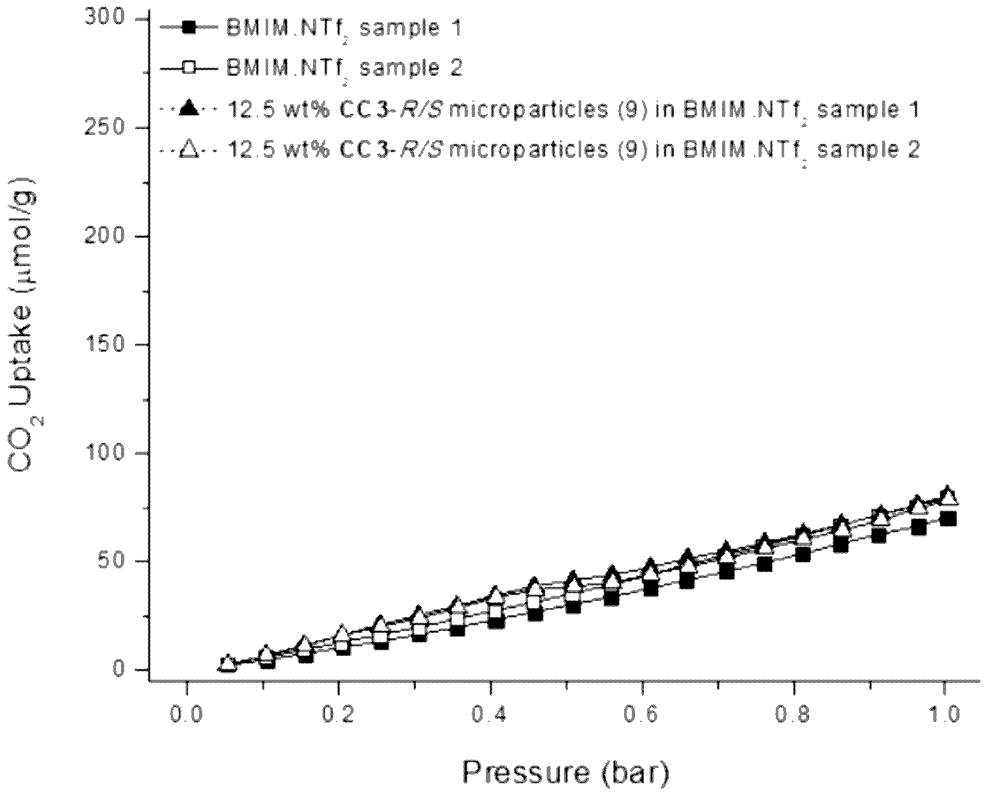

Figure 15k

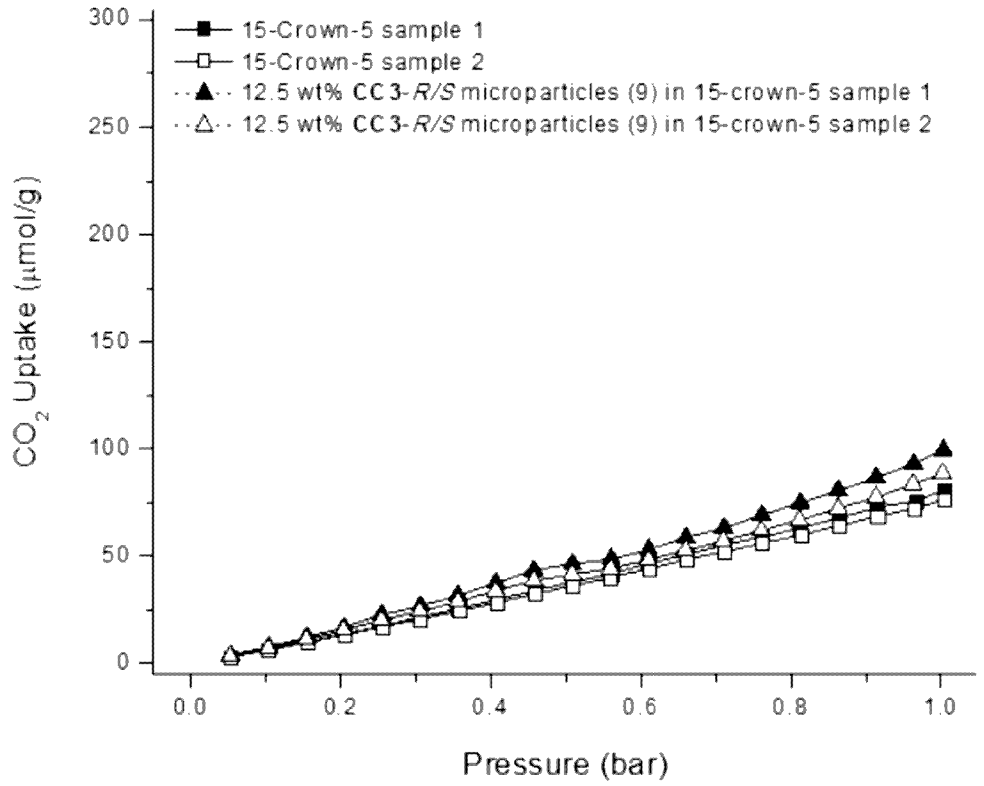

Figure 15l

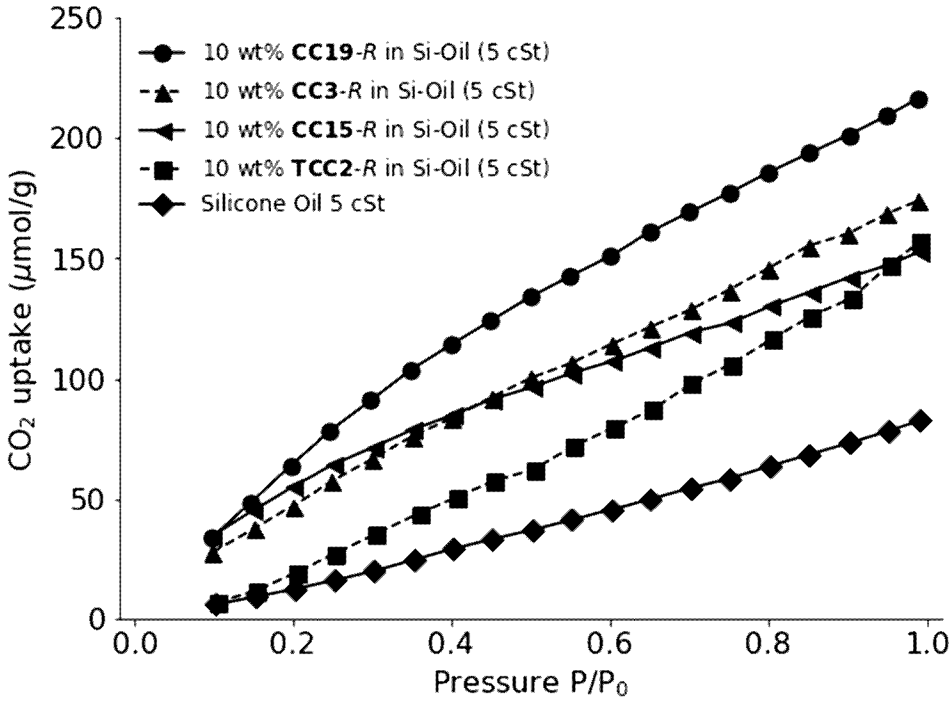

Figure 15m

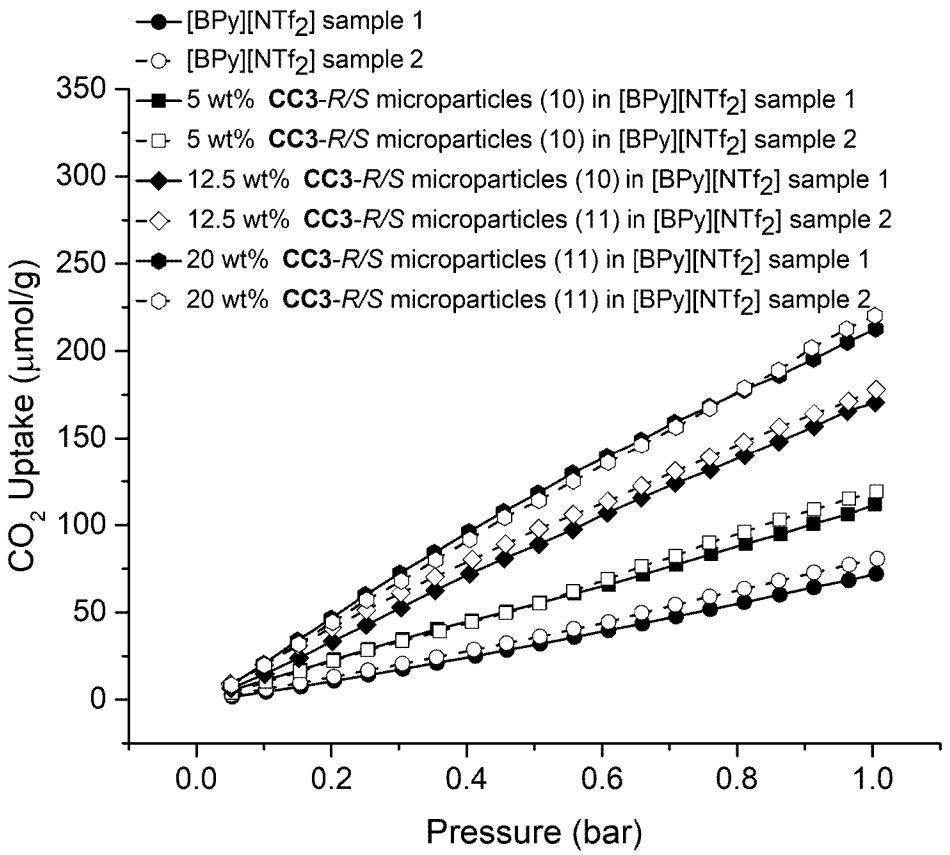

Figure 15n

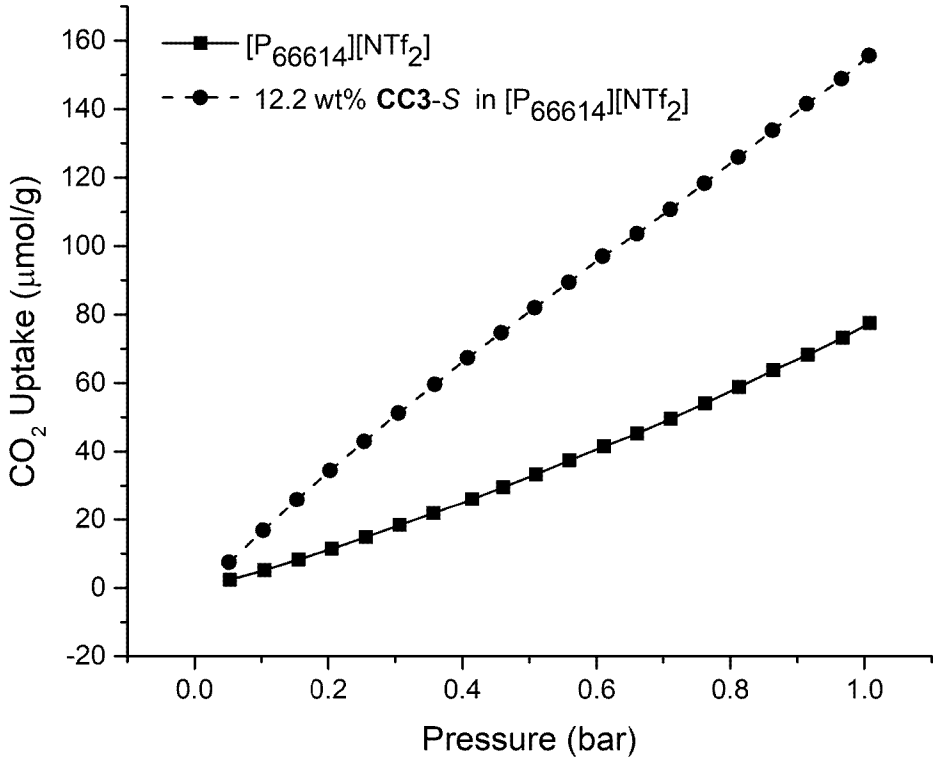

Figure 15o

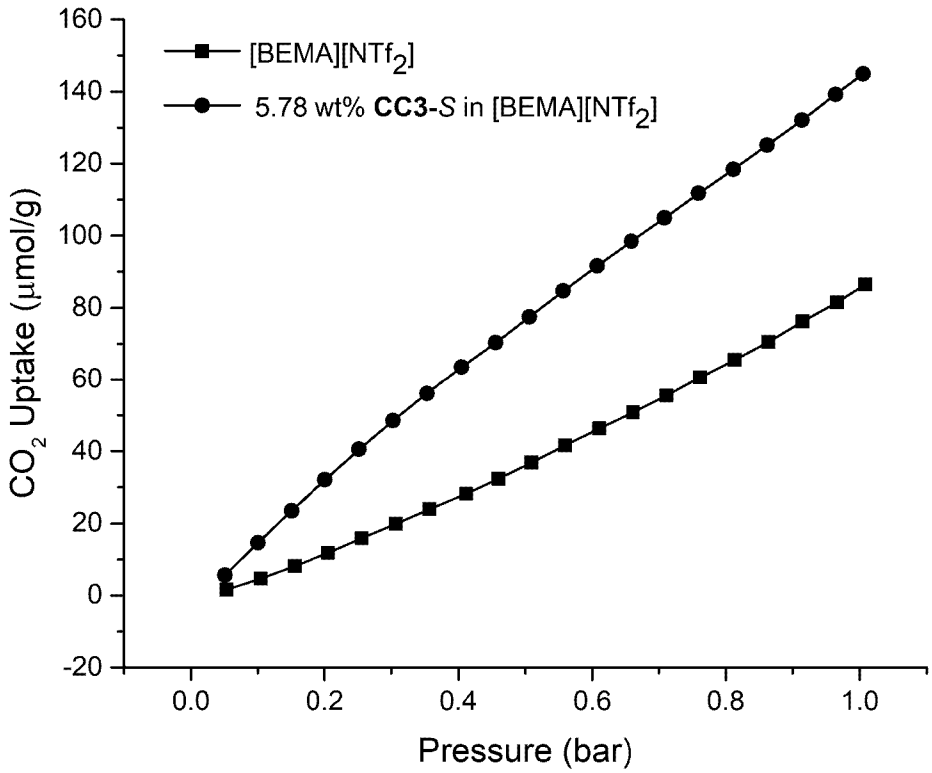

Figure 15p

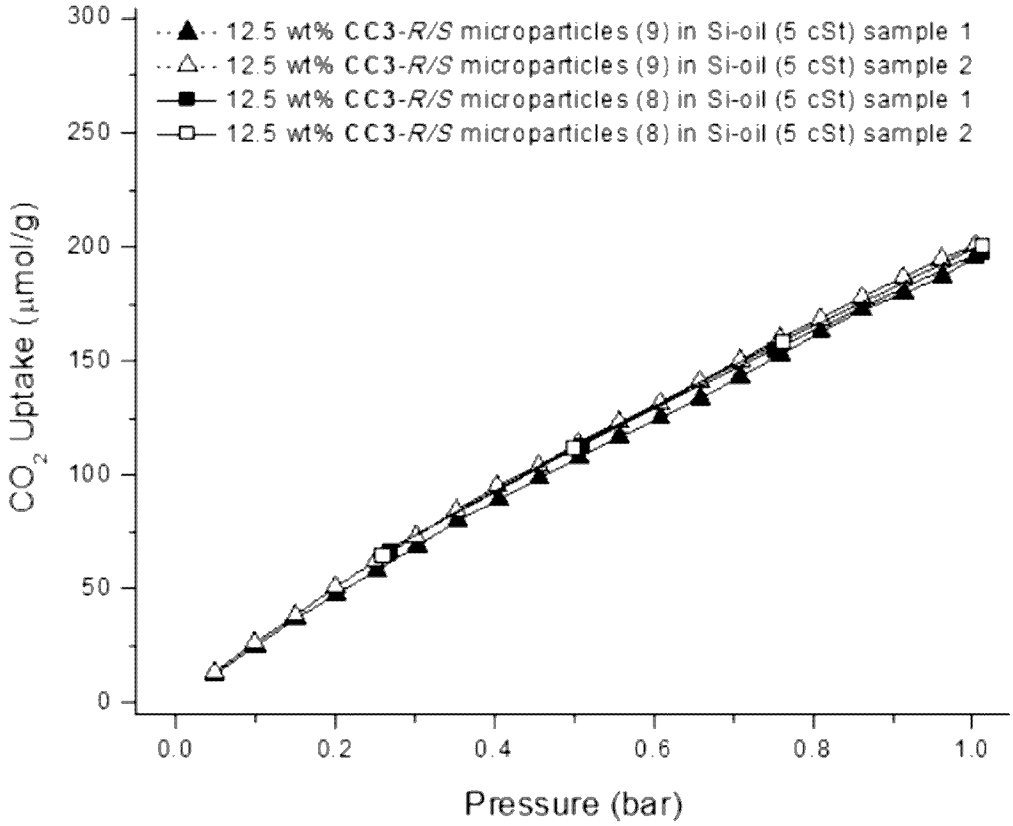

Figure 16

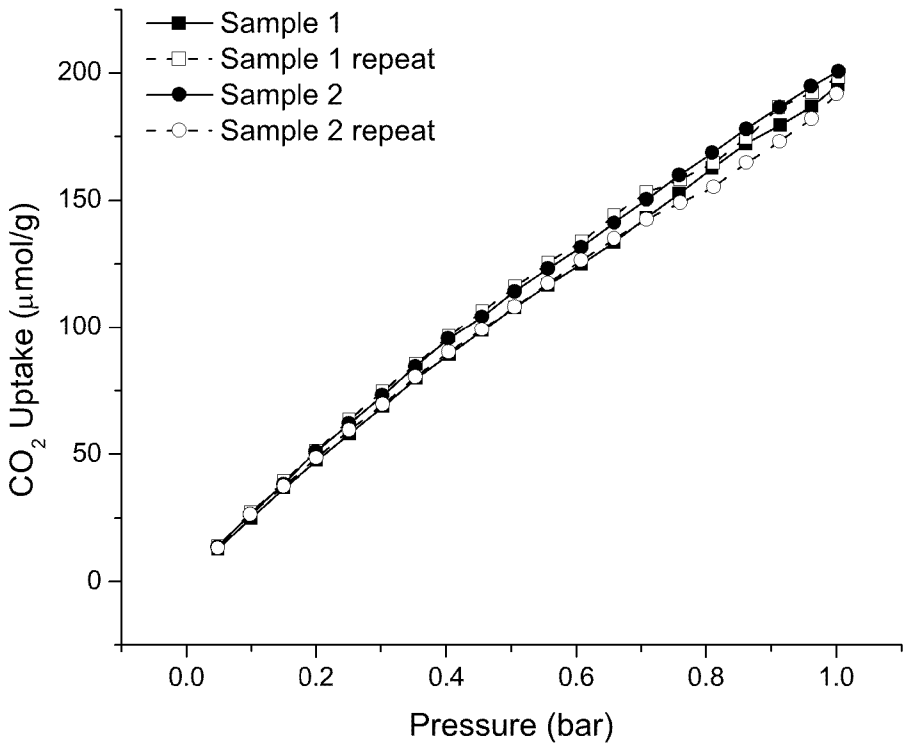

Figure 17a

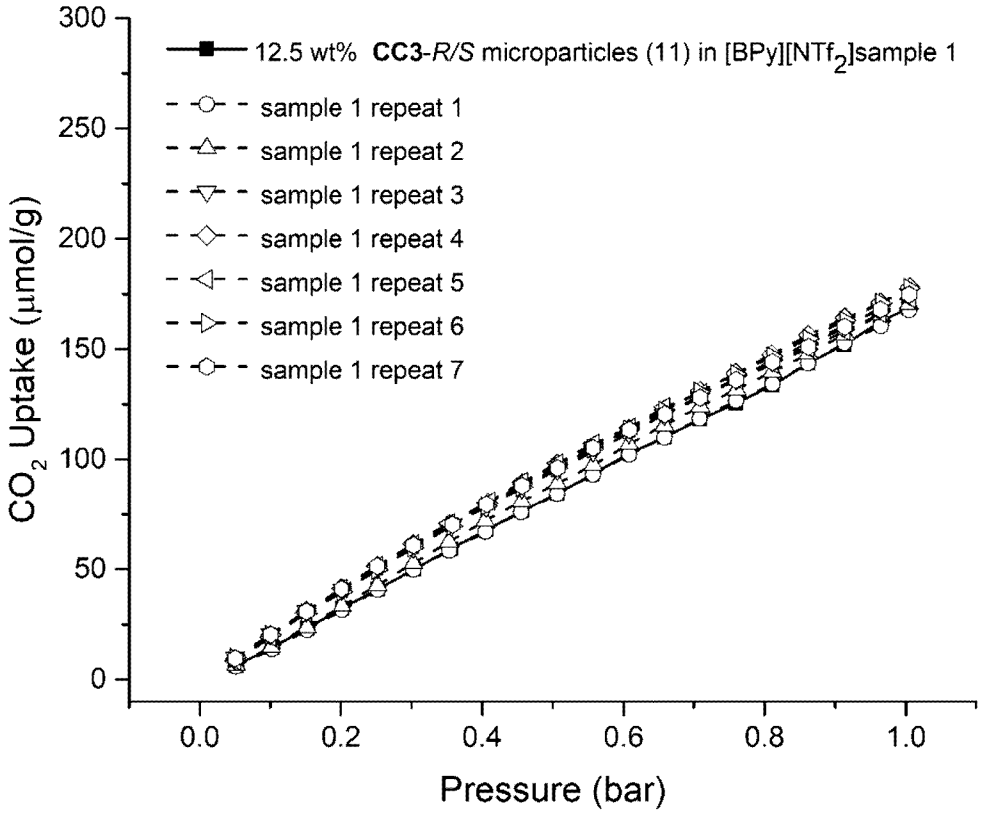

Figure 17b

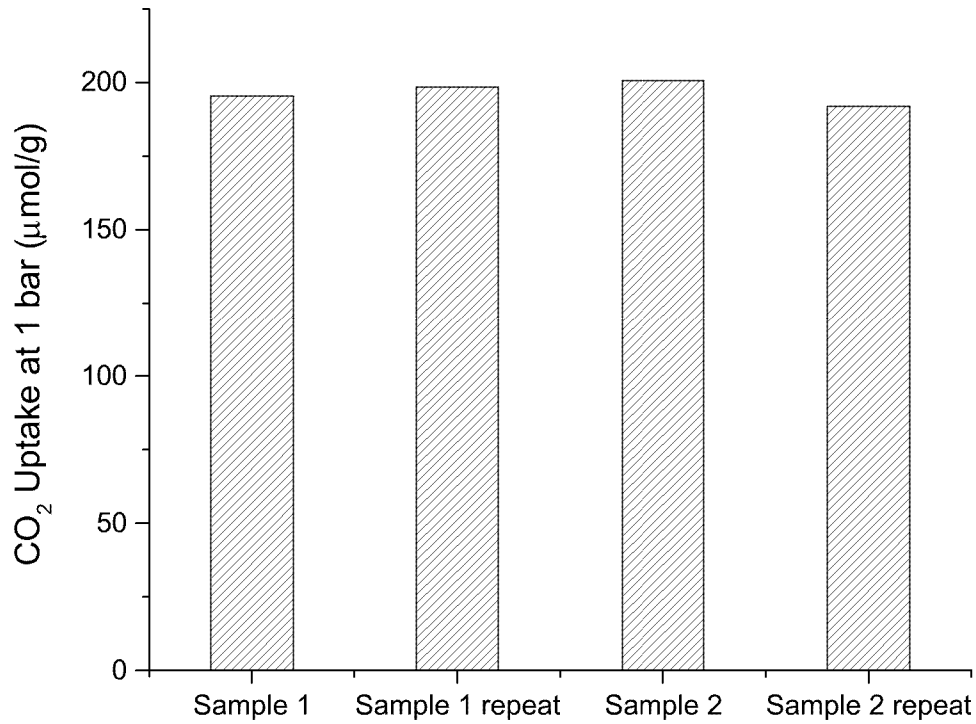

Figure 18a

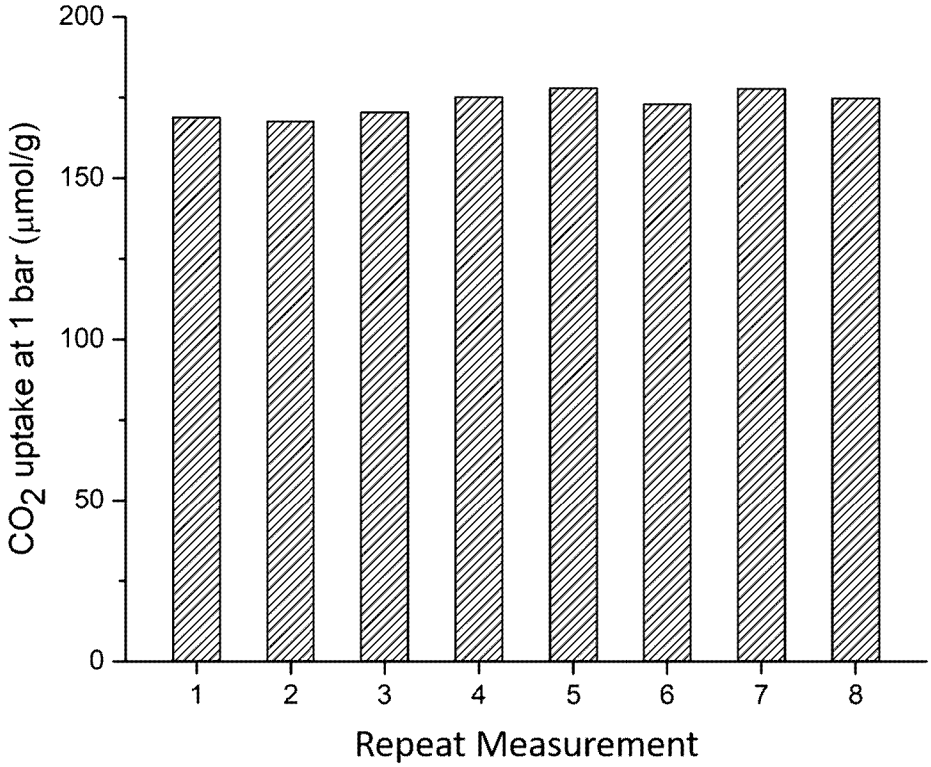

Figure 18b

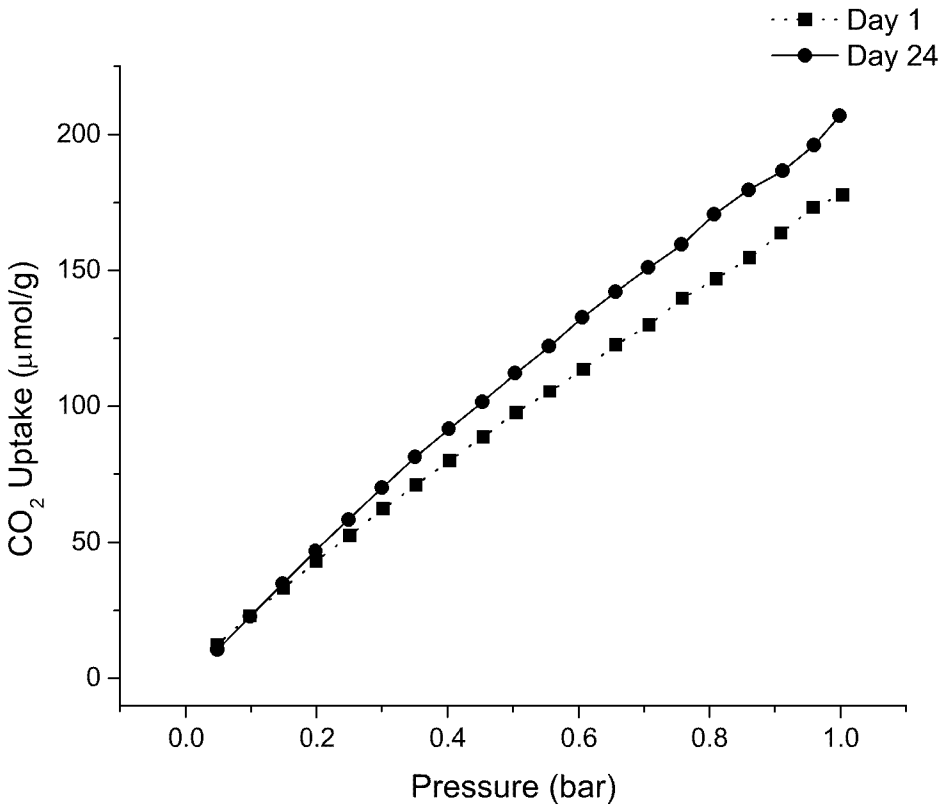

Figure 19a

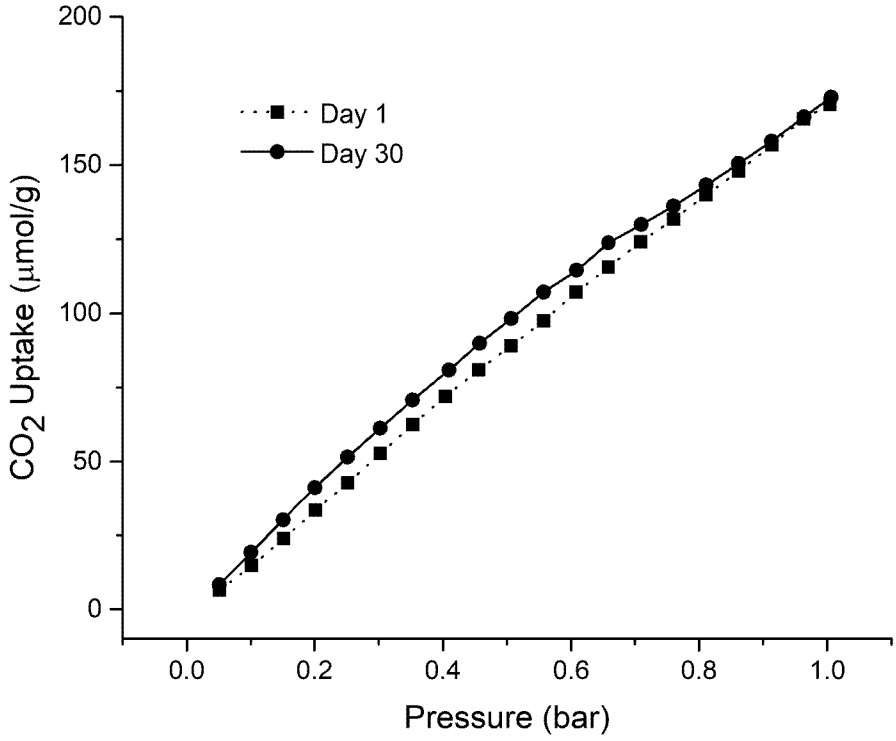

Figure 19b

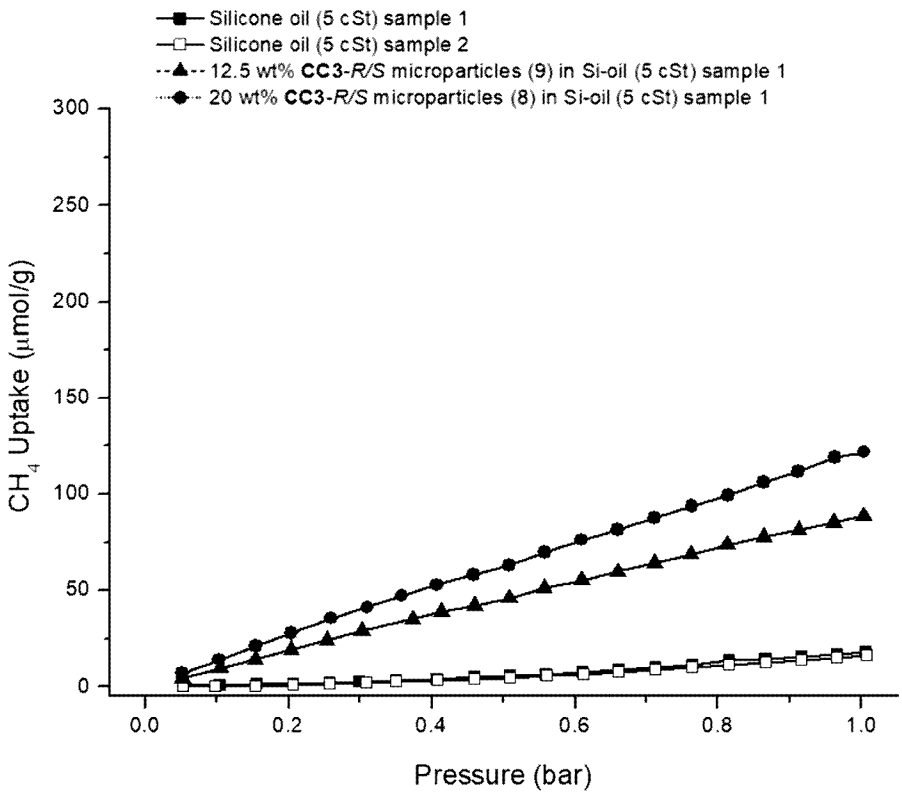

Figure 20a

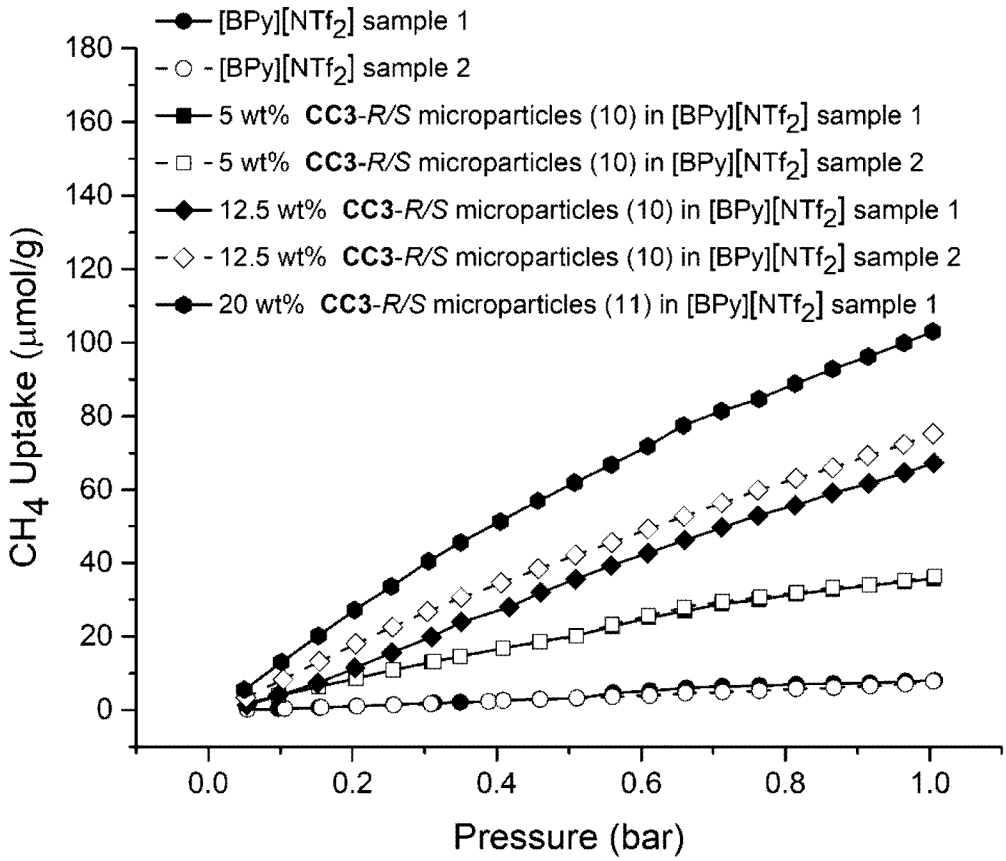
[BPy][NTf2] sample 1
[BPy][NTf2] sample 2
5 wt% CC3-R/S microparticles (10) in [BPy][NTf2] sample 1
5 wt% CC3-R/S microparticles (10) in [BPy][NTf2] sample 2
12.5 wt% CC3-R/S microparticles (10) in [BPy][NTf2] sample 1
12.5 wt% CC3-R/S microparticles (10) in [BPy][NTf2] sample 2
20 wt% CC3-R/S microparticles (11) in [BPy][NTf2] sample 1
CH4 Uptake (μmol/g)
Pressure (bar)
0
20
40
60
80
100
120
140
160
180
0.0
0.2
0.4
0.6
0.8
1.0

Figure 20b

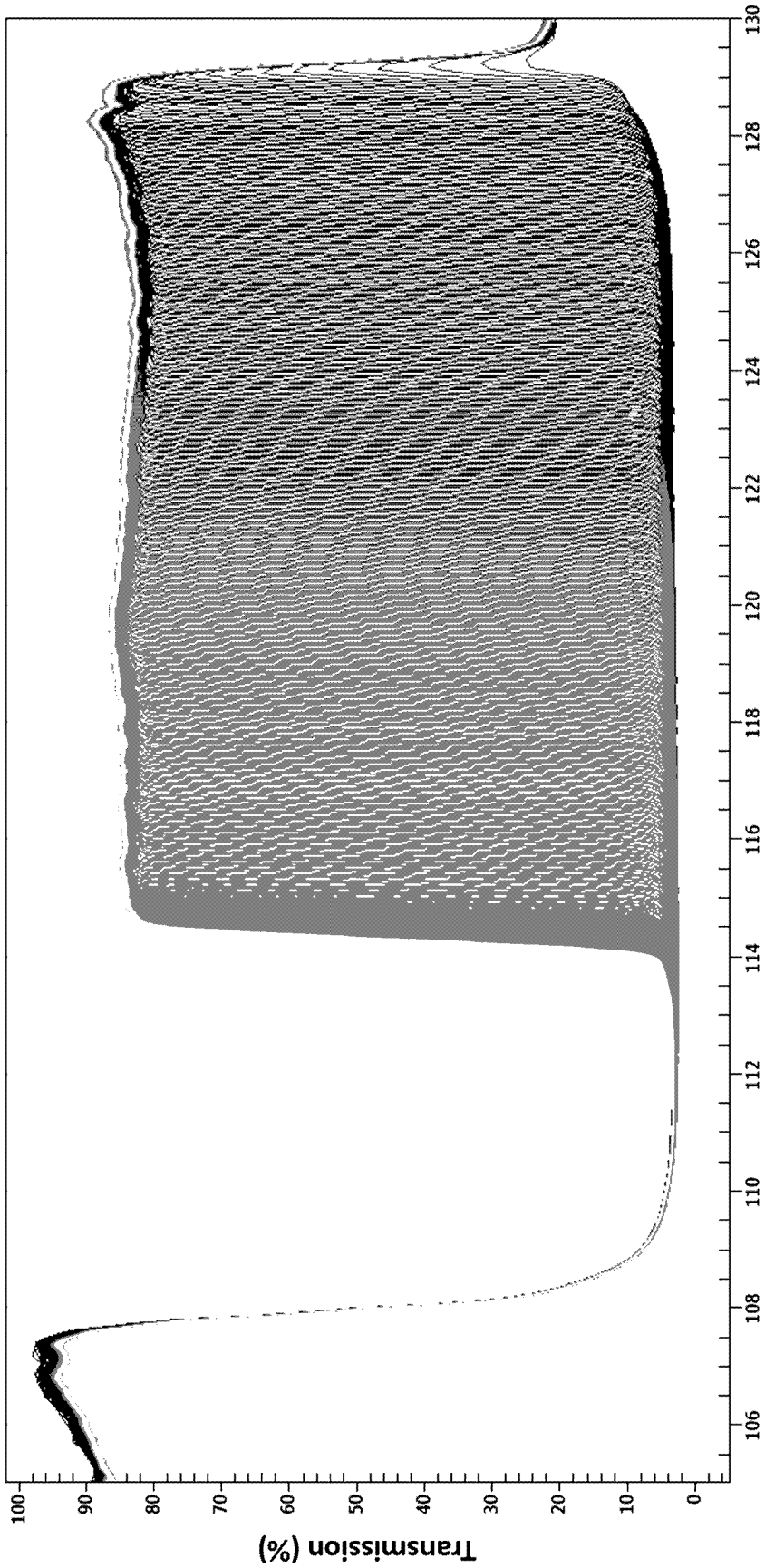
Transmission (%)
100
90
80
70
60
50
40
30
20
10
0
106
108
110
112
114
116
118
120
122
124
126
128
130
Position in mm

Figure 21a

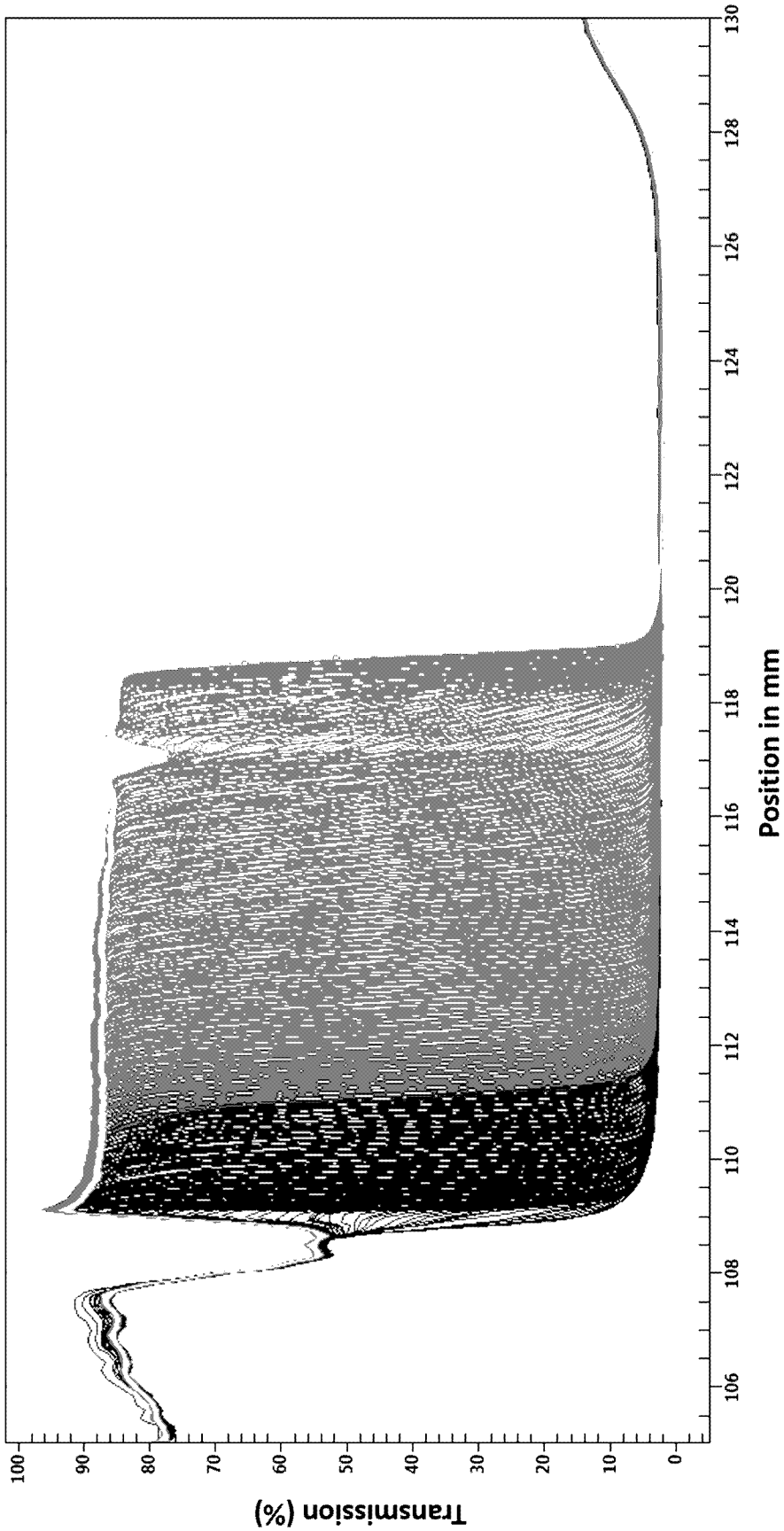
Transmission (%)
100
90
80
70
60
50
40
30
20
10
0
106
108
110
112
114
116
118
120
122
124
126
128
130
Position in mm

Figure 21b

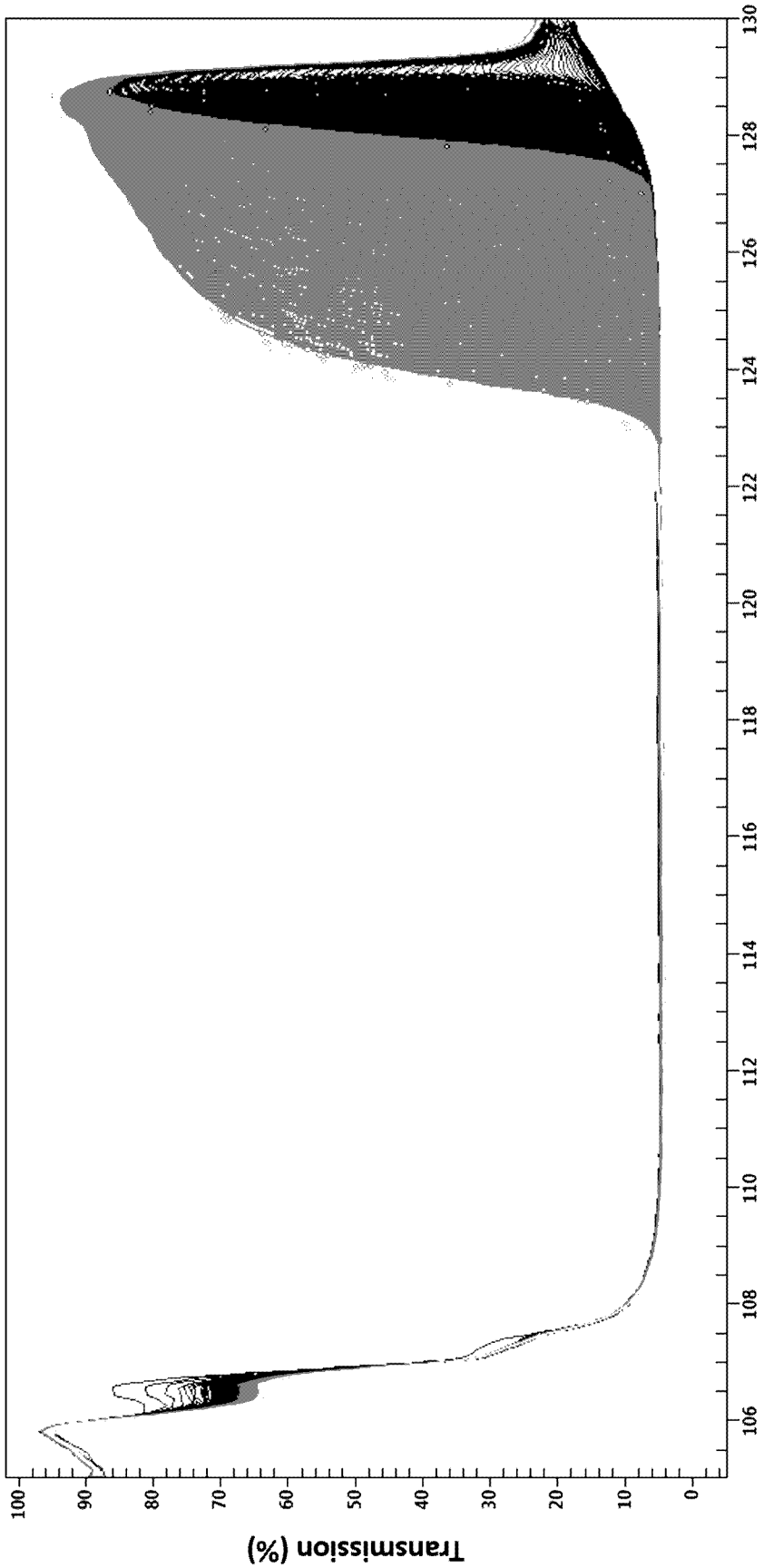
Transmission (%)
100
90
80
70
60
50
40
30
20
10
0
106
108
110
112
114
116
118
120
122
124
126
128
130
Position in mm

Figure 21c

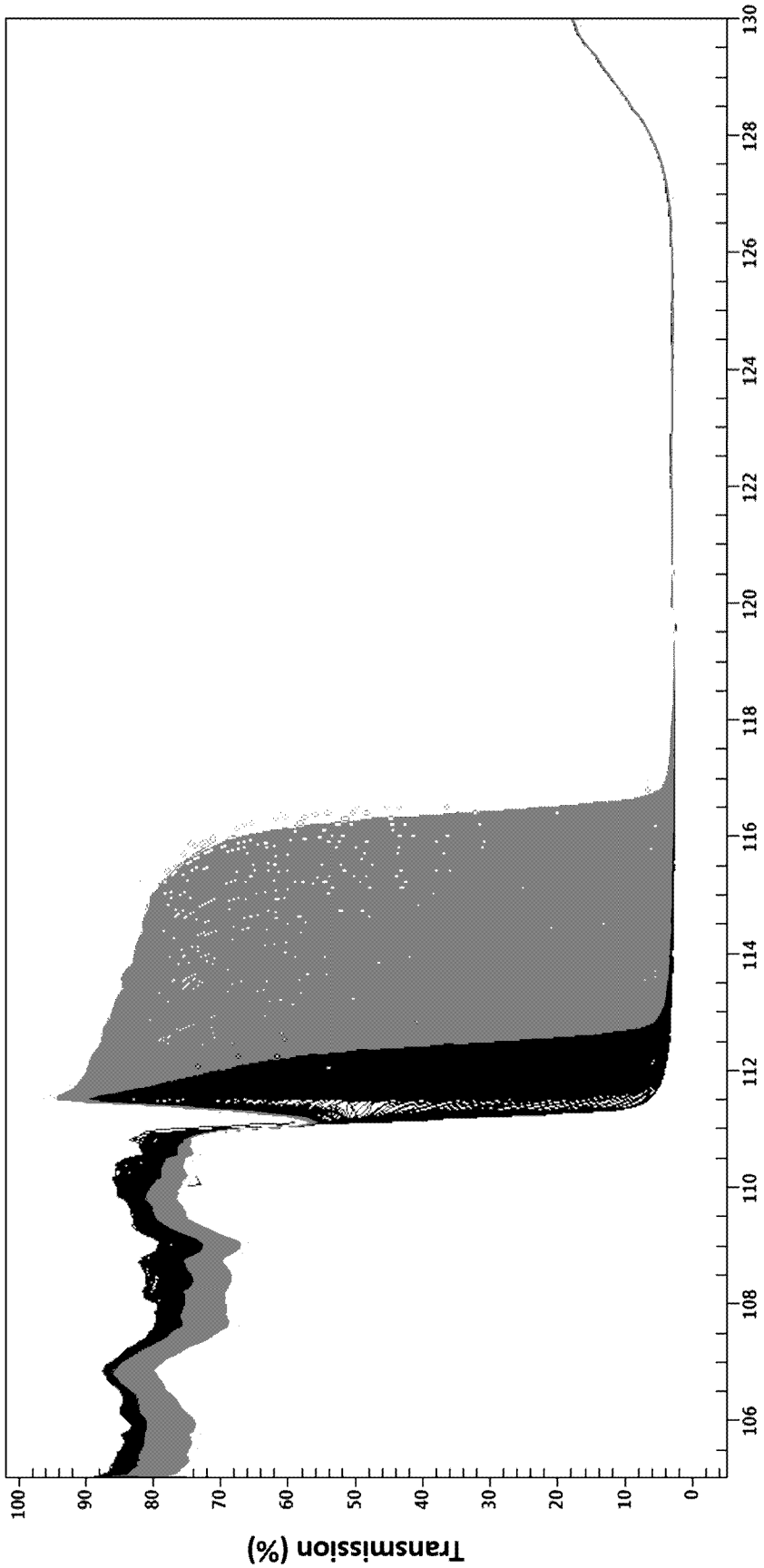
Transmission (%)
100
90
80
70
60
50
40
30
20
10
0
106
108
110
112
114
116
118
120
122
124
126
128
130
Position in mm

Figure 21d

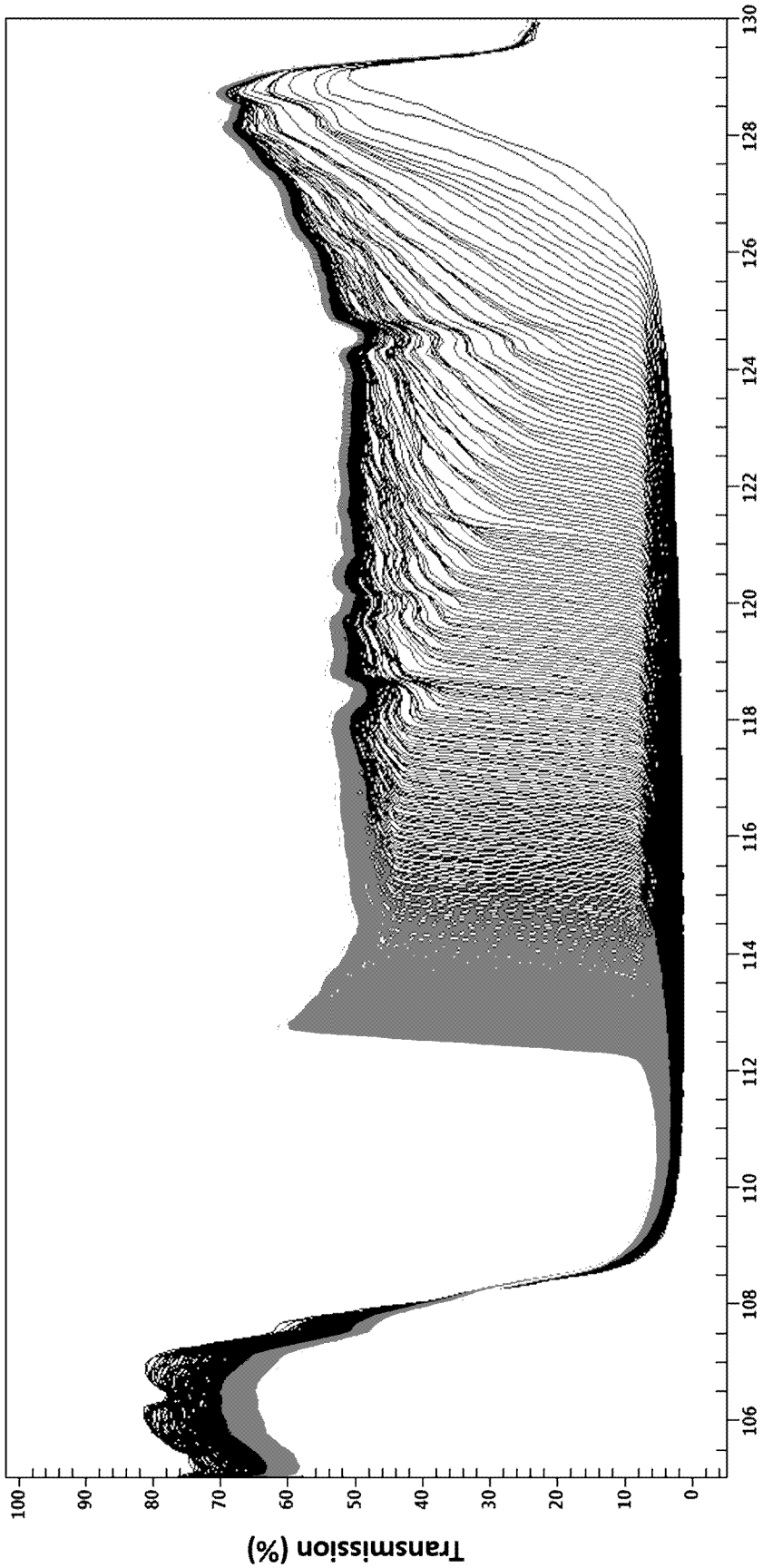
Transmission (%)
100
90
80
70
60
50
40
30
20
10
0
106
108
110
112
114
116
118
120
122
124
126
128
130
Position in mm

Figure 21e

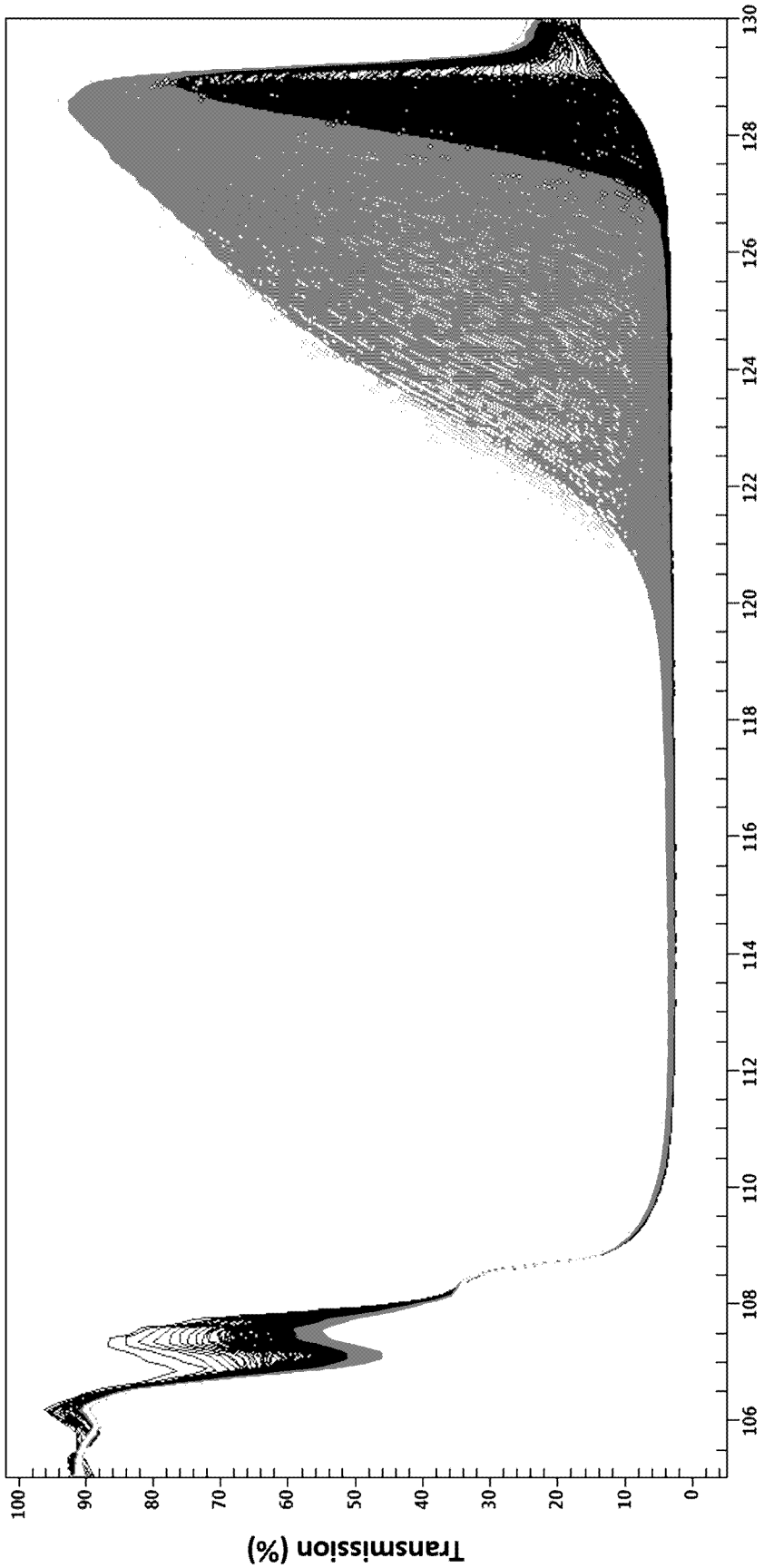
Transmission (%)
100
90
80
70
60
50
40
30
20
10
0
106
108
110
112
114
116
118
120
122
124
126
128
130
Position in mm

Figure 21f

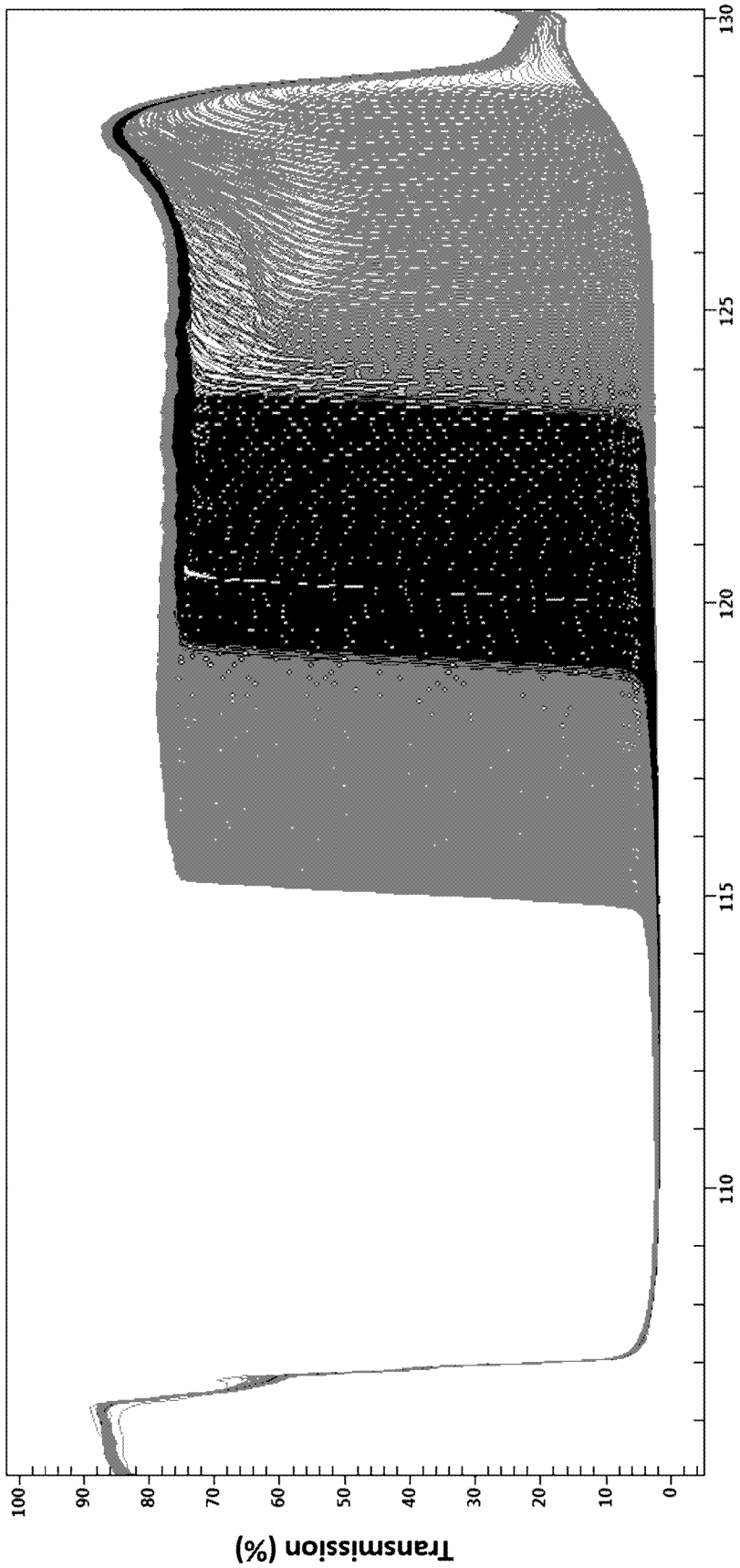
Transmission (%)
100
90
80
70
60
50
40
30
20
10
0
110
115
120
125
130
Position in mm

Figure 21g

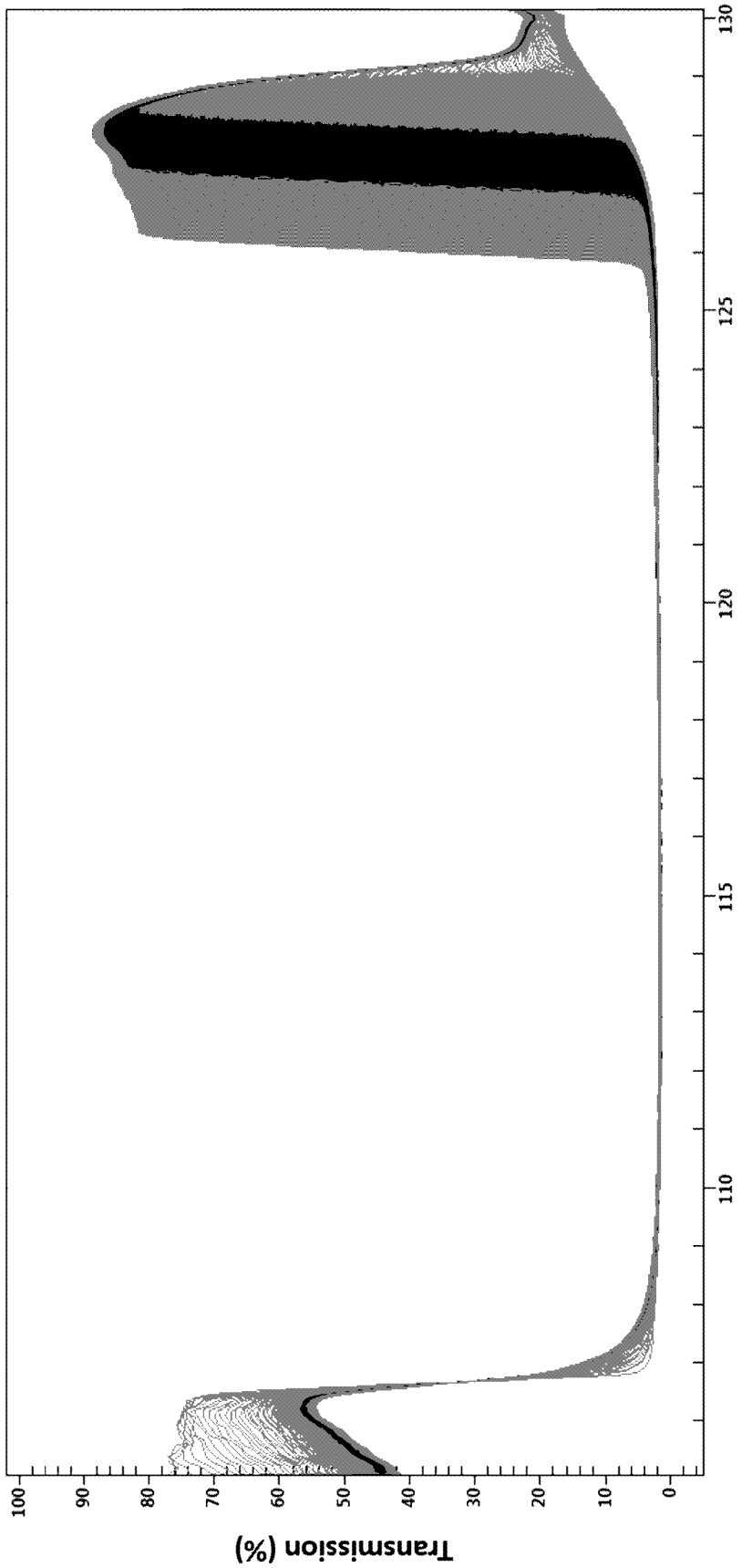
Transmission (%)
100
90
80
70
60
50
40
30
20
10
0
110
115
120
125
130
Position in mm

Figure 21h

INTERNATIONAL SEARCH REPORT

International application No
PCT/GB2019/052557

A. CLASSIFICATION OF SUBJECT MATTER
INV. B01D53/14 B01J20/26 B01J20/28
ADD.

According to International Patent Classification (IPC) or to both national classification and IPC

B. FIELDS SEARCHED

Minimum documentation searched (classification system followed by classification symbols)
B01D G01N B01J

Documentation searched other than minimum documentation to the extent that such documents are included in the fields searched

Electronic data base consulted during the international search (name of data base and, where practicable, search terms used)
EPO-Internal

C. DOCUMENTS CONSIDERED TO BE RELEVANT

Category*	Citation of document, with indication, where appropriate, of the relevant passages	Relevant to claim No.
X	NICOLA GIRI ET AL: "Liquids with permanent porosity", NATURE, vol. 527, no. 7577, 12 November 2015 (2015-11-12), pages 216-220, XP055632799, London ISSN: 0028-0836, DOI: 10.1038/nature16072	1-3,7-17
Y	including description of fig. 4 on page 219; page 219; figure 4 2nd paragraph; page 218, left-hand column	3-6

-/--

[X] Further documents are listed in the continuation of Box C. [ ] See patent family annex.

* Special categories of cited documents :

"A" document defining the general state of the art which is not considered to be of particular relevance

"E" earlier application or patent but published on or after the international filing date

"L" document which may throw doubts on priority claim(s) or which is cited to establish the publication date of another citation or other special reason (as specified)

"O" document referring to an oral disclosure, use, exhibition or other means

"P" document published prior to the international filing date but later than the priority date claimed

"T" later document published after the international filing date or priority date and not in conflict with the application but cited to understand the principle or theory underlying the invention

"X" document of particular relevance; the claimed invention cannot be considered novel or cannot be considered to involve an inventive step when the document is taken alone

"Y" document of particular relevance; the claimed invention cannot be considered to involve an inventive step when the document is combined with one or more other such documents, such combination being obvious to a person skilled in the art

"&" document member of the same patent family

Date of the actual completion of the international search	Date of mailing of the international search report
3 December 2019	20/12/2019

Name and mailing address of the ISA/	Authorized officer
European Patent Office, P.B. 5818 Patentlaan 2 NL - 2280 HV Rijswijk Tel. (+31-70) 340-2040, Fax: (+31-70) 340-3016	Pöhlmann, Robert

1

Form PCT/ISA/210 (second sheet) (April 2005)

C(Continuation). DOCUMENTS CONSIDERED TO BE RELEVANT

Category*	Citation of document, with indication, where appropriate, of the relevant passages	Relevant to claim No.
X	SEYED HOSSEIN JAMALI ET AL: "Thermodynamic and Transport Properties of Crown-Ethers: Force Field Development and Molecular Simulations", JOURNAL OF PHYSICAL CHEMISTRY PART B, vol. 121, no. 35, 25 August 2017 (2017-08-25), pages 8367-8376, XP055648123, US ISSN: 1520-6106, DOI: 10.1021/acs.jpcb.7b06547	1,2
Y	abstract sentence before headline "Acknowledgements"; page 2650	3-6

X	REBECCA L. GREENAWAY ET AL: "Understanding gas capacity, guest selectivity, and diffusion in porous liquids", CHEMICAL SCIENCE, vol. 8, no. 4, 31 January 2017 (2017-01-31), pages 2640-2651, XP055648171, United Kingdom ISSN: 2041-6520, DOI: 10.1039/C6SC05196K	1,2,9
Y	paragraph "Introduction"; page 2640 description to figure 4; page 2643 figure 4	3-6

Y	A. G. SLATER ET AL: "A solution-processable dissymmetric porous organic cage", MOLECULAR SYSTEMS DESIGN & ENGINEERING, vol. 3, no. 1, 9 October 2017 (2017-10-09) , pages 223-227, XP055648618, DOI: 10.1039/C7ME00090A figure 1 abstract	3,4

Y	ANNA G. SLATER ET AL: "Computationally-Guided Synthetic Control over Pore Size in Isostructural Porous Organic Cages", ACS CENTRAL SCIENCE, vol. 3, no. 7, 20 June 2017 (2017-06-20), pages 734-742, XP055648656, ISSN: 2374-7943, DOI: 10.1021/acscentsci.7b00145 Scheme 1; page 735 paragraph "Conclusions"; page 740 - page 741	5,6

1